Analysis of heat shock-, sodium arsenite- and proteasome inhibitor-induced *heat shock protein* gene expression in *Xenopus laevis*

by

Jordan T.F. Young

A thesis
presented to the University of Waterloo
in fulfillment of the
thesis requirement for the degree of
Master of Science
in
Biology

Waterloo, Ontario, Canada, 2009

Author's Declaration

I hereby declare that I am the sole author of this thesis. This is a true copy of the thesis, including any required final revisions, as accepted by my examiners. I understand that my thesis may be made electronically available to the public.

Abstract

Previous studies have focused on the effect of individual stressors on *hsp* gene expression in eukaryotic organisms. In the present study, I examined the effect of concurrent low doses of sodium arsenite and mild heat shock temperatures on the expression of *hsp30* and *hsp70* genes in *Xenopus laevis* A6 kidney epithelial cells. Northern hybridization and western blot analysis revealed that exposure of A6 cells to 1-10 μM sodium arsenite at a mild heat shock temperature of 30˚C enhanced *hsp30* and *hsp70* gene expression to a much greater extent than found with either stress individually. In cells treated simultaneously with 10 μM sodium arsenite and different heat shock temperatures, enhanced accumulation of HSP30 and HSP70 protein was first detected at 26˚C with larger responses at 28 and 30 ˚C. HSF1 activity was involved in combined stress-induced *hsp* gene expression since the HSF1 activation inhibitor, KNK437, inhibited HSP30 and HSP70 accumulation. Immunocytochemical analysis revealed that HSP30 was present in a granular pattern primarily in the cytoplasm in cells treated simultaneously with both stresses. Finally, prior exposure of A6 cells to concurrent sodium arsenite (10 μM) and heat shock (30 ˚C) treatment conferred thermotolerance since it protected them against a subsequent thermal challenge at 37 ˚C. Acquired thermotolerance was not observed with cells treated with the two mild stresses individually. It is likely that the enhanced accumulation of HSPs under these conditions permits the organism to cope with multiple environmental stresses encountered in their natural aquatic habitat.

Previous studies have shown that inhibiting the activity of the proteasome also leads to the accumulation of damaged or unfolded proteins within the cell. In the second phase of this study, I report that inhibition of proteasome activity by the inhibitors carbobenzoxy-L-leucyl-L-leucyl-L-leucinal (MG132) and lactacystin induced the accumulation of HSP30 and HSP70 as well as their respective mRNAs. The accumulation of HSP30 and HSP70 in A6 cells recovering from MG132 exposure was still relatively high 24 h after treatment and it decreased substantially after 48 h. Exposing A6 cells to simultaneous MG132 and mild heat shock enhanced the accumulation of HSP30 and HSP70 to a much greater extent than with each stressor alone. HSP30 localization in A6 cells was primarily in the cytoplasm as revealed by immunocytochemistry. In some A6 cells treated with higher concentrations of MG132 and lactacystin, HSP30 was also found to localize in relatively large cytoplasmic foci. In some MG132-treated cells, HSP30 staining was substantially depleted in the cytoplasmic regions surrounding these foci. The activation of HSF1 may be involved in MG132-induced *hsp* gene expression in A6 cells since KNK437 inhibited the accumulation of HSP30 and HSP70. Lastly, MG132 treatment also conferred a state of thermotolerance in A6 cells such that they were able to survive a subsequent thermal challenge. Analysis of this phenomenon is important given the fact that impaired proteasomal activity has been suggested as an explanation for some of the late-onset neurodegenerative diseases such as Parkinson's and Alzheimer's disease.

Acknowledgements

My years as a member of Club Heikkila have been great. I would like to thank, first and foremost, my supervisor Dr. John Heikkila for all of his guidance and advice during both my undergraduate and graduate education. He has really helped me become a confident and independent scientist. I would also like to thank all of the Club Heikkila members past and present: Julie Gauley, Anne Mulligan Tuttle, Laurie Manwell, Janine Voyer, Jessica Woolfson, Shantel Walcott, Ashley Rammeloo and Saad Khan. I would like to extend acknowledgement to Dale Weber for his help with confocal microscopy and also to Linda Zepf and Mila Kaufman for their administrative assistance. Additionally, I would like to express gratitude to my committee members, Drs. Brendan McConkey and Bruce Reed, for taking the time to read and evaluate my work. Last but not least, I would like to thank my girlfriend Nicole and my family and friends for having to constantly listen to my non-stop ramblings about biology.

Table of Contents

List of Figures viii

1 Introduction 1

1.1 Heat shock proteins 1

1.2 The heat shock response 2

1.3 The small heat shock proteins 3

1.4 The HSP30 family 8

1.5 The HSP70 family 10

1.6 Biological effects of arsenic exposure 13

1.7 The effect of concurrent stressors on *hsp* gene expression 14

1.8 Cellular proteolysis 15

1.9 Protein homeostasis: cooperation of molecular chaperones and the UPS 23

1.10 Diseases and biomedical implications of cellular protein homeostasis 28

1.11 *Xenopus laevis* as a model organism 29

1.12 Objectives 31

2 Materials and Methods 33

2.1 *Xenopus laevis* cell culture and embryo maintenance 33

2.2 Antisense riboprobe production 35

2.3 Northern hybridization analysis 38

2.4 *Xenopus laevis* HSP30C antibody purification 40

2.5 Western blot analysis 46

2.6 Densitometry and statistical analysis 50

2.7 Immunocytochemistry and laser scanning confocal microscopy 50

3 Results 53

3.1 The effect of concurrent sodium arsenite and mild heat shock on the expression of *hsp* genes in *Xenopus laevis* A6 cells 53

3.1.1 The effect of simultaneous sodium arsenite and mild heat shock on *hsp30* and *hsp70* gene expression in A6 cells 53

3.1.2 Involvement of HSF activation in the accumulation of HSP30 and HSP70 in A6 cells exposed concurrently to sodium arsenite and heat shock 65

3.1.3 HSP30 localization in A6 cells exposed concurrently to sodium arsenite and heat shock treatment 65

3.1.4 The effect of pre-treating A6 cells simultaneously with sodium arsenite and heat shock on the acquisition of thermotolerance 68
3.2 The effect of proteasomal inhibition on the expression of *Xenopus laevis hsp* genes..... 76
3.2.1 Examination of ubiquitinated protein accumulation in A6 cells exposed to different stressors 76
3.2.2 Analysis of the expression of *hsp30* and *hsp70* genes in A6 cells exposed to MG132 79
3.2.3 The effect of MG132 on the localization of HSP30 in A6 cells..... 84
3.2.4 Analysis of HSP30 and HSP70 accumulation in A6 cells recovering from MG132 treatment 91
3.2.5 The effect of concurrent MG132 and mild heat shock on the accumulation of HSP30 and HSP70 in A6 cells 94
3.2.6 Involvement of HSF1 activation in the accumulation of HSP30 and HSP70 in A6 cells treated with MG132 99
3.2.7 The effect of MG132 on the acquisition of thermotolerance in A6 cells 104
3.2.8 The effect of MG132 treatment on the accumulation of HSP30 and HSP70 in *Xenopus laevis* tadpoles 111
3.2.9 The effect of lactacystin on *hsp30* and *hsp70* gene expression in A6 cells 112
3.2.10 The effect of lactacystin on the localization of HSP30 in A6 cells..... 117
4 Discussion 126
References 138

List of Figures

Figure 1. Current model for the regulation of *hsp* gene transcription by HSF1 4
Figure 2. A model illustrating the degradation of a cellular protein by the UPS 17
Figure 3. Structural diagrams of two proteasome inhibitors, MG132 and lactacystin 21
Figure 4. Model of functionally distinct HSP70 chaperone complexes 26
Figure 5. Purification of the *Xenopus laevis* HSP30C recombinant protein 44
Figure 6. *Hsp30* and *hsp70* mRNA accumulation in A6 cells treated simultaneously with different concentrations of sodium arsenite and mild heat shock 54
Figure 7. HSP30 and HSP70 protein accumulation in A6 cells treated concurrently with various concentrations of sodium arsenite and mild heat shock 56
Figure 8. Analysis of HSP30 and HSP70 protein accumulation in A6 cells exposed simultaneously to various temperatures and 10 μM sodium arsenite 59
Figure 9. Time course of HSP30 and HSP70 protein accumulation in A6 cells treated concurrently with sodium arsenite and mild heat shock 61
Figure 10. HSP30 and HSP70 protein accumulation in A6 cells recovering from simultaneous treatment with sodium arsenite and mild heat shock 63
Figure 11. Effect of KNK437 on the accumulation of HSP30 and HSP70 protein in A6 cells treated with concurrent sodium arsenite and mild heat shock. 66
Figure 12. Detection of HSP30 localization in A6 cells exposed to various stressors by LSCM 69
Figure 13. HSP30 localization in A6 cells maintained at 30 ºC in combination with different concentrations of sodium arsenite 71
Figure 14. Cytoprotective effects of pre-treating A6 cells with concurrent sodium arsenite and mild heat shock prior to a 37 ºC thermal challenge 73
Figure 15. Analysis of ubiquitinated protein accumulation in A6 cells treated with heat shock, sodium arsenite, MG132 or lactacystin 77
Figure 16. The accumulation of *hsp30* and *hsp70* mRNA in A6 cells treated with different concentrations of the proteasome inhibitor, MG132 80
Figure 17. The accumulation of HSP30, HSP70 and actin protein in A6 cells exposed to different concentrations of MG132 82
Figure 18. Time course of HSP30, HSP70 and actin protein accumulation in A6 cells treated with MG132 85
Figure 19. Detection of HSP30 localization in A6 cells exposed to different MG132 concentrations by LSCM 87

Figure 20. HSP30 and HSP70 protein accumulation in A6 cells recovering from MG132 treatment 92
Figure 21. HSP30 localization in A6 cells recovering from MG132 exposure 95
Figure 22. Analysis of HSP30 and HSP70 protein accumulation in A6 cells exposed to elevated temperatures plus MG132. 97
Figure 23. Time course of HSP30 and HSP70 protein accumulation in A6 cells treated with concurrent MG132 and mild heat shock 100
Figure 24. Effect of KNK437 on the accumulation of HSP30 and HSP70 protein in A6 cells treated with MG132 102
Figure 25. Effect of KNK437 on the localization of HSP30 in A6 cells exposed to MG132 105
Figure 26. Cytoprotective effects of pre-treating A6 cells with MG132 prior to a 37 ˚C thermal challenge 108
Figure 27. HSP30 and HSP70 protein accumulation in *Xenopus laevis* tadpoles treated with MG132 113
Figure 28. The accumulation of *hsp30* and *hsp70* mRNA in A6 cells treated with different concentrations of the proteasome inhibitor, lactacystin 115
Figure 29. The accumulation of HSP30, HSP70 and actin protein in A6 cells exposed to different concentrations of lactacystin 118
Figure 30. Time course of HSP30, HSP70 and actin protein accumulation in A6 cells treated with lactacystin 120
Figure 31. HSP30 localization in A6 cells exposed to different lactacystin concentrations by LSCM 122

1 Introduction

Metazoan cells, tissues and organs are constantly challenged by conditions that cause acute or chronic stress. Consequently, adaptation and survival has orchestrated the evolution of networks of responses that identify, monitor and respond to all types of stress stimuli. At the cellular level, while all macromolecules are affected by stress, the most sensitive of these are proteins (Morimoto, 2008). Polypeptides, whose amino acid composition is determined by genes, perform almost all cellular functions including metabolism, division, differentiation and communication. The tertiary structure of proteins, which depends not only on amino acid composition but also post-translational modifications, is highly essential to their function. Stressful stimuli, both environmental and physiological, can often disrupt protein structure causing aberrant cellular processes and in some instances disease (Morimoto, 2008). Polypeptides with abnormal structure or folding are also prone to cytotoxic aggregation if left unprotected. The cell must have complex systems in place to combat these unfolded polypeptides. Two surveillance mechanisms have evolved to protect the cell: molecular chaperones and the protein degradation pathways.

1.1 Heat shock proteins

Heat shock proteins (HSPs), the largest group of molecular chaperones, were first discovered in the salivary glands of *Drosophila* by Ritossa in 1962 and have been found in all prokaryotic and eukaryotic organisms studied to date (Heikkila *et al.*, 1997b; Robert, 2003; Stromer *et al.*, 2003). HSPs are involved in many cellular metabolic processes including protein synthesis, folding/assembly, membrane translocation and degradation in normally growing cells (Morimoto, 2008). Some HSPs are expressed

constitutively, aiding in numerous cellular processes and are regulated at the level of mRNA synthesis, mRNA stability, translational efficiency or post-translational modifications (Katschinski, 2004). Under stress conditions, proteins may unfold and aggregate, causing the expression of stress-inducible HSPs. These chaperones prevent the irreversible intracellular aggregation of unfolded proteins, and then act with regulatory co-chaperones in the process of refolding and restoring a functional conformation. Although HSPs were named after their discovery in response to heat shock, they were later shown to respond to other factors including chemical exposure. As such, HSPs are often referred to generally as 'stress proteins'. HSPs are grouped and named according to their molecular weight. There are six main families of HSPs, which include the small heat shock proteins (sHSPs), the HSP40s, the HSP60s, the HSP70s, the HSP90s and the HSP105/110s (Morimoto, 2008).

1.2 The heat shock response

The heat shock response (HSR) is a rapid and transient response to stress that is mediated by HSPs (Lindquist and Craig, 1988; Parsell and Lindquist, 1993; Ehrnsperger *et al.*, 1997). *Hsp* genes are transcribed upon the activation of heat shock factor (HSF). Activation of HSF can occur as a result of environmental (anoxia, heavy metals, heat shock and ethanol) or physiological (fever, inflammation, oxidative stress, growth and development and differentiation) stresses that cause the cellular accumulation of unfolded protein. HSFI is the stress-responsive member of the HSF family and is responsible for the activation of the HSR in higher organisms (Morimoto *et al.*, 1994). The structure of HSFI is highly conserved, consisting of 100 amino acids in a helix-turn-helix DNA binding motif, as well as a transcriptional transactivation domain, a carboxy-terminal

hydrophobic region and an oligomerization domain essential for trimer formation. As outlined in figure 1, HSFI, which exists as an inactive monomer in the cytoplasm, is bound by HSP70 and HSP90. HSFI is converted to an active homotrimer in the nucleus upon stress conditions, following its release from HSP70 and HSP90 (Heikkila, 2003; Katschinski, 2004). It has been demonstrated that HSP70 and HSP90 release HSF1 to combat unfolded protein in the cell. Once active, HSFI interacts with the 5' upstream heat shock element (HSE) on the *hsp* gene, initiating transcription by RNA polymerase II (Feige *et al.*, 1996; Morimoto, 1998). Once these proteins are in circulation within the cell, they bind to unfolded or denatured proteins, maintaining them in a folding competent state until the stress is no longer a threat to survival. Following the removal of the stressor, the cell stops producing excess HSPs and their levels return to pre-stress conditions (Heikkila, 2003). At least one HSE is present within all promoters of stress-inducible *hsp* genes, mediating the response to heat shock as well as other stressors, such as agents that alter protein conformation (Mosser *et al.*, 1990; Shamovsky and Nudler, 2008). The activation of HSF1 appears to be initiated by the presence of unfolded, misfolded or damaged protein (Voellmy, 2004; Morimoto, 2008).

1.3 The small heat shock proteins

The small heat shock protein (sHSP) family is made up of HSPs whose molecular weights are between 16 and 43 kDa and include the lens protein α-crystallin (Buchner *et al.*, 1998; Heikkila, 2003; Stromer *et al.*, 2003). The sHSP family differs from other HSP families in its lack of conservation. The number, size and sequence of the family members vary widely from species to species and within a species the variation is relatively small (Arrigo and Landry, 1994; Stromer *et al.*, 2003). Plants have five families

Figure 1. Current model for the regulation of *hsp* gene transcription by HSF1. (1) Stress stimuli causes native proteins to unfold; (2) Unfolded proteins sequester the HSF1 bound-HSP70 and HSP90 chaperones to maintain them in a folding competent state, resulting in free HSF1 in the cytoplasm; (3) Free HSF1 moves to the nucleus and undergoes trimerization; (4) HSF1 homotrimers are now active and can induce *hsp* gene expression by interacting with HSEs; (5) Stress-induced HSPs are expressed and also act as chaperones to maintain unfolded protein in a folding competent state (Morimoto, 2008).

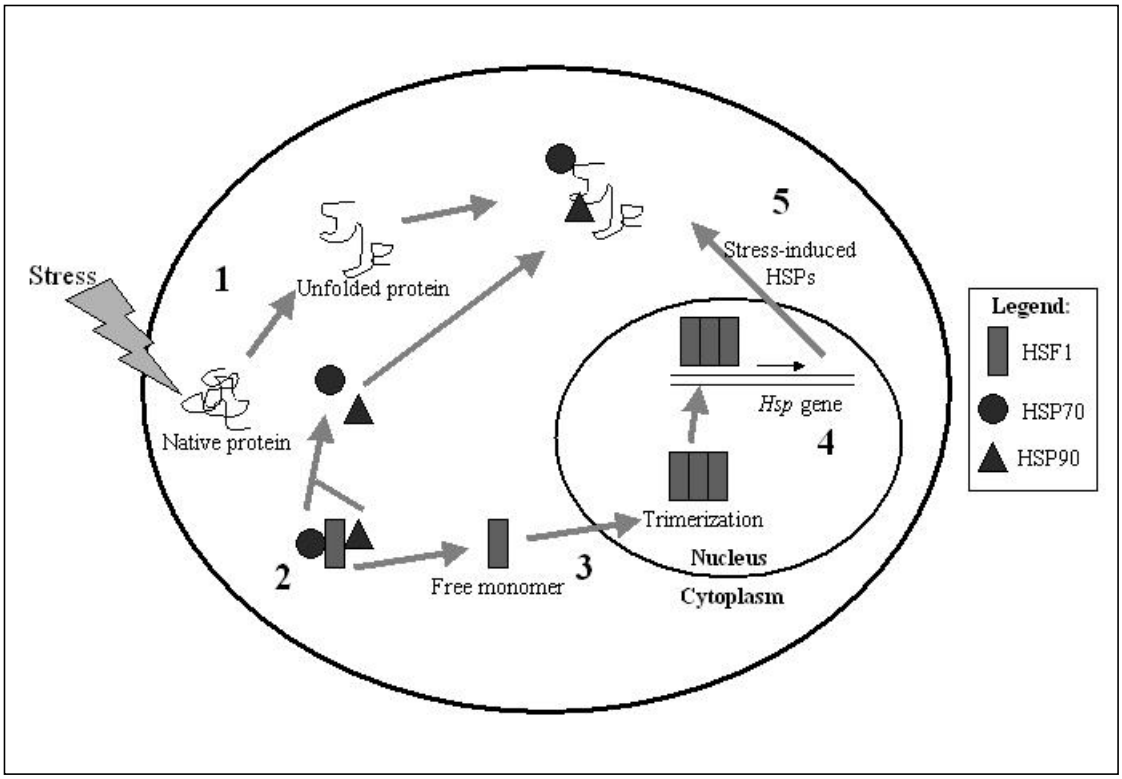
Stress
1
Unfolded protein
Native protein
2
Free monomer
3
Trimerization
Nucleus
Cytoplasm
4
Hsp gene
5
Stress-induced HSPs
Legend:
HSF1
HSP70
HSP90

of genes for these proteins (Boston *et al.*, 1996; Waters *et al.*, 1996). There are also multiple genes for sHSPs in *Escherichia coli*, *Saccharomyces cerevisiae*, *Drosophila*, *Caenorhabditis elegans*, *Xenopus*, *Artemia* and mammals (Allen *et al.*, 1992; Wotton *et al.*, 1996; Linder *et al.*, 1996; Michaud *et al.*, 1997; Liang *et al.*, 1997; Ohan *et al.*, 1998a). These genes have evolved through duplication and subsequent modification (Jong *et al.*, 1998). In *Xenopus laevis* and *Poeciliopsis lucida* (a species of fish) a HSP27 and HSP30 family exists, with members of each being more similar to each other than to other *shsp* genes (Norris *et al.*, 1997; Heikkila, 2003).

1.3.1 Structure of sHSPs

Despite the lack of conservation, most sHSPs have either two or three functional domains. These regions include the conserved α-crystallin domain, an amino-terminal domain and a carboxy-terminal extension. The α-crystallin domain is about 90 amino acids and is located towards the carboxy-terminus. This domain is highly conserved between species and consists of a β-pleated sheet conformation (Buchner *et al.*, 1998; MacRae, 2000). It plays a role in binding unfolded proteins during stress as well as potentially binding nucleotides and cytoskeletal proteins (Djabali *et al.*, 1997; Singh *et al.*, 2006). The amino-terminal domain of sHSPs is poorly conserved, with the exception of a conserved WDPF sequence, which contains two α-helices and may play a role in oligomeric formation (Lambert *et al.*, 1999; Ganea, 2001). Carboxy-terminal extensions are variable in sequence and length, but are common in polar properties between sHSPs and are essential for chaperone function (MacRae, 2000; Fernando and Heikkila, 2000). Research has found that in many organisms, with the notable exception of the nematode, the amino-terminal end has little effect on chaperone function whereas deletion of amino

acids from the carboxy-terminal end of sHSPs results in a dramatic reduction in chaperone activity (Takemoto *et al.*, 1993; Fernando and Heikkila, 2000; Abdulle *et al.*, 2002).

1.3.2 Expression and function of sHSPs

Expression of sHSPs depends on growth conditions, developmental state as well as the oncogenic status of the cell (Haslbeck, 2002). Comparing the stress-induced expression of sHSP to other HSPs, it was demonstrated that sHSPs are some of the most strongly induced HSPs (Arrigo and Landry, 1994; Haslbeck, 2002). sHSPs accumulate in different organs and tissues, and levels vary in a stage-, tissue- and stress-specific manner (Ciocca *et al.*, 1993). For example, HSP25 is most abundant in lens, heart, stomach, colon, lung and bladder in rodents (Klemenz *et al.*, 1993), whereas HSP27 is detected in muscle, nervous, connective tissue and female reproductive tract in human (Ciocca *et al.*, 1993). Developmental or tissue-specific controls in gene expression may be regulated at the level of chromatin structure or organization (Heikkila, 2003). Intracellular localization of sHSPs changes according to the physiological state of the cells and to the type and intensity of the stressor (Beaulieu *et al.,* 1989; Adhikari *et al.,* 2004; Gellalchew and Heikkila, 2005). *Drosophila* sHSPs are peculiar in their specific association to different intracellular compartments. The intracellular localization of *Drosophila* sHSPs are as follows: HSP22 in the mitochondrion (Morrow *et al.*, 2000), HSP23 and HSP26 in the cytoplasm (Michaud *et al.*, 2002) and HSP27 in the nucleus (Marin and Tanguay, 1996; Michaud *et al.*, 1997).

In order to function within the cell, sHSPs form oligomeric complexes (Freeman and Yamamoto, 2002; Azzoni *et al.*, 2004) that are between 9 and 30 subunits in size

(Ohan *et al.*, 1998b; Heikkila, 2003; Stromer *et al.*, 2003). This organization is conserved in a number of organisms including yeast, crustaceans, insects, nematodes, mammals and amphibians. As molecular chaperones, sHSPs are competent at binding with non-native substrate proteins, keeping them soluble and preventing their aggregation. Once the stress has been removed, the sHSPs are responsible for bringing their substrate protein to ATP-dependent HSPs, like HSP70, which will refold the protein into its native state (MacRae, 2000). The sHSPs are removed from the complex through phosphorylation, which alters the secondary structure and inhibits oligomerization (Fernando *et al.*, 2003).

sHSPs have been associated with cellular differentiation, the modulation of redox parameters and actin capping and decapping (Heikkila, 2003). Like other HSPs, the sHSP family has both constitutive and inducible members in many animal development systems including *Drosophila*, mouse, rat, brine shrimp and nematode (Heikkila, 2003). Many sHSPs interact with the p38 mitogen-activated protein kinase (MAPK) pathway including murine HSP25 and human HSP27 which are phosphorylated by the pathway (Stokoe *et al.*, 1992). It has also been determined that the MAPK pathway has a role in phosphorylating HSP30C in *Xenopus laevis* following both heat or chemical stress (Fernando *et al.*, 2003). In the case of HSP30C, phosphorylation inactivates it as a molecular chaperone, altering its secondary structure and inhibiting oligomerization. This causes the release of the substrate from HSP30C (Fernando *et al.*, 2003), which allows for other HSPs, including HSP70 to bind and refold it.

1.4 The HSP30 family

The HSP30s are a family of stress-inducible sHSPs that act as molecular chaperones. *Hsp30* genes have only been isolated in fish, frog and bird species. Most of

these animals have external embryo development where temperatures are not constant and the probability for thermal stress during embryogenesis is high (Katoh *et al.*, 2004). The number of *hsp30* genes within a family varies depending on the species: three members have been identified in chicken (Panasenko *et al.*, 2003), at least five members have been isolated in *Xenopus laevis* (Ohan and Heikkila, 1995; Tam and Heikkila, 1995), up to 18 isoforms have been identified in *Poeciliid* fishes (Norris *et al.*, 1995) and as many as ten have been found in *Rana catesbeiana* (Helbing *et al.*, 1996).

1.4.1 HSP30 in *Xenopus laevis* embryos and somatic cells

Four complete genes in two gene clusters have been isolated from the HSP30 family in *Xenopus laevis*, two of which give rise to functional proteins (Ohan and Heikkila, 1995; Tam and Heikkila, 1995). The first cluster includes *hsp30A* and *hsp30B*, neither of which are representative of the HSP30 gene family, as *hsp30A* contains a 21 base pair insertion in the coding region and *hsp30B* has been identified as a pseudogene (Bienz, 1984a; Bienz, 1984b). The second cluster contains *hsp30C*, *hsp30D* and a portion of *hsp30E*. All are intronless and share a conserved α-crystallin domain and *hsp30C* and *hsp30D* both encode for 24 kDa proteins (Heikkila, 2003). *Hsp30C*, the most extensively studied *hsp30* gene in *Xenopus*, contains 2 TATA boxes, 3 HSEs and a CCAAT box within its 5' promoter region while the 3' UTR is AT-rich and contains both a polyadenylation element and an mRNA instability region (Heikkila, 2003).

Experiments employing RNase protection analysis and reverse transcription-polymerase chain reaction (RT-PCR) assays were able to narrow down the developmental stage at which *Xenopus laevis hsp30A* and *hsp30C* genes were first heat-inducible to the late neurula/early tailbud stage (Ali *et al.*, 1993; Lang *et al.*, 1999). Whole mount *in situ*

hybridization and immunocytochemical analysis of heat shock-treated midtailbud embryos revealed a preferential accumulation of *hsp30* mRNA and protein in the cement gland, lens placode, somites and proctodeum (Lang *et al.*, 1999). These experiments suggested that certain embryonic tissues were more sensitive in the activation of *hsp* gene expression than others in the midtailbud embryo. In A6 kidney epithelial cells, HSP30 accumulation was induced by heat shock, sodium arsenite, herbimycin A and hydrogen peroxide treatment (Briant *et al.*, 1997; Fernando *et al.*, 2003; Muller *et al.*, 2004). The intracellular localization was determined to be primarily in the cytoplasm and perinuclear regions of A6 cells (Gellalchew and Heikkila, 2005). *Xenopus* HSP30 recombinant protein demonstrated its ability to act as a molecular chaperone by inhibiting heat-induced aggregation of client protein and maintaining them in a soluble and folding competent state (Fernando and Heikkila, 2000; Abdulle *et al.*, 2002; Fernando *et al.*, 2002).

1.5 The HSP70 family

HSP70 was suggested to be the most conserved protein in evolution, present from archaebacteria to humans (Daugaard *et al.*, 2007). The HSP70 family includes multiple highly conserved 68 to 74 kDa molecular chaperones that regulate protein folding under both normal and stressful conditions. HSP70 members are important molecular chaperones involved in the protection of denatured proteins from aggregation as well as proper folding or refolding of cellular proteins (Katschinski, 2004). This gene family has been comprehensively studied and includes several functional members, including cytoplasmic stress-inducible HSP70, cytoplasmic constitutively expressed HSC70, mitochondrial p75 and ER-resident GRP78 or BiP (Morimoto, 1998). The high identity

within and between species has facilitated the identification of *hsp70* genes from several organisms. The functional domains for HSP70 include: a conserved ATPase domain, a protease sensitive region, a peptide binding domain and a carboxy-terminal domain responsible for intracellular localization and substrate interaction (Morimoto and Milarski, 1990).

1.5.1 Expression and function of HSP70

Some HSP70 family members are expressed in a stress-dependant manner. Human cytoplasmic stress-inducible HSP70 has at least two regulatory elements in its 5' upstream promoter region that interact with HSF1 (Wu *et al.*, 1996). HSP70 is also expressed in a cell type and cell-cycle dependent manner during normal steady-state conditions (Daugaard *et al.*, 2007). Like any cell modulator, expression of HSP70 needs to be tightly regulated, since over-expression of this protein can be problematic. *Drosophila* larvae with excess accumulation of HSP70 have additional protection against immediate damage caused by heat stress but have decreased growth, development and survival to adulthood (Krebs and Feder, 1997).

HSP70 family members have been associated in processes such as protein transport, degradation of unstable and misfolded protein, folding and refolding proteins, uncoating of clathrin-coated vesicles and regulatory protein control (Daugaard *et al.*, 2007). The most well-known function of HSP70 is as a molecular chaperone, as it has been shown that it can repair thermally denatured target enzymes in combination with other co-chaperones (Freeman and Morimoto, 1996). *Hsp70* gene expression has been reported in response to stressful conditions including elevated temperature, chemical and heavy metal exposure. During periods of stress, HSP70 is synthesized and protects the

cell from aggregation of unfolded proteins and also directs the refolding of these proteins (Boorstein *et al.*, 1994). For protein folding HSP70 requires the help of co-chaperones like HIP, HOP and HSP40 (Katschinski, 2004). The BAG-1 protein has been shown to act as a nucleotide exchange factor for HSP70 in eukaryotes (Sondermann *et al.*, 2001) as it binds to the ATPase domain of HSC/HSP70 via its carboxy-terminal BAG domain and stimulates ADP release and substrate unloading from the chaperone. Therefore, BAG-1 inhibits substrate folding and has an important role in protein degradation which will be described in section 1.9.2. In addition to functioning as chaperones, HSP70 family members are important in assembly and transport of cellular proteins between intracellular compartments. Stress initiates translocation of HSC70 and HSP70 to the nucleus, which is facilitated by the presence of a nuclear localization signal (NLS) (Ali *et al.*, 1996a). HSP70 plays an inhibitory role in stress kinase pathways (Sreedhar and Csermely, 2004) and in apoptosis (Mosser *et al.*, 2000). The ability of HSP70 to prevent apoptosis has been reported by several groups (Beere, 2001; Parcellier *et al.*, 2003; Garrido *et al.*, 2006).

1.5.2 HSP70 in *Xenopus laevis* embryos and somatic cells

The regulation of cytoplasmic stress-inducible *hsp70* gene expression during early *Xenopus laevis* embryogenesis has also been well established. *Xenopus laevis hsp70* was not heat inducible until after the midblastula transition (MBT) even though HSF was detectable and heat responsive in cleavage-stage embryos (Krone and Heikkila, 1988; Ovsenek and Heikkila, 1990). Whole mount *in situ* hybridization was employed to examine the spatial pattern of *hsp70* mRNA accumulation in control and stress-treated *Xenopus laevis* embryos (Lang *et al.*, 2000). *Hsp70* mRNA was not detected

constitutively at any of the developmental stages examined. It was also determined that heat shock-induced *hsp70* mRNA accumulation was enriched in a tissue-specific manner in *Xenopus laevis* embryos. For example, in heat shocked (33 ºC) early tailbud embryos, *hsp70* mRNA accumulated primarily in the anterior head region, including the lens placode and cement gland (Lang *et al.*, 2000). In A6 cells, *hsp70* mRNA was not detected constitutively at 22 ºC but an enhanced accumulation of *hsp70* was detected at 30 ºC with peak levels at 35-37 ºC (Gauley and Heikkila, 2006). The stress-induced accumulation of *hsp70* mRNA was also observed in A6 cells treated with 50 μM sodium arsenite for 1-6 h, 200 μM cadmium chloride for 5 h and 6% ethanol for 5 h (Gauley and Heikkila, 2006).

1.6 Biological effects of arsenic exposure

Arsenic is a known human carcinogen that is most commonly encountered in drinking water but is also found in the metal and glass making industries. Arsenic exposure in humans results in increased risk for cancer, diabetes, spontaneous abortions, gangrene, atherosclerosis and ischemic heart disease (Chen *et al.*, 1996; Nickson *et al.*, 1998; Gebel, 2001; Hughes, 2002; Tseng *et al.*, 2002). Examination of cells exposed to arsenic has revealed many side effects including apoptosis, malignant cell transformation, cell cycle arrest, inhibition of cell proliferation and cytoskeletal injury (Chou 1989, Li and Chou, 1992; Liu *et al.*, 2001; Bode and Dong, 2002). While many side effects of arsenic exposure are known, the exact mechanism of toxicity to the cells is not. It has been suggested that changes to DNA repair and methylation or the induction of reactive oxygen species may be involved in this mechanism (Harris and Shi, 2003). Sodium arsenite and other arsenic compounds can induce the accumulation of HSPs in eukaryotic cells (reviewed in Del Razo *et al.*, 2001). It is likely that the accumulation of damaged

protein produced by sodium arsenite leads to the activation of HSF and the expression of *hsp* genes (Zou *et al.*, 1998; Voellmy, 2004).

1.7 The effect of concurrent stressors on *hsp* gene expression

Most of the studies that examined sodium arsenite-induced *hsp* gene expression have focused on the effect of this stressor, alone, at normal culture temperatures. However, organisms may encounter multiple stressors simultaneously in their natural habitats. In general, the study of the effect of simultaneous multiple stresses on *hsp* gene expression has been quite limited. In cultured mouse lymphocytes, short-term simultaneous treatment to elevated temperature and ethanol, which alone do not induce *hsp* gene expression, resulted in the enhanced induction of *hsp* genes (Rodenhiser *et al.*, 1986). Furthermore, low amounts of iron and aluminium exposed concurrently to human neural (HN) cells resulted in the enhanced expression of the *hsp27* gene (Alexandrov *et al.*, 2005). C6 rat glioma cells treated simultaneously with sodium arsenite and either diethyl maleate or buthionine sulfoximine, agents that lower levels of glutathione, had an enhanced expression of *hsp27* and *αβ crystallin* (Ito *et al.*, 1998). In aquatic animals, which are particularly vulnerable to multiple environmental toxicants or stresses, enhanced *hsp* gene expression was described with the following concurrent stresses: heat shock and non-ionic pollutants in freshwater sponge; wound stress and hypoxia in sea star; pesticide and viral infection in salmon and heat shock plus herbimycin A, hydrogen peroxide or cadmium chloride in *Xenopus* kidney cells (Muller *et al.*, 1995; Briant *et al.*, 1997; Muller *et al.*, 2004; Eder *et al.*, 2007; Holm *et al.*, 2008; Woolfson and Heikkila, 2009). Additional understanding of the effect of multiple stressors on *hsp* gene expression is also of importance given the substantial interest in the modulation of the heat shock

response in the potential treatment of human diseases of protein conformation (Westerheide and Morimoto, 2005).

1.8 Cellular proteolysis

Sixty years ago protein components of the body were viewed as essentially stable constitutes that were subject to only minor defects as time progressed. The discovery of the lysosome between 1953 and 1955 was a turning point in the studies of protein turnover as this organelle contains a vast array of proteases with different specificities. However, between the mid-1950s and the late 1970s, increasing evidence suggested that not all protein was degraded in the lysosome. In the early 1980s, components of the ubiquitin-proteasome system (UPS) were beginning to be discovered (Hershko *et al.*, 1980; Ciechanover *et al.*, 1980; Wilkinson *et al.*, 1980) and by 1987 a mechanism that described ubiquitin conjugation and targeted degradation in the 26S proteasome was established (Hough *et al.*, 1987). In fact, it was later determined that approximately 80-90% of celluar proteins are degraded in the proteasome (Lee and Goldberg, 1998a). Studies with lysosomal inhibitors have established that this structure normally plays only a minor role in non-specific degradation, eliminating approximately 10-20% of cellular proteins (Lee and Goldberg, 1998a).

1.8.1 The ubiquitin-proteasome system (UPS)

In eukaryotic cells, the proteasome is the site for degradation of most proteins and is necessary for viability. The proteasome constitutes up to 1% of the total protein in mammalian cells (Tanaka *et al.*, 1986). Proteasomes are present in the cytoplasm and nucleus, and some particles are found to be associated with the endoplasmic reticulum and with the cytoskeleton (Rivett *et al.*, 1992; Scherrer and Bey, 1994). It is an essential

component of the ATP-dependent proteolytic pathway, which assists the degradation of many enzymes, transcriptional regulators and other critical regulatory proteins. The proteasome is also responsible for the degradation of abnormal unfolded proteins (due to mutation, translational error and stress).

The 26S proteasome complex consists of the 20S particle and two 19S particles. The barrel-shaped 20S particle comprises four stacked rings that enclose a central chamber where proteolysis occurs (Lee and Goldberg, 1998a). The two central β-rings contain multiple proteolytic sites that function together in protein degradation. In eukaryotes, two of these sites are chymotrypsin-like, two are trypsin-like and two are caspase-like in their specificity. The outer two α-rings surround a small opening where polypeptide subunits enter. These α-rings are essential for proteasome function but have no role in proteolysis. The 19S particles contain binding sites for ubiquitinated proteins, enzymes that depolymerise the ubiquitin chain and six different ATPases that appear to unfold the substrate and assist its entry into the 20S particle (Lee and Goldberg, 1998a). It appears that some proteins can be degraded in the proteasome without being ubiquitinated via an unknown mechanism.

Within a eukaryotic cell (as illustrated in Figure 2), a protein is marked for degradation by the addition of ubiquitin molecules by three classes of enzymes: the ubiquitin-activating enzyme (E1), the ubiquitin-conjugating enzymes (E2s) and the ubiquitin ligases (E3s). First, the ubiquitin-activating enzyme (E1) adenylates the carboxy-terminus of ubiquitin and then forms a thioester bond between the ubiquitin carboxy-terminus and a catalytic E1 cysteine residue (Haas and Rose, 1982; Neutzner *et*

Figure 2. A model illustrating the degradation of a cellular protein by the UPS. Polypeptides are marked for proteasomal degradation by the addition of ubiquitin molecules. Ubiquitin moieties are recognized by the 19S particle and the protein is subsequently degraded within the 26S proteasome resulting in small peptide chains. These peptides are further degraded into amino acids, which are reused during translation or transported to the cell surface for antigen presentation by binding to major histocompatibility complex (MHC) class 1 molecules (Lee and Goldberg, 1998).

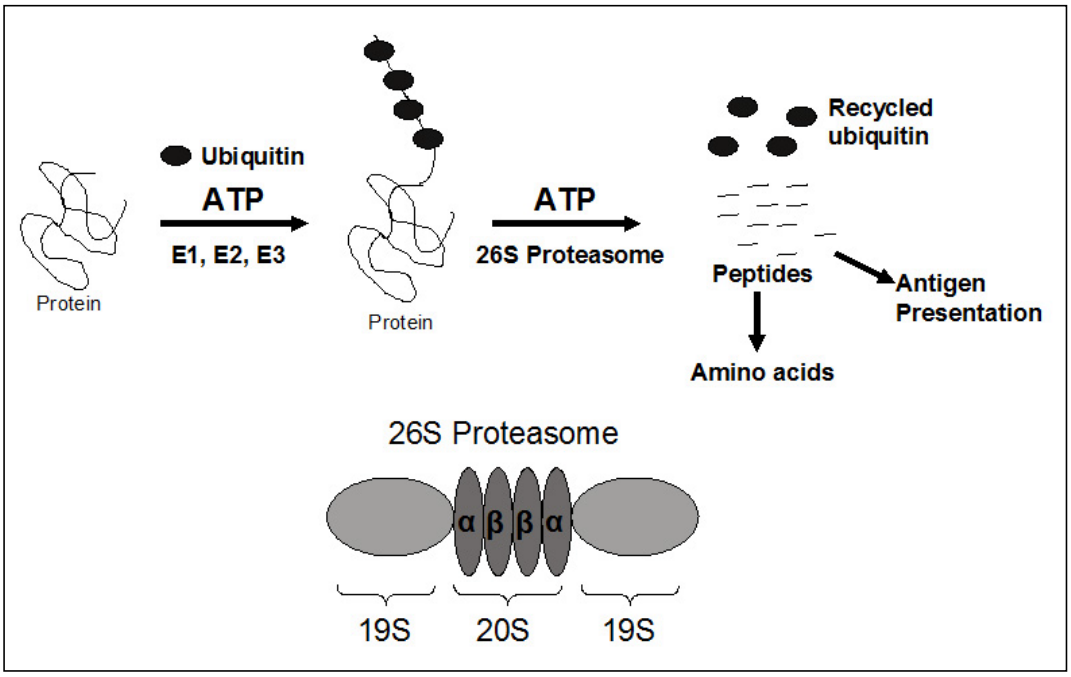
Protein
Ubiquitin
ATP
E1, E2, E3
Protein
ATP
26S Proteasome
Recycled ubiquitin
Peptides
Antigen Presentation
Amino acids
26S Proteasome
α
β
β
α
19S
20S
19S

al., 2008). To be fully functional, the E1 must non-covalently bind to and adenylate a second ubiquitin protein. Next, the thioester-linked ubiquitin is transferred from E1 onto the active-site cysteine residue of an ubiquitin-conjugating enzyme (E2), where it is again linked by a thioester bond. With the aid of a third enzyme, an E3 ubiquitin ligase, ubiquitin is transferred from the E2 to a lysine residue of a substrate protein. This transfer of ubiquitin results in an isopeptide bond between the ε-amino group of a substrate lysine and the carboxy-terminal carboxylate of ubiquitin. This mechanism continues until the substrate protein is polyubiquitinated. Furthermore, ubiquitination occurs most often on the carboxy-terminus of substrate proteins. However, in some rare cases ubiquitin chains can be added to the amino-terminus (Breitschopf *et al.*, 1998; Aviel *et al.*, 2000; Reinstein *et al.*, 2000). Ubiquitin ligases (E3s) provide the specificity to the ubiquitin pathway since they recognize and bind to specific substrate sequences or degrons . Only one type of E1 enzyme has been isolated in eukaryotes (Uba1) and there are approximately 10-30 E2s. The number of E3s is currently unknown but it is certainly much larger than the number of E2s. In most cases, the E3 ligases are the only component of the pathway subjected to regulation (Glickman and Ciechanover, 2002). The ubiquitinated substrate is then hydrolysed by the 26S proteasome via an ATP-dependent mechanism. Deubiquitination enzymes present on the 19S particle will then allow recycling of ubiquitin molecules. Most peptide products are hydrolysed into amino acids by exopeptidases, but some are also transported to the cell surface for antigen presentation by binding to major histocompatibility complex (MHC) class 1 molecules (Lee and Goldberg, 1998a).

1.8.2 Inhibitors of the proteasome

There are several low-molecular-weight inhibitors of the proteasome that have been identified. The most popular of these are the peptide aldehydes, which include carbobenzoxy-L-leucyl-L-leucyl-L-leucinal (MG132). These agents are substrate analogues and inhibitors, primarily of the chymotrypsin-like activity of the proteasome (Rock *et al.*, 1994). Numerous studies suggest that the chymotryptic site is rate-limiting in protein degradation (Rock *et al.*, 1994; Lee and Goldberg, 1998a). The inhibition of proteolysis by MG132 is readily reversed by its removal.

Peptide aldehydes also inhibit some lysosomal proteases and the calpains (Omura *et al.*, 1991). A proteasome inhibitor that does not affect these proteases is lactacystin, which has a much higher specificity for inhibiting the proteasome. Lactacystin and its derivative *clasto*-lactacystin β-lactone are natural products structurally different from the peptide aldehydes. Lactacystin was isolated originally from actinomycetes by its ability to promote neurite outgrowth from cultured neurons and to block cell division (Omura *et al.*, 1991). It was later discovered that it acts as a pseudosubstrate and binds covalently to the hydroxyl groups on the active site threonine of the proteasome's 20S β subunits (Fenteany *et al.*, 1995). Therefore, proteasomal inhibition by lactacystin is irreversible. In aqueous solution, lactacystin is converted to the β-lactone derivative, which is the active form of this proteasome inhibitor. This conversion is actually beneficial because the β-lactone derivative enters cells much more readily (Dick *et al.*, 1996). Structural depictions of both MG132 and lactacystin are shown in figure 3.

Figure 3. Structural diagrams of two proteasome inhibitors, MG132 and lactacystin. The molecular formulas for these molecules are $C_{26}H_{41}N_3O_5$ and $C_{15}H_{24}N_2O_7S$, respectively.

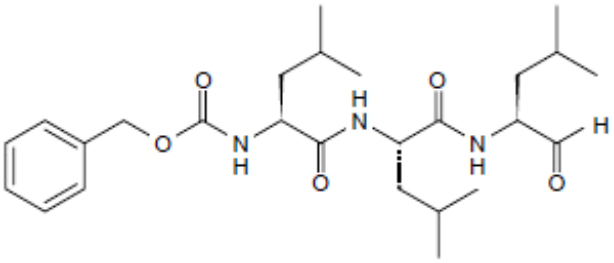

Peptide aldehyde (MG132)

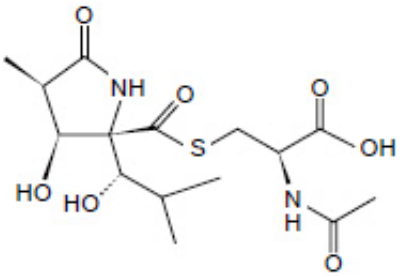

Lactacystin

1.9 Protein homeostasis: cooperation of molecular chaperones and the UPS

Homeostasis is the tendency for a system to maintain internal stability, owing to a coordinated response of its parts to any situation or stimulus that may disrupt its normal condition and function (Silverthorn, 2004). Homeostasis is often discussed in complex physiological processes but it also exists on a cellular and molecular level. Protein homeostasis refers to the regulation and coordination of cellular processes that impact protein synthesis, degradation and quality control. Recent studies have established connections between these processes. For example, a direct feedback mechanism that maintains homeostasis between protein synthesis and degradation exists. Several proteins involved in the UPS have roles in pre-ribosomal RNA processing and therefore can regulate both protein synthesis and degradation (Tabb *et al.*, 2001; Fatica *et al.*, 2003). Furthermore, molecular chaperones involved in polypeptide quality control, also have roles in proteasome assembly and function. For example, an HSP70 family member, HSC73, is required for the final maturation steps of the 20S proteasome complex (Kloetzel, 2001). Moreover, HSP90 has been shown to participate in the ATP-dependent assembly of the 26S proteasome (Imai *et al.*, 2003). As a chaperone, HSP70 has several functions within the cell which do not only involve folding of non-native proteins but also presentation of abnormal or misfolded polypeptides to the UPS for degradation.

1.9.1 CHIP: a chaperone associated ubiquitin ligase

There are several explanations for the molecular cooperation between protein degradation pathways and the molecular chaperones. The most established model is that chaperones have an active role in the degradation process by acting as substrate

recognition factors and actively transferring the bound proteins to the proteasome. Intriguingly, the characterization of a chaperone cofactor, named CHIP (carboxy-terminus of HSP70 interacting protein), provided experimental evidence for this model.

CHIP is intimately involved in the regulation of molecular chaperones, namely in the HSP70 and HSP90 families, and their cooperation with the UPS (Ballinger *et al.*, 1999). CHIP possesses an amino-terminal tetratricopeptide repeat (TPR) domain and a carboxy-terminal U-box domain. The U-box domain is structurally similar to RING-finger domains present in numerous ubiquitin ligases, which suggests a role for CHIP in ubiquitin conjugation (Cyr *et al.*, 2002). Studies have determined that CHIP utilizes its U-box domain for binding to E2 enzymes of the Ubc4/5 family and functions as an E3 ubiquitin ligase during the ubiquitination of several chaperone substrates (Murata *et al.*, 2001). Therefore, CHIP shifts the mode of action of HSP70 and HSP90 from protein folding to protein degradation.

1.9.2 Degradation versus folding: CHIP, BAG-1, HIP and HOP

The chaperone/CHIP complex may be viewed as a multi-subunit ubiquitin ligase that contains either HSP70 or HSP90 as the main substrate recognition factor. During targeting of chaperone substrates to the proteasome, CHIP may cooperate with the BAG-1 nucleotide exchange factor of HSP70. BAG-1 possesses a BAG domain which is responsible for mediating HSP70 binding and regulation (Jentsch and Pyrowolakis, 2000). Additionally, BAG-1 also has an ubiquitin-like domain which is used as a coupling factor between HSP70 and the proteasome (Luders *et al.*, 2000). The cooperation of BAG-1 and CHIP in targeting substrates to the proteasome seems to involve the ability of the two cofactors to simultaneously associate with HSP70

(Ballinger *et al.*, 1999). BAG-1 interacts with the amino-terminal ATPase domain of HSP70 and CHIP binds to the carboxy-terminus. It remains to be determined if BAG-1 is a necessary factor of the CHIP ubiquitin ligase complex as *in vitro* studies have shown CHIP-mediated degradation of some protein substrates can be carried out without BAG-1 (Xu *et al.*, 2002).

Folding or degradation of denatured proteins in the cell would involve initial recognition by molecular chaperones in order to avoid aggregation. The interaction of HSP70 with various cofactors, shown in Figure 4, determines the fate of the chaperone-bound polypeptide: interaction of HSP70 with CHIP and BAG-1 would lead to degradation of the substrate, whereas attempts to fold the bound protein would occur upon interaction with the folding cofactors, such as HIP and HOP. Interestingly, CHIP and HOP compete in HSP70 binding (Connell *et al.*, 2001), as both proteins bind the same sites at the carboxy-terminus (Scheufler *et al.*, 2000). A similar competition occurs at the amino-terminal end of HSP70 where BAG-1 and HIP attempt to bind to the chaperone (Hohfeld and Jentsch, 1997). The intracellular levels of the competing cofactors are suggested to set the threshold for protein folding versus degradation. Under normal conditions, the levels of BAG-1 and CHIP are low compared to HIP and HOP, so the cell seems to favour folding instead of degradation. However, there is very little research about how the expression of these cofactors is regulated. As you can see, there is an extensive cooperation between molecular chaperones and the UPS to ensure protein homeostasis within the cell.

Figure 4. Model of functionally distinct HSP70 chaperone complexes. The degrading complex is characterized by an interaction of BAG-1 with the amino-terminus of HSP70, while CHIP is bound to the carboxy-terminus. BAG-1 mediates an association of HSP70 with the proteasome and CHIP acts as a chaperone-associated ubiquitin ligase to target substrates for degradation in the proteasome. In the folding complex, HOP competes with CHIP in binding the carboxy-terminus of HSP70, while HIP competes with BAG-1 for the amino-terminus. When both are bound to HSP70 the chaperone complex mediates substrate folding.

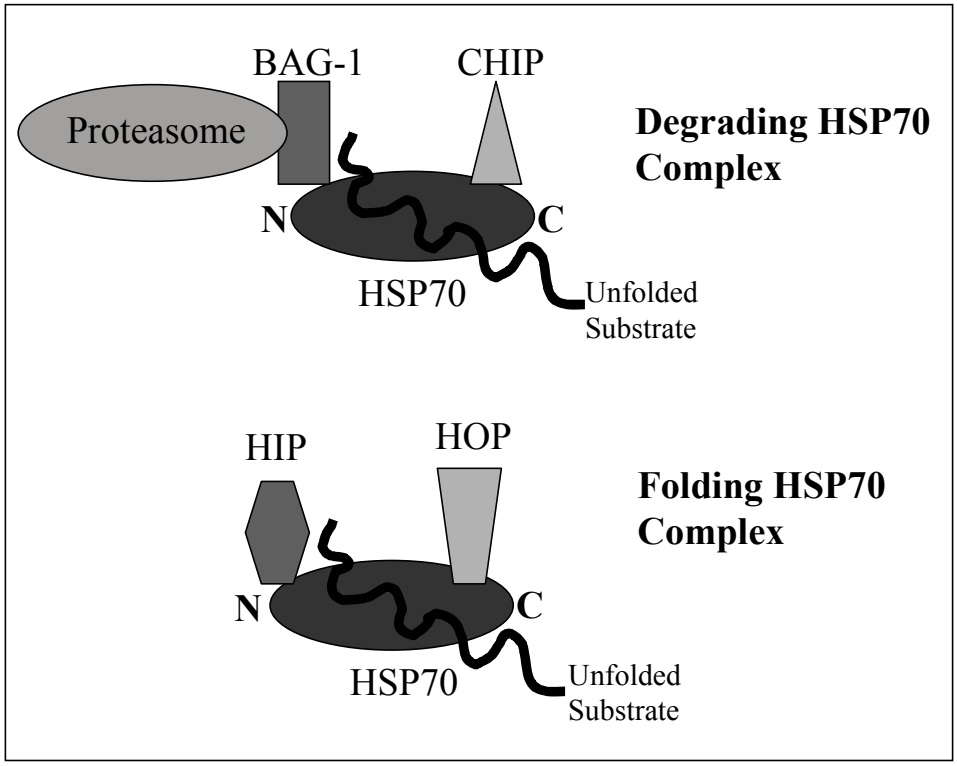
BAG-1
CHIP
Proteasome
Degrading HSP70 Complex
N
C
HSP70
Unfolded Substrate
HIP
HOP
Folding HSP70 Complex
N
C
HSP70
Unfolded Substrate

1.10 Diseases and biomedical implications of cellular protein homeostasis

Protein homeostasis within the cell involves a coordinated regulation of protein folding, re-folding, synthesis and degradation. Many diseases have been implicated in the deregulation of these processes. The synthesis or mutation of sHSPs have been associated with a variety of diseases including cancer, muscle myopathy, cataracts, multiple sclerosis, Alzheimer's disease and a number of other neuropathologies (Quinlan and van den Ijssel, 1999; Heikkila, 2003). Recent genetic evidence points to mutations in two human homologs of *Methanococcus jannaschii*, αA-crystallin and αB-crystallin, which are responsible for autosomal dominant congenital cataract and desminrelated myopathy, respectively (Quinlan and van den Ijssel, 1999; van den Ijssel *et al.*, 1999). HSP overexpression has been observed in numerous cancers and is believed to protect cancer cells from cell death (Brodsky and Chiosis, 2006). HSPs are present in great abundance in a variety of mouse and human tumours compared to normal tissues. In recent studies, inhibition of HSP70 expression in cancer cells lead to caspase-dependent apoptotic cell death and is therefore a novel therapeutic modality for cancer. HSPs have also been implicated in many cardiovascular diseases (Gupta *et al.*, 2004). Multiple investigations have demonstrated an elevation of HSPs in patients with systemic hypertension, coronary artery disease, carotid atherosclerosis, and myocardial infarction and ischemia. There are many human diseases which have been linked to chaperone and proteasome dysfunction that are pathologically defined by the abnormal deposition of misfolded polypeptides. Among these diseases are severe neurodegenerative diseases like prion pathologies, Alzheimer's and Huntington's, in which misfolded proteins aggregate in fibrillar

structures, known as amyloids (Taylor *et al.*, 2002). Another disease that involves protein folding and degradation is Parkinson's disease. The mechanism by which brain cells are lost may consist of an abnormal accumulation of the protein α-synuclein bound to ubiquitin in the damaged cells. The α-synuclein-ubiquitin complex cannot be directed and degraded in the proteasome. This protein's accumulation forms proteinaceous cytoplasmic inclusions called Lewy bodies which are cytotoxic (Masliah *et al.*, 2000).

1.11 *Xenopus laevis* as a model organism

Xenopus laevis is one of the most intensively used non-mammalian laboratory research animals. For decades, *Xenopus* has been a useful amphibian model organism for development, and its cell and molecular biology have also been extensively examined. There are 7 species within the *Xenopus* genus, and 7 subspecies of *Xenopus laevis*. The South African clawed frog is native to Southern and Western Africa. These animals are entirely aquatic, spending little if any time on land (Deuchar, 1975). *Xenopus* generally prefer stagnant pools of water and gulp air for respiration. In such an environment, prone to severe temperature changes, *Xenopus* would be exposed to a broad temperature range, rendering it an interesting organism for stress response research.

Xenopus continuous cell lines are useful tools for *in vitro* molecular analyses. Several *Xenopus* cell lines have been established and include: A6, B3.2, KR, XF, XL2, XL110, XL-177 and XTC-2 (Smith and Tata, 1991). The most popular *Xenopus* cell line used today is the A6 somatic cell line, which was used in this study. This cell line was initiated by Rafferty (1965), by a primary culture derived from normal adult male kidney cells. A6 cells appear to be mostly epithelial as they have a cuboidal or short columnar morphology. The A6 cell line is easy to maintain and has fast cell division and growth,

making it an excellent tool for cellular and molecular biology research. A6 cells have been utilized as an experimental system in many areas of research including: cellular proliferation and differentiation (Bjerregaard, 2007), physiological mechanisms of the renal epithelium (Fronius *et al.*, 2001; Guerra *et al.*, 2004) and the effects of gravitational force on cells by clinorotation and space-station experiments (Tanaka and Atomi, 2000; Ichigi and Asashima, 2000). The largest number of studies employing A6 cells have come from our laboratory, where we have examined the expression and function of amphibian HSPs. A6 cells have been used to characterize the expression of numerous *Xenopus hsp* genes including: *hsp30*, *hsp47*, *hsp70*, *hsp90*, *hsp110* and *BiP* (Darasch *et al.*, 1988; Tam and Heikkila, 1995; Ali *et al.*, 1996b; Miskovic *et al.*, 1997; Briant *et al.*, 1997; Hamilton and Heikkila, 2006; Gauley and Heikkila, 2006). A6 cells have also been utilized to study the expression of *hsp* genes in response to various stressors including: heat shock, sodium arsenite, herbimycin A, hydrogen peroxide and cadmium chloride (Darasch *et al.*, 1988; Briant *et al.*, 1997; Muller *et al.*, 2004; Gauley and Heikkila, 2006; Woolfson and Heikkila, 2009). HSP functional studies have also been carried out in A6 cells. For example, studies in A6 cells established that HSP30 assembles into high molecular weight aggregates in order to function as a molecular chaperone (Ohan *et al.*, 1998b).

Additionally, *Xenopus laevis* is a model organism for vertebrate development. The ability to stimulate egg induction hormonally, and fertilize eggs *in vitro*, provides a great deal of control to the researcher (Sive *et al.*, 2000). The large egg size yields a large amount of protein and nucleic acids for analysis, allows visual observation of developmental progression and facilitates microinjection. Although *Xenopus laevis* are

tetraploid organisms, they have served very well as model amphibian organisms in both cellular and genetic studies (Graf and Kobel, 1991). Using another species in the genus, *Xenopus tropicalis*, can be advantageous for genetic research as this organism is diploid.

1.12 Objectives

The objectives of this Master's of Science project were two-fold: (1) an investigation of the effect of simultaneous mild sodium arsenite and heat shock on the expression of *hsp30* and *hsp70* genes in *Xenopus laevis* A6 kidney epithelial cells and (2) the examination of the effect of proteasomal inhibition on the expression of *Xenopus laevis hsp* genes. The present research on the effect of simultaneous stressors on *hsp* gene expression builds on a preliminary study, which examined only a single set of stress parameters in A6 cells (Heikkila *et al.*, 1987). The findings gathered by the Heikkila *et al.* (1987) study were verified during my Biology 499 undergraduate research project. In the present study, a more comprehensive analysis of this phenomenon was performed and the objectives were:

- To determine the effect of concurrent sodium arsenite and heat shock on the accumulation of *hsp30* and *hsp70* mRNA and protein in *Xenopus laevis* A6 kidney epithelial cells
- To determine the accumulation of HSP30 and HSP70 protein in A6 cells recovering from simultaneous sodium arsenite and heat shock treatment
- To investigate whether HSF1 activation was involved in the accumulation of HSP30 and HSP70 in A6 cells exposed to combined sodium arsenite and heat shock
- To analyze the localization of HSP30 in A6 cells treated concurrently with sodium arsenite and heat shock
- Lastly, to explore whether concurrent sodium arsenite and heat shock treatment could confer an acquired state of thermotolerance in A6 cells

In the second stage of this project, proteasome inhibitors were employed to determine their effect on the expression of *Xenopus laevis hsp* genes. Most research examining the stress-induced expression of HSPs involved thermal and chemical stresses. However in the present study, inhibition of a cellular protein degradation pathway and its effect on stress-induced *hsp* gene expression was investigated. The objectives for this phase of the study included:

- To analyze the accumulation of cellular protein conjugated to ubiquitin in A6 cells treated with proteasome inhibitors
- To determine the effect of proteasomal inhibition on the expression of *hsp30* and *hsp70* genes in *Xenopus laevis* A6 cells and embryos
- To analyze the accumulation of HSP30 and HSP70 protein in A6 cells recovering from proteasomal inhibition
- To investigate the accumulation and localization of HSP30 in A6 cells exposed to proteasome inhibitors
- To determine the effect of concurrent proteasome inhibition and heat shock on the accumulation of HSP30 and HSP70 in A6 cells
- To investigate whether HSF1 activation was involved in the accumulation of HSP30 and HSP70 in A6 cells exposed to proteasome inhibitors
- To determine if proteasomal inhibition can confer a state of acquired thermotolerance in A6 cells

2 Materials and Methods

2.1 *Xenopus laevis* cell culture and embryo maintenance

Xenopus laevis A6 kidney epithelial cells were acquired from ATCC (CCL-102; American Type Culture Collection, Rockville, Maryland). The cells were cultured in Leibovitz (L)-15 media (Sigma, Oakville, Ontario) supplemented with 10% fetal bovine serum (FBS; Sigma) and 1% penicillin/streptomycin (100 U/mL and 100 µg/mL, respectively; Sigma) and were grown at 22 ºC in T75 cm^2 flasks. Upon confluency, cells were washed with 1 mL versene [0.02% (w/v) KCl, 0.8% (w/v) NaCl, 0.02% (w/v) KH_2PO_4, 0.115% (w/v) Na_2HPO_4, 0.02% (w/v) sodium ethylenediaminetetraacetic acid (Na_2EDTA)], followed by another 1 min incubation with 2 mL of fresh versene. Then 1 mL of 1X trypsin (Sigma) diluted in 100% Hank's balanced salt solution (HBSS; Sigma) was added until cells began to detach from the flask. Ten mL of fresh media was then added to the detached cells, which were divided into additional flasks. Cell treatments were performed 1 or 2 days after cell splitting to allow the cells to reach 90-100% confluence.

Collection and maintenance of *Xenopus laevis* embryos was performed as described in Sive *et al.* (2000). *Xenopus* female frogs (Boreal, St. Catharines, ON) were injected with 50 U human chorionic gonadotropin (hCG; Sigma) in sterile 0.65% NaCl (w/v) in the dorsal lymph sac with a 26 gauge needle 5 days prior to fertilization to prime for ovulation. Frogs were then injected with 1000 U hCG 9 h prior to egg collection to induce ovulation. Eggs were collected, by applying gentle pressure to the abdomen of the frogs, into 1X Modified Barth's Saline [MBS; 88 mM NaCl, 1 mM KCl, 0.7 mM $CaCl_2$, 1mM $MgSO_4$, 5mM HEPES-KOH, 2.5 mM $NaHCO_3$, pH 7.8].

Sperm for fertilization was obtained by dissecting out the testes of a male *Xenopus* frog which were then stored in 1X MBS. Fertilization was carried out manually by first removing the MBS from the eggs, and then touching each egg with a portion of the cut testes. Eggs were then immersed in 0.1X MBS and left to fertilize for 30 min on an orbital shaker. Fertilization was determined by observing cortical rotation, which results in the animal pole of the eggs oriented upward. Following fertilization, the jelly coat of the embryo was removed by 2% L-cysteine (Sigma) in 0.1X MBS (w/v), pH 8.0 for 2-5 min. Once embryos were dejelled they were immediately washed 6 times in 0.1X MBS to remove the L-cysteine. Embryos were subsequently maintained in 0.1X MBS at 22°C throughout development. Embryos were regularly monitored and if any were dead or deformed they were removed from the media.

Sodium arsenite was dissolved in distilled water to make a stock solution of 100 mM. The stock was further diluted to make a 1 mM working solution. The proteasome inhibitors MG132 (Sigma) and lactacystin (Sigma) were dissolved in dimethylsulphoxide (DMSO; Sigma) and distilled water, respectively. Stock solutions for MG132 and lactacystin were both 5 mg/mL. Stock solutions of KNK437 (N-formyl-3,4-methylenedioxy-benzylidene-γ-butyrolactam; Calbiochem, Gibbstown, New Jersey) were prepared at 5 mg/mL in DMSO. The appropriate volume of the above chemicals were added to 10 mL of (L)-15 media (for A6 cell treatments) or 10 mL of 0.1X MBS (for embryo treatments) to produce the desired concentration. Heat shock treatments at 33 ºC were for 2 h, followed by a 2 h recovery period at 22 ºC. These treatments were conducted in a water bath that was periodically monitored using a digital thermometer (Fisher Scientific, Ottawa, Ontario). Immediately following treatment, cell were

harvested by washing in 2 mL of 65% HBSS, and then removed in 1mL of 100% HBSS by scraping. The cells were pelleted at 14,000 rpm for 1 min and stored at -80°C until protein or RNA isolation.

2.2 Antisense riboprobe production

2.2.1 *Hsp30C* and *hsp70* template construction

The open reading frame of the *hsp30C* gene was previously inserted into the pRSET expression vector (Invitrogen, Carlsbad, California) by Pasan Fernando (Fernando and Heikkila, 2000). Plasmids containing the *hsp30C* insert were transformed into *Escherichia coli* DH5α cells. Individual colonies were inoculated into 15 mL centrifuge tubes and grown overnight in 5 mL of LB broth [1% (w/v) tryptone-peptone, 0.5% (w/v) yeast extract, 1% (w/v) NaCl, pH 7.5] containing 100 μg/mL ampicillin (Bioshop, Burlington, Ontario) at 37 ºC. The coding region of *hsp70* genomic DNA was previously isolated (Lang *et al.*, 2000) and inserted into the plasmid pSP72 (Promega, Napean, Ontario). Plasmids containing the *hsp70* insert were also inoculated into 15 mL centrifuge tubes and grown overnight in 5 mL of LB broth containing 100 μg/mL ampicillin (Bioshop) at 37 ºC.

2.2.2 Plasmid isolation

Bacterial cells were pelleted in a centrifuge at 5,000 rpm for 10 min at 4 ºC. Plasmid DNA was isolated by resuspending the pelleted cells in 200 μL of ice-cold solution #1 [50 mM glucose, 25 mM Tris (pH 8.0), 1 mM EDTA (pH 8.0)] and transferring the mixture into a microcentrifuge tube where the cells were lysed by mixing gently with 200 μL of solution #2 [0.2 M NaOH, 1% (w/v) sodium dodecyl sulfate (SDS)]. The tubes were kept on ice for the remainder of the plasmid isolation experiment.

Ice-cold solution #3 [3 M potassium acetate, 5 M glacial acetic acid] was added and the tubes were again mixed gently and placed on ice for 5 min. Following centrifugation at 14,000 rpm for 5 min at 4 ºC, the supernatant was transferred to a new tube. A 2 h RNase A treatment (10 µg/mL; BioShop) was performed at 37 ºC to remove RNA from the sample. This was followed by the addition of 600 µL of phenol:chloroform (1:1) and subsequent vortexing. The tube was centrifuged at 14,000 rpm for 3 min at 4 °C and the upper aqueous layer was transferred to a new tube. A 600 µL solution of isoamyl alcohol:chloroform (1:24) was added and the tube was vortexed and centrifuged again. The upper aqueous layer was again transferred to a new tube. To precipitate the nucleic acids, 600 µL of isopropanol was added. The samples were vortexed and incubated at room temperature for 2 min. They were then centrifuged at 14,000 rpm for 5 min at room temperature. The supernatant was removed and 500 µL of 70% ethanol was added to wash the pellet. The sample was centrifuged at 14,000 rpm for 2 min at 4 °C. The ethanol was removed and the wash step was repeated. The pellets were allowed to air dry and were then resuspended in 50 µL distilled water and stored at -20 °C.

2.2.3 *In vitro* transcription

The plasmid containing the *hsp30C* or *hsp70* insert as mentioned above was linearized using the *Pvu*II or *Mlu*NI restriction enzyme, respectively (Roche, Laval, Quebec). The cut plasmid was then electrophoresed on a 1% (w/v) agarose gel in 1X TAE. The *hsp30C* or *hsp70* insert was cut out using a razor blade and extracted from the gel using a DNA extraction column (Millipore Corp., Bedford, Massachusetts) which was centrifuged at 5,000 rpm for 10 min. The DNA passed through the filter in the TAE buffer. The filter was removed and the DNA was precipitated by adding 100% ice-cold

ethanol (2X volume) and 3 M sodium acetate (pH 5.2, 1/10 of volume). The tube was placed at -80 ºC for 30 min and then centrifuged at 14,000 rpm for 10 min at 4 ºC. The supernatant was discarded and the pellet was washed in 1 mL of 70% ice-cold ethanol and centrifuged at the settings mentioned above. The ethanol was removed and the ethanol wash step was repeated. The pellet was air dried and resuspended in 20 µL of sterile water and kept at -20 °C.

In vitro transcription was used to generate digoxygenin (DIG)-labelled riboprobes. Each *in vitro* transcription reaction contained 4 µL of linearized DNA template, 4 µL of rNTP mix [2.5 mM rGTP, 2.5 mM rATP, 2.5mM rCTP, 1.625 mM rUTP (Promega, Nepean, Ontario), 0.875 mM DIG-11-UTP (Roche), 1.5 µL diethylpyrocarbonate (DEPC)-treated water, 4 µL of 100 mM dithiothreitol to a final concentration of 20 mM (Promega), 4 µL of 5X transcription buffer to a final concentration of 1X (Fermentas, Burlington, Ontario), 0.5 µl RNase inhibitor (Fermentas) and 40 IU of SP6 RNA polymerase (Roche)]. The *in vitro* transcription reaction was performed for 1 h at 37°C. To remove any remaining DNA template, 2 µL of RNase-free DNase 1 (Roche) was added for 10 min at 37 ºC. *In vitro* transcripts were then precipitated with the addition of 10 µL of 3 M sodium acetate (pH 5.2), 80 µL of TES [10 mM Tris-HCl (pH 7.4), 5 mM EDTA (pH 8.0), 1% (w/v) SDS] and 220 µL of ice-cold 100% filtered ethanol. The reaction was incubated at -80 ºC for 30 min and then centrifuged at 14,000 rpm for 15 min at 4 ºC. The supernatant was removed and the pellet was air dried and resuspended in 21 µL of DEPC-treated water. One µL was electrophoresed to verify the presence of the *in vitro* transcript. The remaining 20 µL was stored at -80 ºC until Northern hybridization analysis.

2.3 Northern hybridization analysis

2.3.1 RNA isolation

RNA was isolated from A6 cells using the QIAgen RNeasy Mini Kit (QIAgen, Mississauga, Ontario) as described in the RNeasy Mini Handbook (2009) animal cell protocol. Isolated RNA was suspended in DEPC-treated water and quantified using the NanoDrop ND-1000 (NanaDrop, Waltham, Massachusetts) spectrophotometer at a wavelength of 260 nm. RNA integrity was analysed by running 2 µg of each RNA sample on a 1.2% (w/v) formaldehyde agarose gel [1.2% (w/v) agarose, 10% (v/v) 10X MOPS, 16% (v/v) formaldehyde]. Prior to loading, 10 µL of loading buffer [1 µL 10X MOPS, 1.6 µL formaldehyde, 2 µL RNA loading dye (0.2% bromophenol blue, 1 mM EDTA (pH 8.0), 50% (v/v) glycerol), 5 µL formamide, 0.5 µg/mL ethidium bromide] was added to each sample. Samples were then heat denatured for 10 min at 68 ºC, cooled on ice for 5 min, and then loaded onto the gel and run for 1 h at 90 V. Distinct 18S and 28S rRNA banding indicated intact RNA.

2.3.2 Northern hybridization analysis

For Northern hybridization analysis, an antisense riboprobe for *Xenopus hsp30* and *hsp70* (produced above) was used. Ten µg of total isolated RNA was electrophoresed in a 1.2% formaldehyde agarose gel as described previously. The loading buffer contained all components except ethidium bromide and the gel was electrophoresed for 3 h at 65V. Following electrophoresis, the RNA in the gel was denatured by soaking the gel in 0.05 N NaOH for 20 min. Then the gel was rinsed in DEPC-treated water and soaked twice for 20 min each in fresh 20X SSC buffer [3 M sodium chloride, 300 mM sodium citrate]. The RNA was then transferred overnight to a positively charged nylon membrane

(Roche; 11417240001) by capillary action. A piece of 3MM Whatman filter paper, which served as a wick, was pre-soaked in 20X SSC and placed on a plexiglass support over a Pyrex dish containing approximately 500 mL of 20X SSC. The inverted gel was placed onto the wick, followed by a piece of nylon membrane slightly larger in dimensions than the gel. This was then covered by two pieces of 3MM Whatman filter paper cut to the same size as the gel. Paper towels (same size as gel) were then stacked about 6-7 cm high on top of the blotting paper. A plexiglass support and a weight of approximately 250 g were placed on top of the apparatus to aid transfer. The following morning, the apparatus was disassembled and lanes were marked on the membrane using a lead pencil. RNA on the membrane was UV-crosslinked twice using a UVC-515 Ultraviolet Multilinker. The quality of the transfer was checked using 1X reversible blot stain (Sigma). The stained blot was photographed and then incubated in 50 mL of pre-heated prehybridization buffer [50% (v/v) formamide, 5X SSC, 0.02% (w/v) SDS, 0.01% (w/v) N-lauryl sarcosine, 2% (w/v) blocking reagent] in a hybridization bag at 68 ºC for 4 h in a Shake N' Bake Hybridization Oven. After prehybridization, the buffer was replaced with hybridization buffer (same components as prehybridization buffer) containing 20 µL of either *hsp30* or *hsp70* DIG-labelled antisense riboprobe (produced in section 2.2) and the membrane was returned to the hybridization oven overnight. The following morning, the membrane was then washed to remove any unbound probe. It was first washed twice in 2X SSC at room temperature, then once each in 0.5X SSC and 0.1X SSC, both at 68ºC for 15 min. Each of these three SSC washing solutions contained 0.1% (w/v) SDS. The blot was then equilibrated for 1 min at room temperature in washing buffer [100 mM maleic acid buffer, 0.3% (v/v) Tween-20] and blocked using blocking solution [2% (w/v) blocking

reagent, 10% (v/v) maleic acid buffer] for 1 h at room temperature. The blot was then incubated in blocking solution containing 1:8000 alkaline phosphatase conjugated anti-DIG-Fab fragments for 30 min. The membrane was then washed twice in washing buffer for 10 min each and then equilibrated in detection buffer [0.1 M Tris-HCl (pH 9.5), 0.1 M NaCl] for 2 min prior to detection using CDP-star, a chemiluminescent reagent, which was applied to the membrane and allowed to develop in a hybridization bag for 10 min. The membrane was then visualized on a DNR Chemiluminescent Imager (DNR Bioimaging Systems, Kirkland, Quebec) for up to 12 min depending on the strength of the signal.

2.4 *Xenopus laevis* HSP30C antibody purification

2.4.1 Expression of HSP30C recombinant protein

As previously mentioned, the open reading frame of the *hsp30C* gene was inserted into the pRSET expression vector (Invitrogen) by Pasan Fernando and transformed into *E. coli* DH5α cells. Although DH5α cells are good hosts for storing plasmids, they are not optimal for producing recombinant protein (Kroll et al, 1993). The pRSETB plasmid was therefore isolated from the DH5α cells and transformed into *E. coli* BL21 (DE3) cells. BL21 cells are much more efficient in producing recombinant protein.

Transformed DH5α cells were grown from a glycerol stock and pRSETB plasmids were isolated as in section 2.2.2. The pRSET plasmids were then digested as described in section 2.2.3 and then both cut and uncut plasmids were electrophoresed in a 1% agarose gel to determine that the plasmid insert was the correct size.

BL21 cells, from a glycerol stock previously used in our laboratory, were grown overnight on LB plates [1% bacto-tryptone, 0.5% yeast extract, 1% NaCl, 1.5% agar, pH

7.0]. A single colony was used to inoculate 5 mL of ZB media [1% N-Z-Amine A, 0.5% NaCl] and was left to grow overnight at 37 ºC. $CaCl_2$ was used to transform BL21 cells with the pRSETB plasmid containing the *hsp30C* insert. Transformed cells were grown overnight on ZB plates containing 100 μg/mL ampicillin. As the pRSETB plasmid contains an ampicillin resistance gene, this ensured that only cells containing the plasmid would grow. A single colony of transformed BL21 cells were grown overnight in a 10 mL culture of ZB plus ampicillin (100 μg/mL). Ten mL of overnight culture was added to 500 mL of M9ZB plus ampicillin [1% N-Z-Amine A, 0.5% NaCl, 0.1% NH_4Cl, 0.3% KH_2PO_4, 0.6% Na_2HPO_4, 0.4% glucose, 1mM $MgSO_4$, 50 μg/mL ampicillin]. Isopropyl-β-D-thiogalactopyranoside (IPTG) was added to a final concentration of 1.0 mM to induce the production of recombinant protein. After cells grew for 4-5 h, they were homogenized in guanidium lysis buffer (6.0 M guanidine hydrochloride, 20 mM Na_2HPO_4, 500 mM NaCl, pH 7.8) and sonicated using a Fisher Scientific Sonic Dismembrator 100 (Fisher Scientific) for 15 bursts (60% duty cycle and 4.5 output), then centrifuged at 5,000 rpm in a Sorval RC 5B Plus centrifuge using the SS-34 rotor for 30 min at 4 ºC to pellet the cellular debris. The lysate (supernatant) was removed and stored at -20ºC until purification.

2.4.2 Purification of HSP30C recombinant protein

HSP30C recombinant protein was purified using a Poly Prep chromatography column (BioRad) using ProBond resin (Invitrogen) containing nickel under denaturing conditions. Three mL of resin was added to the column and centrifuged at 1,000 rpm for 2 min. The overlaying storage buffer was removed and the column was washed twice with 5 mL of distilled water and then twice with 8 mL of denaturing buffer [8.0 M urea,

20 mM $NaPO_4$, 0.5 M NaCl, pH 7.8]. Five mL of bacterial lysate, pH adjusted to 7.8, was added to the column and bound for 45 min at room temperature on an orbital nutator and then centrifuged at 2,000 rpm to separate unbound lysate, which was then removed. This process was repeated several times with additional bacterial lysate. The washing process consisted of agitation on the orbital nutator for 2 min, centrifugation at 2,000 rpm for 3 min and the removal of the supernatant. The following buffers were adjusted to the proper pH immediately before addition to the column. The column was washed three times with 5 mL denaturing buffer at pH 6, five times at pH 5.3 and three times at pH 5. The protein was then eluted off the column in 5 mL denaturing buffer at pH 4 in 1 mL fractions. The resin was packed by centrifugation at 2,000 rpm for 30 s and an additional 5 mL denaturing buffer at pH 4 was added to the column. The protein was again eluted in 1 mL aliquots. Twenty µL was removed from each of the aliquots and analyzed by sodium dodecyl sulphate-polyacrylamide gel electrophoresis (SDS-PAGE; as outlined in section 2.5.4) to determine which aliquots contained the recombinant protein. The aliquots containing recombinant protein were then dialyzed to remove the urea. The dialysis tubing was prepared by soaking in 500 mL distilled water for 15 min and then in 10 mM sodium bicarbonate at 80 ºC for 30 min. The tubing was transferred to 500 mL of 100 mM EDTA for 30 min and then to 500 mL of distilled water at 80 ºC for 30 min. Finally the tubing was washed inside and out with distilled water and soaked in TEN buffer [50 mM Tris, 25 mM NaCl, 0.2 mM EDTA, pH 8.0] for 15 min. The eluted protein was poured inside the tubing and clamped at both ends. The tubing was placed in a beaker containing 100 to 1,000 times the amount of eluted protein and stirred gently at 4 ºC for 3 h. The tubing was then transferred to a beaker containing fresh TEN buffer and

stirred gently overnight at 4 ºC. The protein was concentrated using a MicroSep 3K Concentrator Column (Pall Filtration Corp.) by centrifugation at 5000 rpm at 4 ºC until the sample was concentrated to the desired volume. The protein was quantified with a BCA assay as described in section 2.5.3 and was stored at –20 ºC. Twenty µL of purified recombinant protein was electrophoresed by SDS-PAGE along with 20 µL samples of uninduced bacterial lysate and unpurified recombinant protein and was visualized using Coomassie Brilliant Blue R-250 staining (Figure 5).

2.4.3 Polyclonal antibody purification

The rabbit anti-HSP30 serum had been previously prepared in our laboratory by Anne Mulligan Tuttle. HSP30 recombinant protein was diluted to 1.0 µg/µL in sterile 0.85% saline solution followed by the addition of an equal volume of Freund's Complete Adjuvant (Sigma) and injected into the rabbit using an 18-gauge needle. Three additional protein injections were given at 3-week intervals with the Freund's Incomplete Adjuvant (Sigma) being substituted for Freund's Complete Adjuvant. At the end of the twelve week period, the rabbit was euthanized. The serum was separated from the rest of the blood and was stored at -20 ºC. In order to separate the anti-HSP30 antibody from the crude rabbit serum, ProBond resin was added to a PolyPrep Chromatography Column and centrifuged. Unless otherwise mentioned, all wash steps were performed on an orbital nutator and followed by centrifugation at 1,000 rpm for 2 min and followed by the removal of the supernatant. Five mL of distilled water was used to wash the column 3 times. The column was then washed in 8 mL of equilibration buffer [50 mM Tris, 2 mM NaCl, pH 7.4] 3 times. Five mL of recombinant protein was diluted to a final volume of 8 mL in equilibration buffer. The column was agitated for 1 h on an orbital nutator at 4 ºC.

Figure 5. Purification of the *Xenopus laevis* HSP30C recombinant protein. *Xenopus laevis* HSP30C was overexpressed in BL21 cells by induction with IPTG. The histidine tagged recombinant HSP30C was purified by means of nickel affinity column chromatography. The recombinant protein was then purified as described in Section 2.4.2 and analysed by SDS-PAGE and visualized by Coomassie Brilliant Blue R-250 staining. Lane 1, molecular weight markers shown in kDa; lane 2, uninduced bacterial lysate; lane 3, induced bacterial lysate; lane 4, purified recombinant HSP30C protein (indicated by the arrow).

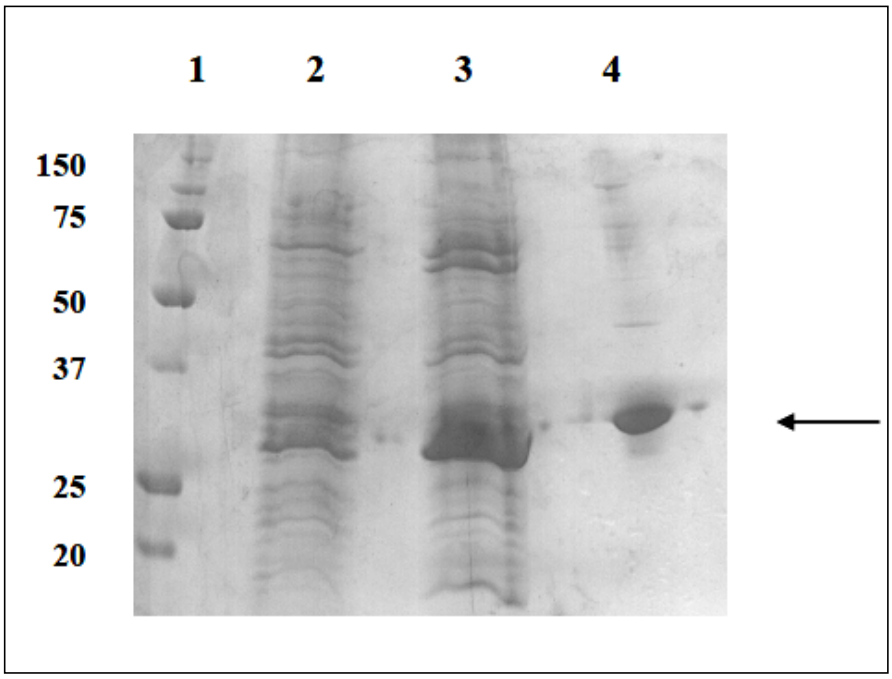
1
2
3
4
150
75
50
37
25
20

Eight mL of Tris-Buffered Saline with Tween-20 [TBS-T; 25 mM Tris, 150 mM NaCl, 2.5 mM KCl, 0.1% (v/v) Tween-20 (Sigma)] was added to wash the column. The rabbit anti-HSP30 serum was diluted 1:4 in TBS-T and bound to the column overnight at 4 ºC and then washed in 5 mL of TBS-T 3 times. The column was washed 5 times with 5 mL of equilibration buffer, and then 5 times in 5 mL of wash buffer [50 mM Tris, 150 mM NaCl, pH 7.4]. The antibody was eluted from the column with the addition of 2 mL of 4 M $MgCl_2$ for 15 min at 4 ºC. The supernatant was allowed to drain out the column and collected. Another 2 mL of $MgCl_2$ was added and the flow through was collected again. The flow through was combined and the antibody was dialyzed and concentrated as described in section 2.4.2. The antibody was then stored at -20 ºC.

2.5 Western blot analysis

2.5.1 Protein isolation from A6 cells

The pellet of harvested A6 cells was thawed on ice and then 500 µl of lysis buffer was added to the microcentrifuge tube. Lysis buffer contained 1% SDS and homogenization buffer [200 mM sucrose, 2 mM EGTA, 1 mM EDTA, 40 mM NaCl, 30 mM HEPES]. This buffer also contained 1X complete protease inhibitor cocktail (Roche). It should be noted here that the lysis buffer used for samples in preparation for western blotting with mouse anti-ubiquitin antibody contained 10 mM N-ethylmaleimide (Sigma) to inhibit ubiquitin conjugating enzymes. The cells were homogenized in the lysis buffer by sonication (output 4.5, 60% duty cycle) for 15 bursts using a Fisher Scientific Sonic Dismembrator 100 (Fisher Scientific). The homogenate was centrifuged at 14,000 rpm for 30 min at 4 ºC. The supernatant was then transferred to a new tube which was stored at -20 ºC until use.

2.5.2 Protein isolation from *Xenopus laevis* embryos

After treatment, *Xenopus* embryos were rapidly frozen in liquid nitrogen and stored at –80 ˚C. For protein isolation, embryos were thawed on ice and then suspended in 200 µL of embryo solublization buffer [ESB; 100 mM NaCl, 50 mM Tris-HCl, pH 7.5, 1% (v/v) NP-40, 1X complete protease inhibitor cocktail (Roche)] for 5 min. The embryos were then homogenized using a 20G needle and a 1 mL syringe and then subsequently centrifuged at 14,000 rpm for 20 min at 4 ˚C. The supernatant, located between the settled debris and the upper fatty layer, was transferred to a new microcentrifuge tube. Centrifugation and supernatant transfer was then repeated and followed by storage at –20 ˚C until use in Western blot analysis.

2.5.3 Protein quantification

Protein was quantified using a bicinchoninic acid (BCA) Protein Assay Kit (Pierce, Rockford, Illinois). A bovine serum albumin (BSA; Bioshop) protein standard was created by diluting BSA in distilled water at concentrations ranging from 0 to 2 mg/mL. Protein samples were diluted to a concentration of 1:2 in distilled water. Ten µL of BSA standards and protein samples were transferred in triplicate into a 96 well polystyrene plate. Then 80 µL of BCA reagent A and B (Pierce) at a ratio 50:1 were added to the BSA and protein samples. The plate was tapped lightly on the side to mix and then incubated at 37°C for 30 min. The plate was then read at 562 nm using a Versamax Tunable microplate reader (Molecular Devices, Sunnyvale, California). A standard curve was created using the concentrations of the BSA protein standards which was used to determine the concentration of the protein samples.

2.5.4 Western blot analysis

Immunoblot analysis was performed using 20, 40 or 60 μg of protein (depending on the primary antibody used) and SDS-PAGE. For SDS-PAGE, gels were electrophoresed on a BioRad TETRA cell electrophoresis system (BioRad; Mississauga, Ontario). Separating gels [10-12% (v/v) acrylamide, 0.32% (v/v) n'n'-bis methylene acrylamide, 0.375 M Tris (pH 8.8), 1% (w/v) SDS, 0.2% (w/v) ammonium persulfate (APS), 0.14% (v/v) tetramethylethylenediamine (TEMED)] were prepared, poured and allowed to polymerize for 25 min with 100% ethanol layered on top. Ethanol was poured off and the stacking gel [4% (v/v) acrylamide, 0.11% (v/v) n'n'-bis methylene acrylamide, 0.125 M Tris (pH 6.8), 1% (w/v) SDS, 0.4% (w/v) APS, 0.21 % (v/v) TEMED] was prepared, poured and allowed to polymerize for 25 min. A6 cell protein samples were aliquoted in loading buffer [0.0625M Tris (pH 6.8), 10% (v/v) glycerol, 2% (w/v) SDS, 5% (v/v) β-mercaptoethanol, 0.0125% (w/v) bromophenol blue] was added, to a final concentration of 1X. Embryo protein samples were prepared in 2X Laemmli buffer [0.125 M Tris-HCl, 4% (w/v) SDS, 20% (w/v) glycerol, 10% (v/v) 2-mercaptoethanol, 0.004% (w/v) bromophenol blue]. Samples were denatured via boiling for 10 min, cooled on ice for 5 min and pulse-centrifuged prior to loading. Gels were electrophoresed with 1X running buffer [25mM Tris, 0.2M glycine, 1 mM SDS] at 90 V until samples reached the separating gel, at which time the voltage was turned up to 160 V until the dye front reached the bottom of the gel. Pure nitrocellulose transfer blot membranes (BioRad) and filter paper (BioRad) were cut to 5.5 cm x 8.5 cm, and membranes were incubated for 30 min in transfer buffer [25 mM Tris, 192 mM glycine, 20% (v/v) methanol]. After electrophoresis, the stacking gel was cut away and the

remainder of the gel was soaked in transfer buffer for 15 min. Protein was transferred to the nitrocellulose membrane with a Trans-Blot Semi-Dry Transfer Cell (BioRad) at 25 volts for 20 min. Blots were then stained with Ponceau S stain [0.19% (w/v) Ponceau S, 5% (v/v) acetic acid] for 10 min to determine the success of the transfer and equal loading. The membrane was destained with MilliQ water and then photographed. The membrane was incubated in 5% blocking solution [20 mM Tris (pH 7.5), 0.1% Tween 20 (Sigma), 300 mM NaCl, 5% (w/v) Nestle® Carnation skim milk powder] for 1 h to prevent non-specific binding. The membrane was then incubated for 1 h in blocking solution containing the primary polyclonal antibody. A list of primary antibodies with their respective dilutions is outlined in table 1. Excess unbound antibody was removed by rinsing the membrane (2 x 10 seconds) with 1X TBS-T [20 mM Tris, 300 mM NaCl, (pH 7.5), 0.1% (v/v) Tween 20 (Sigma)]. The membrane was washed with fresh TBS-T for 15 min, followed by two 10 min washes. The membrane was then incubated for 1 h with blocking solution containing the secondary antibody (AP-conjugated goat-anti-rabbit or mouse (BioRad)). The secondary antibody dilution was dependent on the primary antibody employed, which is also outlined in table 1. The membrane was then washed with TBS-T for 15 min, followed by two 5 min washes. The membrane was incubated in alkaline phosphatase detection buffer [alkaline phosphatase buffer (100 mM Tris base, 100 mM NaCl, 50 mM $MgCl_2$ (pH 9.5)), 0.3% 4-nitro blue tetrazolium (NBT; Roche), 0.17% 5-bromo-4-chloro-3-indolyl30 phosphate, toluidine salt (BCIP; Roche)] until the bands were visible. The blots were then photographed.

Table 1: dilution specifications for antibodies used in Western blot analysis

Primary antibody	Dilution	Secondary antibody; dilution	Comments
Rabbit anti-*Xenopus* HSP30	1:1000	Goat anti-rabbit IgG AP-conjugate; 1:2000	Prepared by Heikkila lab
Rabbit anti-*Xenopus* HSP70	1:200	Goat anti-rabbit IgG AP-conjugate; 1:3000	Prepared by Abgent (San Diego, CA)
Rabbit anti-actin (Sigma)	1:200	Goat anti-rabbit IgG AP-conjugate; 1:3000	
Mouse anti-ubiquitin (Zymed, San Francisco, CA)	1:150	Goat anti-mouse IgG AP-conjugate; 1:1000	Lysis buffer prepared with 10 mM N-ethylmaleimide

2.6 Densitometry and statistical analysis

Densitometry was performed using ImageJ (1.38) software on all blots examining the effect of combined stressors as described previously (Voyer and Heikkila, 2008; Woolfson and Heikkila, 2009). Briefly, experiments were repeated in triplicate, and the average densitometric values for each sample were expressed as a percentage of the maximum hybridization band. The data were graphed with standard deviation represented as vertical error bars. Two-tailed, unpaired T-tests were performed with this data to determine if statistically significant differences existed between samples. Confidence levels used were 95% ($p < 0.05$; *) and 99% ($p < 0.01$; Δ).

2.7 Immunocytochemistry and laser scanning confocal microscopy

Cells were prepared for imaging by laser scanning confocal microscopy (LSCM) on glass coverslips in sterile Petri dishes. In order to clean the glass coverslips, they were placed in small Coplin jars to ensure full contact with the base solution [49.5% (v/v)

ethanol, 0.22M NaOH] for 30 min with periodic shaking at room temperature. The coverslips were then rinsed under running distilled water for 3 h and dried on Whatman paper. Finally, the coverslips were in stored in Petri dishes and then flamed in the laminar flow hood prior to use. To prepare A6 cells for an experiment, coverslips were placed in new sterile Petri dishes and the cell suspension was added to the dish. The cells were then allowed to attach to the coverslips for 12-24 h at 22 °C. For chemical treatments, A6 cells were treated directly in the Petri dishes at 22 °C. In heat shock experiments, the Petri dishes were wrapped with Parafilm and sealed in a plastic bag before being placed in a heated water bath. After treatment, the (L)-15 media was removed and the cells were washed twice in phosphate-buffered saline [PBS; 1.37 M NaCl, 67 mM Na_2HPO_4, 26 mM KCl, 14.7 mM KH_2PO_4, 1 mM $CaCl_2$, 0.5 mM $MgCl_2$, pH 7.4] and the coverslips were transferred to new small Petri dishes (1 coverslip per dish). The cells were fixed with 3.7% (w/v) paraformaldehyde (pH 7.4 in PBS) for 15 min and then washed 3 times in PBS for 5 min. Next, the cells were permeabilized using 0.3% Triton X-100 (Sigma) in PBS for 10 min and then washed 3 times in PBS for 5 min. Finally, the cells were blocked with 3.7% (w/v) bovine serum albumin fraction V (BSA; Sigma) in PBS for 1 h or overnight at 4 ºC. The BSA fraction V was filter-sterilized using a 0.45 μm filter (Pall Filtration Corp.) to remove debris that might negatively affect the imaging. The next day the cells were incubated in primary antibody (rabbit anti-*Xenopus* HSP30 at 1:500 in blocking solution) for 1 h. After three, 5 min washes in PBS, the cells were indirectly labelled by incubation in a fluorescent-conjugated secondary antibody (goat-anti rabbit Alexa Fluor 488 (Molecular Probes, Eugene, OR) at 1:2,000 in blocking solution) for 30 min, in the dark, to avoid photo-bleaching of the fluorescent signal. The cells were then

probed for actin with rhodamine-tetramethylrhodamine-5-isothiocyanate phalloiden (TRITC; Molecular Probes) at 1:60 in PBS for 15 min, in the dark. The cells were then washed three times for 5 min in PBS. The coverslips were mounted (cell side down) in one drop of VectaShield containing 4,6-diamidino-2-phenylindole (DAPI; Vector Laboratories Inc, Burlingame, CA) on a glass slide and sealed with clear nail polish. Once dried, the slides were visualized with a Zeiss Axiovert 200 microscope and LSM 510 META software (Carl Zeiss Canada Ltd., Mississauga, ON). The 63X oil immersion objective was utilized along with the 405 nm (for DAPI), 488 nm (for Alexa-488) and 533 nm (for TRITC) scanning lasers. Pinhole settings were set to 1.0 airy unit. Microscope configurations were kept identical for all imaging experiments.

3 Results

3.1 The effect of concurrent sodium arsenite and mild heat shock treatment on the expression of *hsp* genes in *Xenopus laevis* A6 cells

3.1.1 The effect of simultaneous sodium arsenite and mild heat shock on *hsp30* and *hsp70* gene expression in A6 cells

In the present study, I characterized the accumulation of *hsp30* and *hsp70* mRNA in A6 cells exposed to different concentrations of sodium arsenite (NA) plus mild heat shock (Fig. 6A). Cells were treated with sodium arsenite (1 to 10 μM) and heat shock (30 ºC) either singly or in combination for 1.5 h. A6 cells exposed to either mild heat shock or the low sodium arsenite concentrations alone did not exhibit a detectable accumulation of *hsp30* or *hsp70* mRNA. However, when cells were treated simultaneously with both stressors there was an increase in *hsp30* and *hsp70* transcript accumulation as the concentration of sodium arsenite was increased from 1 to 10 μM. For example, densitometric analysis determined that in cells exposed to 7.5 μM sodium arsenite plus mild heat shock, there was an 11.8- and a 7.2-fold increase in the accumulation of *hsp30* and *hsp70* mRNA, respectively, compared to cells treated with 5 μM sodium arsenite plus heat stress (Fig. 6B). Additionally, at 30 ºC *hsp30* mRNA levels were maximal at 7.5 to 10 μM sodium arsenite whereas *hsp70* mRNA levels were highest at 10 μM sodium arsenite.

The accumulation of HSP30 and HSP70 protein in response to simultaneous exposure of A6 cells to mild heat shock plus sodium arsenite was examined by western blot analysis (Fig. 7A). A6 cells were treated for 3 h followed by a 2 h recovery period at

Figure 6. *Hsp30* and *hsp70* mRNA accumulation in *Xenopus laevis* A6 kidney epithelial cells treated simultaneously with different concentrations of sodium arsenite (NA) and mild heat shock. A) A6 cells were maintained at 22 ºC or exposed to different concentrations of sodium arsenite either singly or in combination with a 30 ºC heat shock for 1.5 h. Cells were harvested and total RNA was isolated and quantified. Total RNA (10 μg) was analysed by northern hybridization analysis using *hsp30* and *hsp70* antisense riboprobes. The bottom panel exhibits a reversible blot stain which confirms equal loading and quality of transfer. B) Image J (Version 1.38) software was used to carry out densitometric analysis of *hsp30* (grey bars) and *hsp70* (black bars) mRNA bands on the northern blot images. Results are expressed as a percentage of the maximum hybridization signal obtained. Standard deviation is represented by the vertical error bars. Significant differences between sets of sodium arsenite exposed cells at 22 ºC and at 30 ºC are indicated as * ($p < 0.05$) or Δ ($p < 0.01$). These results are representative of at least 3 different experiments.

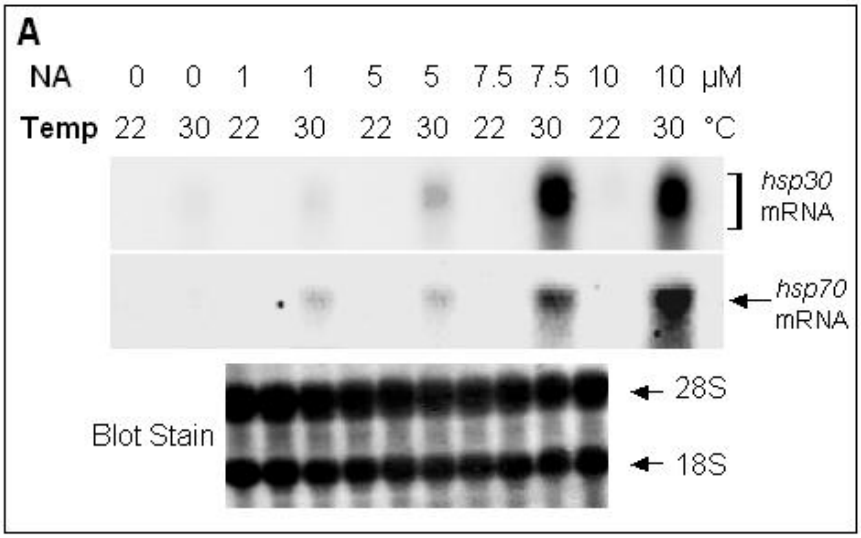
A
NA 0 0 1 1 5 5 7.5 7.5 10 10 µM
Temp 22 30 22 30 22 30 22 30 22 30 °C
hsp30 mRNA
hsp70 mRNA
Blot Stain
28S
18S

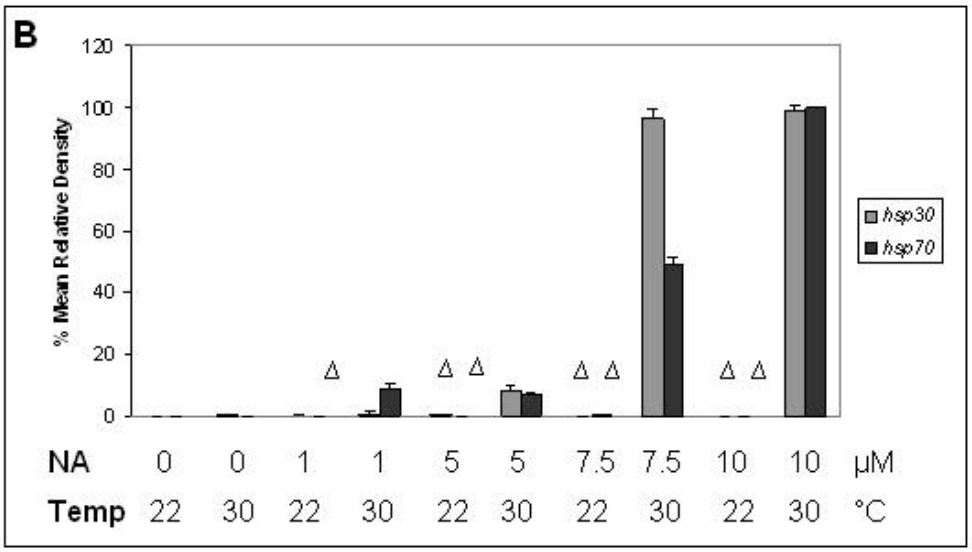
B
% Mean Relative Density
120
100
80
60
40
20
0
hsp30
hsp70
NA 0 0 1 1 5 5 7.5 7.5 10 10 µM
Temp 22 30 22 30 22 30 22 30 22 30 °C

Figure 7. HSP30 and HSP70 protein accumulation in A6 cells treated concurrently with various concentrations of sodium arsenite and mild heat shock. A) Cells were maintained at 22 ºC or exposed to different concentrations of sodium arsenite either singly or in combination with a 30 ºC heat shock for 3 h followed by a 2 h recovery period at 22 ºC. Total protein was isolated and resolved on 12% SDS-polyacrylamide gels. Protein was transferred to nitrocellulose membranes and probed with anti-HSP30 or anti-HSP70 polyclonal antibodies as described in Materials and Methods. A section of a representative Ponceau S stained membrane is included to demonstrate efficient transfer and equal loading of protein. B) Image J (Version 1.38) software was employed to perform densitometric analysis as outlined in the legend of figure 6.

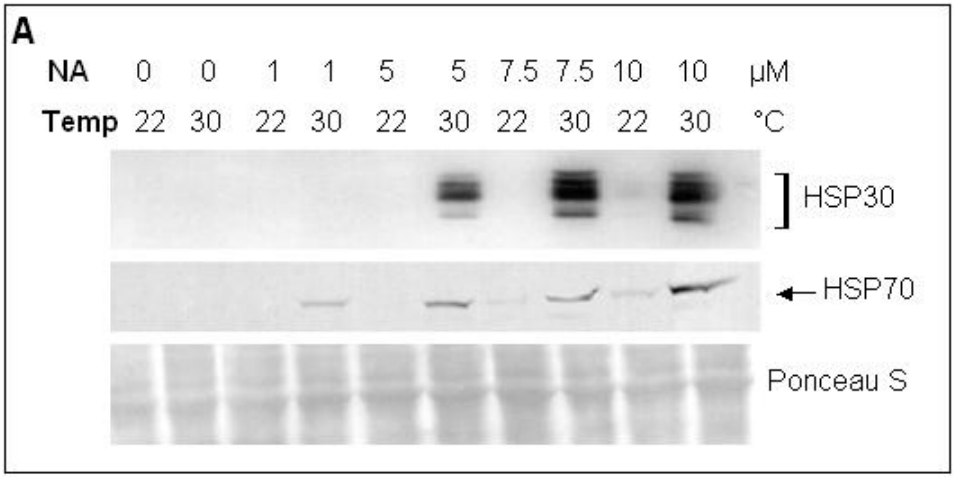
A
NA 0 0 1 1 5 5 7.5 7.5 10 10 µM
Temp 22 30 22 30 22 30 22 30 22 30 °C
HSP30
HSP70
Ponceau S

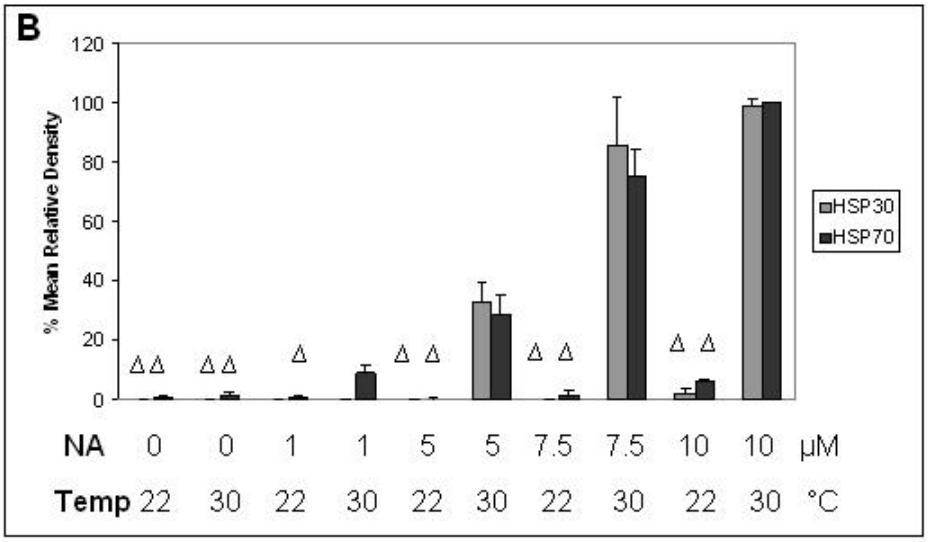
B
% Mean Relative Density
120
100
80
60
40
20
0
HSP30
HSP70
NA 0 0 1 1 5 5 7.5 7.5 10 10 µM
Temp 22 30 22 30 22 30 22 30 22 30 °C

22 ºC. HSP30 and HSP70 accumulation was detected in cells exposed to 5 to 10 μM sodium arsenite plus heat shock. Additionally, there was a low detectable level of HSP70 in cells treated with 1 μM sodium arsenite at 30 ºC. The largest accumulation of HSP30 was detected in cells treated with 7.5 and 10 μM sodium arsenite at 30 ºC, whereas the highest HSP70 accumulation was seen at 10 μM sodium arsenite at 30 ºC. Also, the relative levels of HSP30 or HSP70 accumulation in cells exposed to combined stress was greater than the sum of the HSP levels found with each stressor individually (Fig. 6B; 7B).

The accumulation of HSP30 and HSP70 in response to 10 μM sodium arsenite plus incubation temperatures ranging from 26 to 30 ºC is shown in Figure 8A. HSP30 and HSP70 accumulation in A6 cells exposed to 10 μM sodium arsenite increased from 26 to 30 ºC. Densitometric analysis revealed that HSP70 had a greater relative increase at 26 and 28 ºC than HSP30 (Fig. 8B). In time course studies, A6 cells were treated with 10 μM sodium arsenite at 30 ºC for different time intervals ranging from 2 to 24 h (Fig. 9A). The relative accumulation of HSP30 and HSP70 increased gradually from 2 to 15 h and then decreased at 24 h. Densitometric analysis revealed that the maximum accumulation of HSP30 and HSP70 occurred when cells were exposed to the combined treatment between 8 to 15 h in duration (Fig. 9B). Furthermore, at 15 and 24 h there was a 3.8- and 5.3-fold decrease in the accumulation of HSP30 and HSP70, respectively.

The relative levels of HSP30 and HSP70 were analysed during recovery from the combined treatment (Fig. 10A). A6 cells were exposed to 10 μM sodium arsenite at 30 ºC for 3 h followed by recovery time intervals ranging from 2 to 24 h. A relatively large amount of HSP30 and HSP70 accumulated in cells that were allowed to recover for 2 to 4

Figure 8. Analysis of HSP30 and HSP70 protein accumulation in A6 cells exposed simultaneously to various temperatures and 10 µM sodium arsenite. A) Cells were maintained at 22 ºC or exposed to various elevated temperatures ranging from 26 to 30 ºC in combination with 10 µM sodium arsenite for 3 h followed by a 2 h recovery period at 22 ºC. Total protein was isolated and analysed by immunoblotting as outlined in the legend of figure 7. B) Image J (Version 1.38) software was used to perform densitometric analysis as outlined in the legend of figure 6. Significant differences between the maximum signal and other treatments are indicated as Δ ($p < 0.01$).

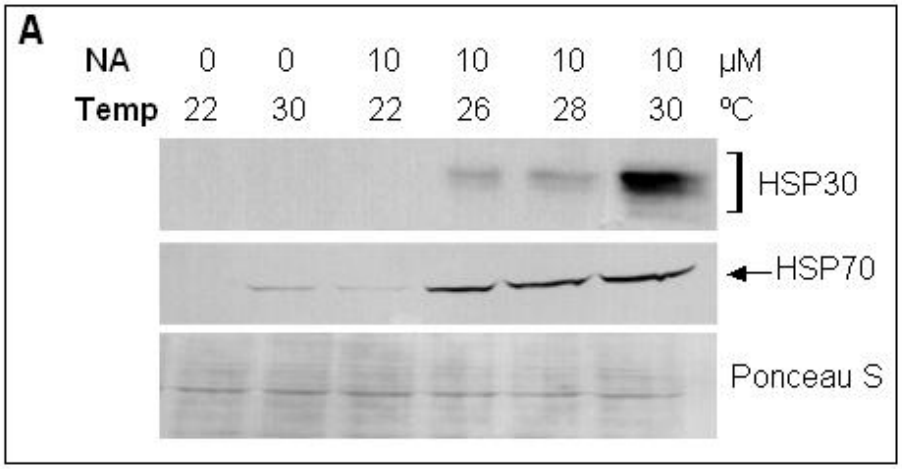
A
NA 0 0 10 10 10 10 µM
Temp 22 30 22 26 28 30 ºC
HSP30
HSP70
Ponceau S

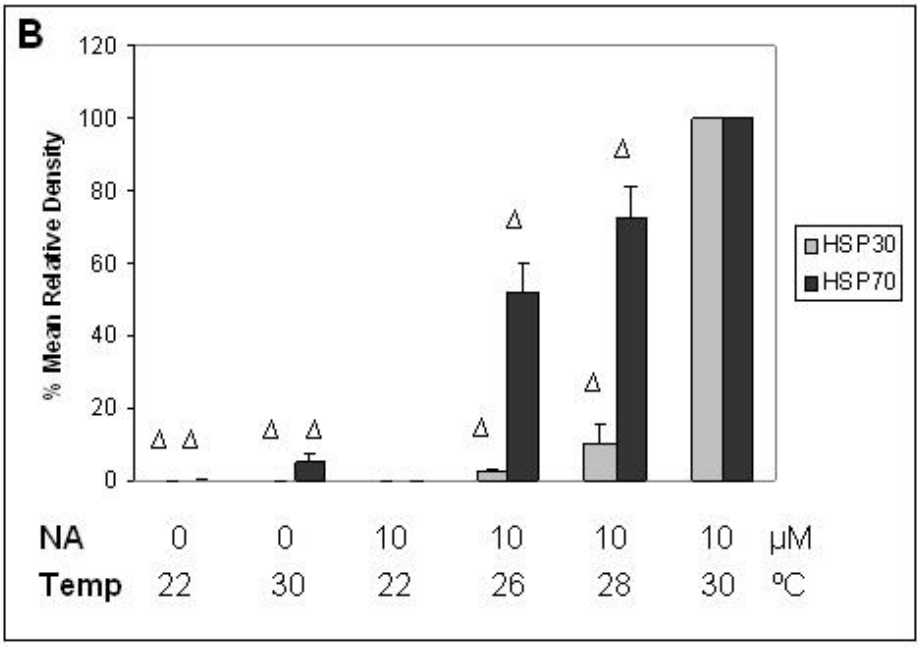
B
% Mean Relative Density
120
100
80
60
40
20
0
HSP30
HSP70
NA 0 0 10 10 10 10 µM
Temp 22 30 22 26 28 30 ºC

Figure 9. Time course of HSP30 and HSP70 protein accumulation in A6 cells treated concurrently with sodium arsenite and mild heat shock. A) Cells were maintained at 22 ºC or exposed to 10 μM sodium arsenite plus a 30 ºC heat shock for time intervals ranging from 2 to 24 h. Total protein was isolated and analysed by immunoblotting as described in the legend of figure 7. B) Image J (Version 1.38) software was used to perform densitometric analysis as detailed in the legend of figure 6. Significant differences between the maximum signal, 15 h for HSP30 and 12 h for HSP70, are indicated as * ($p < 0.05$) or Δ ($p < 0.01$).

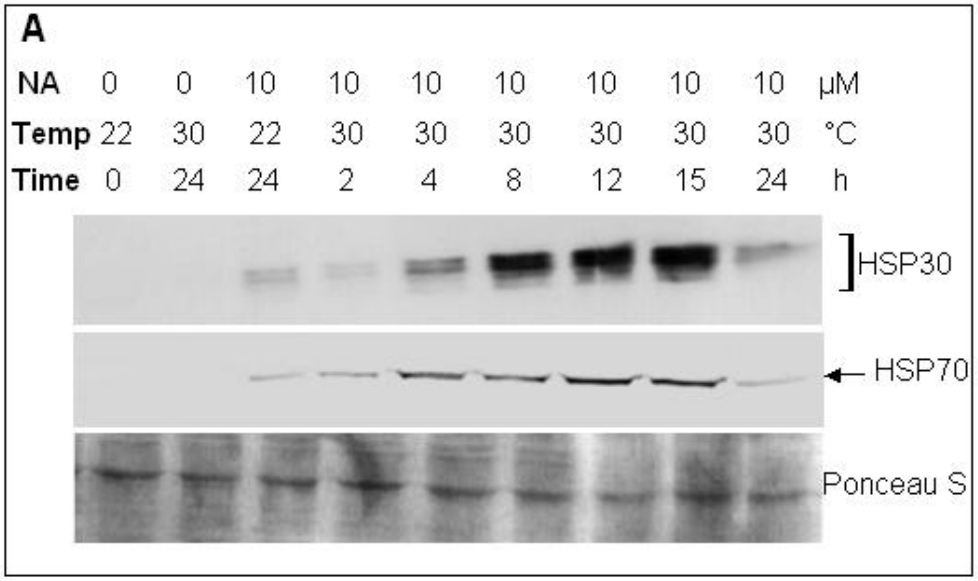
A
NA 0 0 10 10 10 10 10 10 10 µM
Temp 22 30 22 30 30 30 30 30 30 °C
Time 0 24 24 2 4 8 12 15 24 h
HSP30
HSP70
Ponceau S

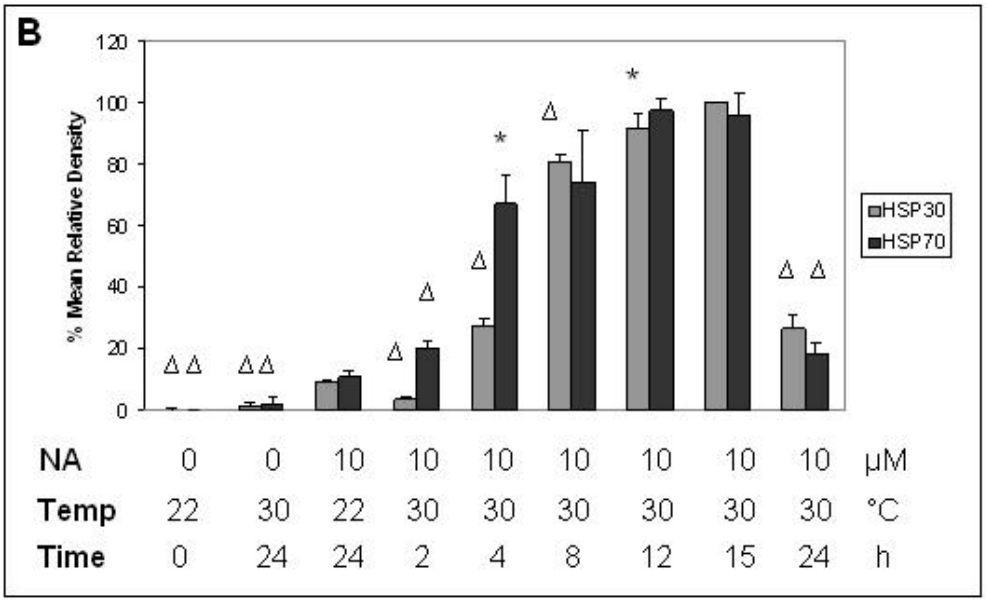
B
% Mean Relative Density
120
100
80
60
40
20
0
HSP30
HSP70
NA 0 0 10 10 10 10 10 10 10 µM
Temp 22 30 22 30 30 30 30 30 30 °C
Time 0 24 24 2 4 8 12 15 24 h

Figure 10. HSP30 and HSP70 protein accumulation in A6 cells recovering from simultaneous treatment with sodium arsenite and mild heat shock. A) Cells were maintained at 22 ºC (C) or exposed to 10 μM sodium arsenite plus a 30 ºC heat shock for 3 h. Cells were allowed to recover in fresh media at 22 ºC for different time intervals ranging from 2 to 24 h. Total protein was isolated and analysed by immunoblotting as described in the legend of figure 7. B) Image J (Version 1.38) software was used to perform densitometric analysis as outlined in the legend of figure 6. Significant differences between the standard 2 h recovery period and the longer recovery times are indicated as Δ ($p < 0.01$).

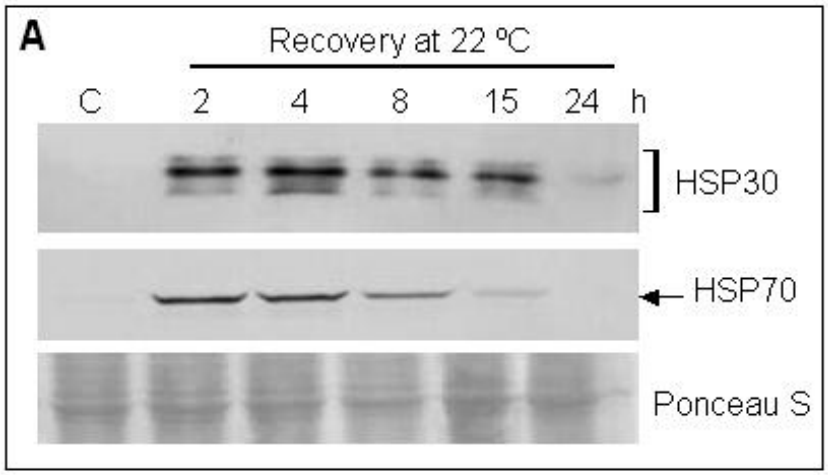
A
Recovery at 22 ºC
C
2
4
8
15
24
h
HSP30
HSP70
Ponceau S

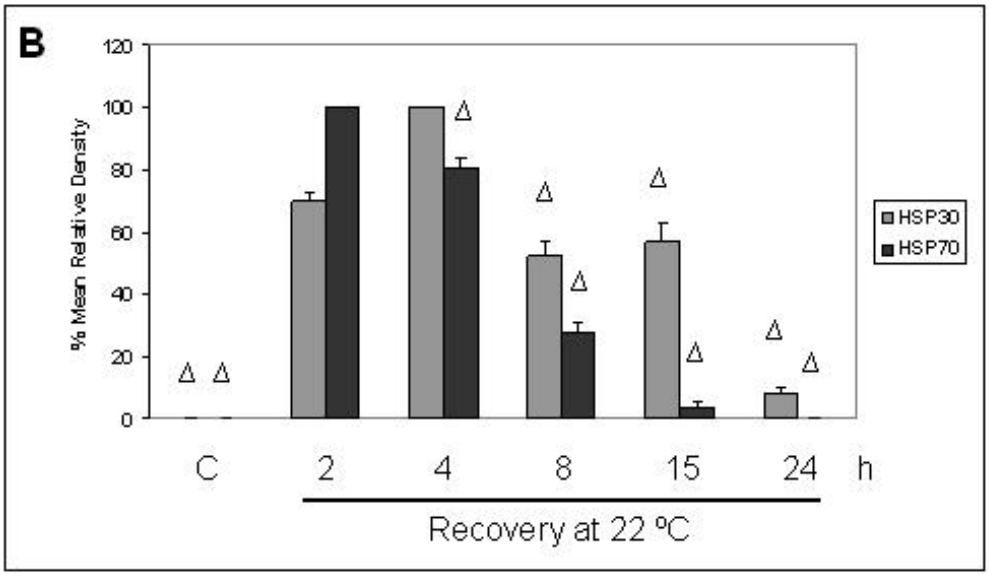
B
% Mean Relative Density
120
100
80
60
40
20
0
HSP30
HSP70
C
2
4
8
15
24
h
Recovery at 22 ºC

h. However, between 4 and 8 h the relative accumulation decreased by 2- and 2.9-fold for HSP30 and HSP70, respectively (Fig. 10B). At 24 h of recovery the relative levels of HSP30 decreased by 11.8-fold while HSP70 was not detectable.

3.1.2 Involvement of HSF activation in the accumulation of HSP30 and HSP70 in A6 cells exposed concurrently to sodium arsenite and heat shock

The expression of *Xenopus laevis hsp* genes in response to heat shock or chemical stress has been shown to be controlled at the level of transcription by the activation of HSF (Ovsenek and Heikkila, 1990; Gordon *et al.*, 1997; Manwell and Heikkila, 2007; Voyer and Heikkila, 2008). In the present study, I utilized a HSF inhibitor, KNK437, to determine if the expression of *hsp30* and *hsp70* genes in A6 cells exposed to sodium arsenite plus mild heat shock was due to HSF activation (Fig. 11A). A6 cells were pretreated with 100 μM KNK437 for 6 h and then exposed to 10 μM sodium arsenite plus a 30 ºC heat shock for 3 h followed by a 2 h recovery period at 22 ºC. Immunoblot and subsequent densitometric analysis demonstrated a KNK437-induced inhibition of 99% and 99.6% of HSP30 and HSP70 accumulation, respectively (Fig. 11B). KNK437 also inhibited HSP accumulation in A6 cells heat shocked at 33 ˚C.

3.1.3 HSP30 localization in A6 cells exposed concurrently to sodium arsenite and heat shock treatment

The accumulation and localization of HSP30 protein was analysed by immunocytochemistry and laser scanning confocal microscopy (LSCM). The accumulation and intracellular localization of HSP70 was not investigated since the affinity-purified, polyclonal anti-HSP70 antibody, which was utilized successfully in immunoblot analysis, was unable to specifically detect HSP70 by immunocytochemistry.

Figure 11. Effect of KNK437 (KNK) on the accumulation of HSP30 and HSP70 protein in A6 cells treated with concurrent sodium arsenite and mild heat shock. A) Cells were maintained at 22 ºC, pretreated with 100 μM KNK437 for 6 h, or pretreated and then exposed to 10 μM sodium arsenite plus a 30 ºC heat shock. Total protein was isolated and analysed by immunoblotting as detailed in the legend of figure 7. B) Image J (Version 1.38) software was used to perform densitometric analysis as described in the legend of figure 6. Significant inhibition of HSP accumulation by KNK437 is indicated as Δ ($p < 0.01$).

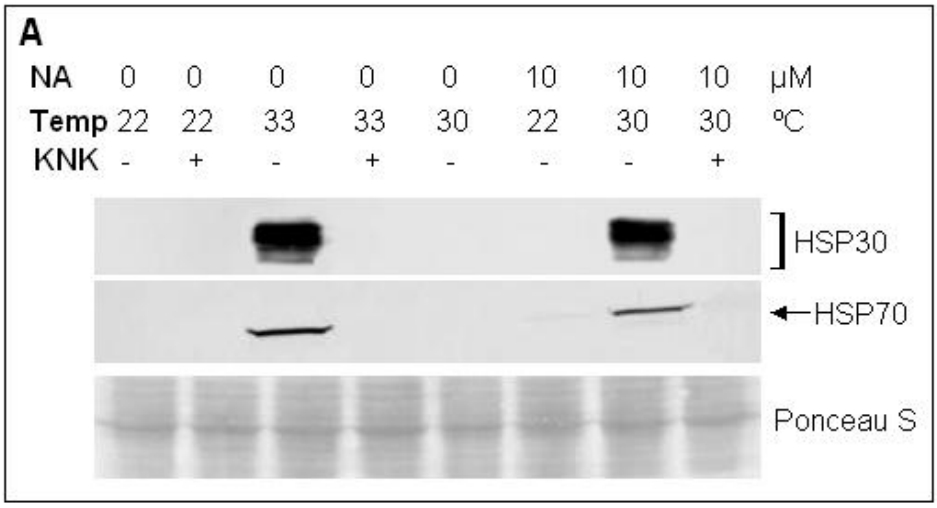
A
NA 0 0 0 0 0 10 10 10 µM
Temp 22 22 33 33 30 22 30 30 ºC
KNK - + - + - - - +
HSP30
HSP70
Ponceau S

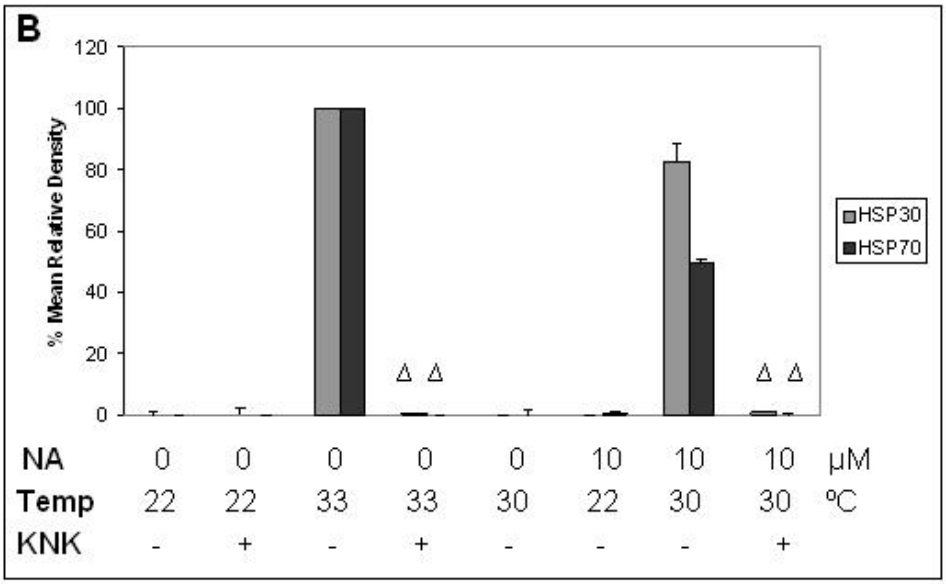
B
% Mean Relative Density
120
100
80
60
40
20
0
HSP30
HSP70
NA 0 0 0 0 0 10 10 10 µM
Temp 22 22 33 33 30 22 30 30 ºC
KNK - + - + - - - +

A6 cells were grown on glass coverslips and maintained at 22 ºC or treated with a 30 ºC or a 33 ºC heat shock. Some cells were also treated with 10 μM sodium arsenite. These treatments were 3 h in duration and were followed by a 2 h recovery period at 22 ºC (Fig. 12). The accumulation of HSP30 was not detectable in control cells maintained at 22 ºC. However, HSP30 did accumulate in cells exposed to a 33 ºC heat shock. Furthermore, there was no detectable accumulation in cells treated singly with a 30 ºC heat shock or 10 μM sodium arsenite. The effect of simultaneous exposure to sodium arsenite and mild heat shock was subsequently investigated (Fig. 13). A6 cells were exposed to different concentrations of sodium arsenite (1 to 10 μM) plus a 30 ºC heat shock. The relative accumulation of HSP30 gradually increased in cells treated with 1 to 10 μM sodium arsenite at 30 ºC, with very little accumulation detected at 1 μM. HSP30 staining induced by the combined stressors occurred primarily in the cytoplasm in a punctate or granular pattern. A small amount of HSP30 staining was also present in the nucleus.

3.1.4 The effect of pretreating A6 cells simultaneously with sodium arsenite and heat shock on the acquisition of thermotolerance

In a previous study, it was established that pre-treatment of A6 cells with a 33 ºC heat shock resulted in the accumulation of HSPs and an acquired state of thermotolerance (Manwell and Heikkila, 2007). In the present study, I examined whether simultaneous exposure to sodium arsenite and heat shock, which induced the accumulation of HSP30 and HSP70, could also acquire thermotolerance. Shifting the incubation temperature of A6 cells from 22 ºC directly to a 37 ºC thermal challenge for 1 h resulted in the collapse of the actin cytoskeleton (Fig. 14A). Cells treated singly with a 30 ºC heat shock or 10 μM sodium arsenite prior to the 37 ºC incubation also displayed a cytoskeletal collapse.

Figure 12. Detection of HSP30 localization in A6 cells exposed to various stressors by LSCM. Cells were grown on glass coverslips in (L)-15 media and were either maintained at 22 ºC, exposed to a 30 ºC or 33 ºC heat shock, or treated with 10 μM sodium arsenite. Treatments were 3 h in length, followed by a 2 h recovery period at 22 ºC. Actin was stained using phalloiden conjugated to TRITC (red) and the nuclei were stained using DAPI (blue). HSP30 was detected indirectly by an anti-HSP30 antibody and Alexa-488 secondary antibody conjugate (green). From left to right the columns display fluorescence detection channels for actin, HSP30 and merged images plus DAPI. The 10 μm white scale bar is shown. These images are representative of at least 3 different experiments.

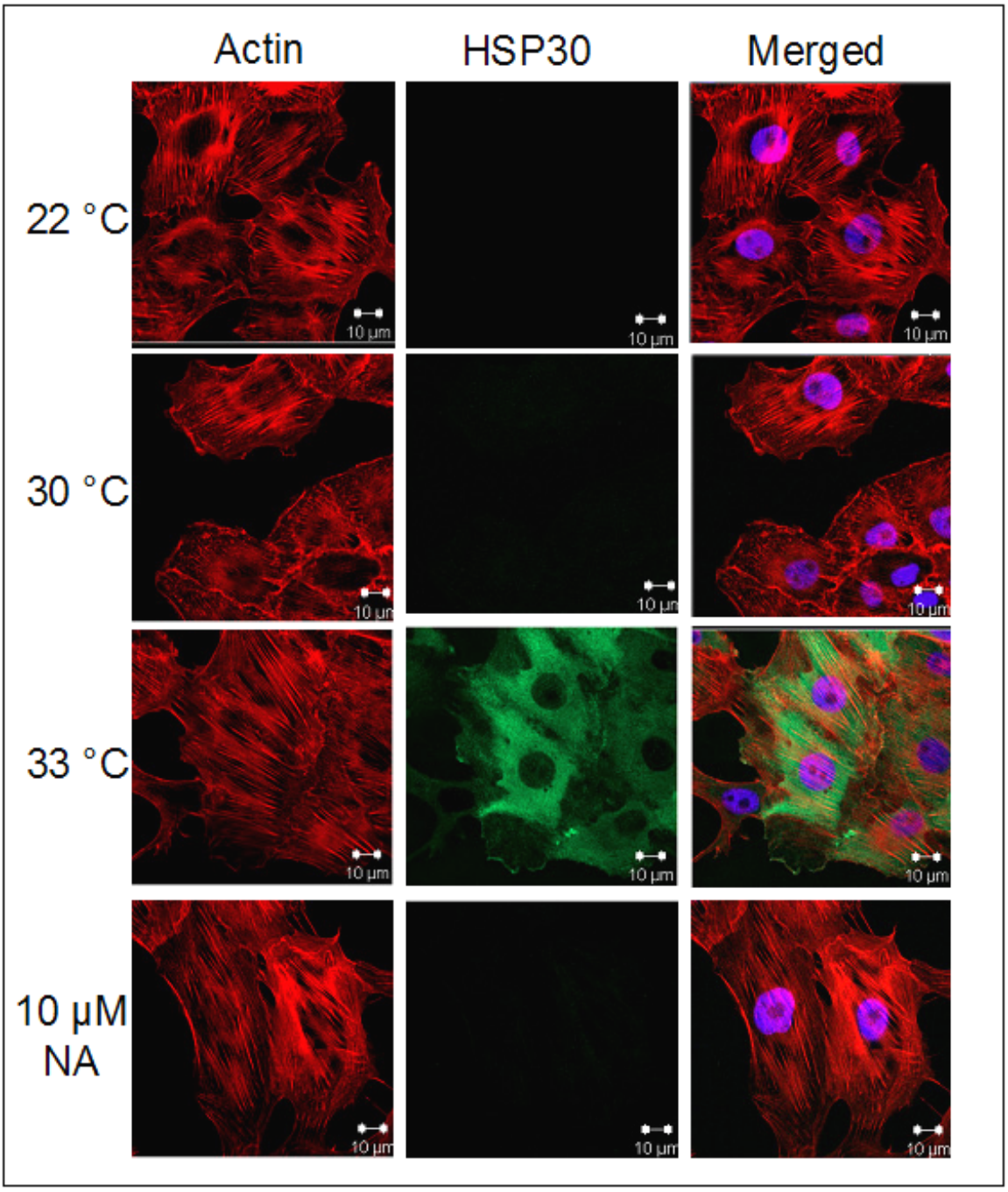
Actin
HSP30
Merged
22 °C
30 °C
33 °C
10 µM NA
10 µm

Figure 13. HSP30 localization in A6 cells maintained at 30 ºC in combination with different concentrations of sodium arsenite. Cells were grown on glass coverslips and exposed to a 30 ºC heat shock plus sodium arsenite concentrations ranging from 1 to 10 μM for 3 h followed by a 2 h recovery period at 22 ºC. Actin and nuclei were stained directly with phalloiden conjugated to TRITC (red) and DAPI (blue), respectively. HSP30 was indirectly detected with an anti-HSP30 antibody and a secondary antibody conjugated to Alexa-488 (green).

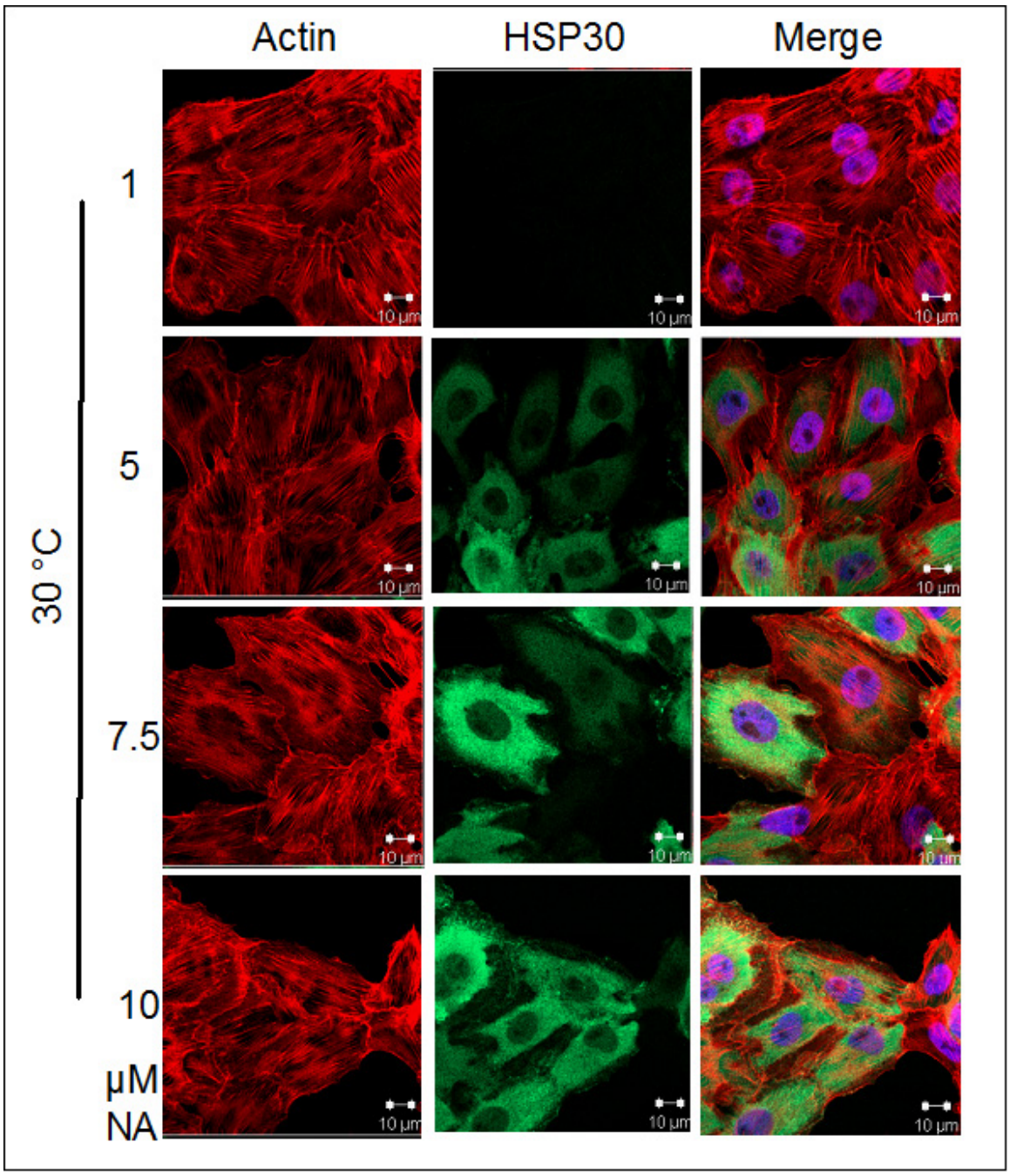
Actin
HSP30
Merge
30 °C
1
5
7.5
10
μM
NA
10 μm

Figure 14. Cytoprotective effects of pre-treating A6 cells with concurrent sodium arsenite and mild heat shock prior to a 37 ºC thermal challenge. A) A6 cells were grown on glass coverslips and were maintained at 22 ºC, heat shocked at 37 ºC, maintained at 30 ºC followed by a 37 ºC heat shock, or exposed to 10 μM sodium arsenite followed by a 37 ºC heat shock. B) A6 cells were subjected to a 33 ºC heat shock or 10 μM sodium arsenite plus a 30 ºC heat shock for 3 h prior to a 37 ºC thermal challenge for 1 h. In the last row, cells were pretreated with 100 μM KNK437 for 6h before the combined treatment and subsequence thermal challenge. All treatments were followed by a 2 h recovery period at 22 ºC. Actin and nuclei were stained directly with phalloiden conjugated to TRITC (red) and DAPI (blue), respectively. HSP30 was indirectly detected with an anti-HSP30 antibody and a secondary antibody conjugated to Alexa-488 (green).

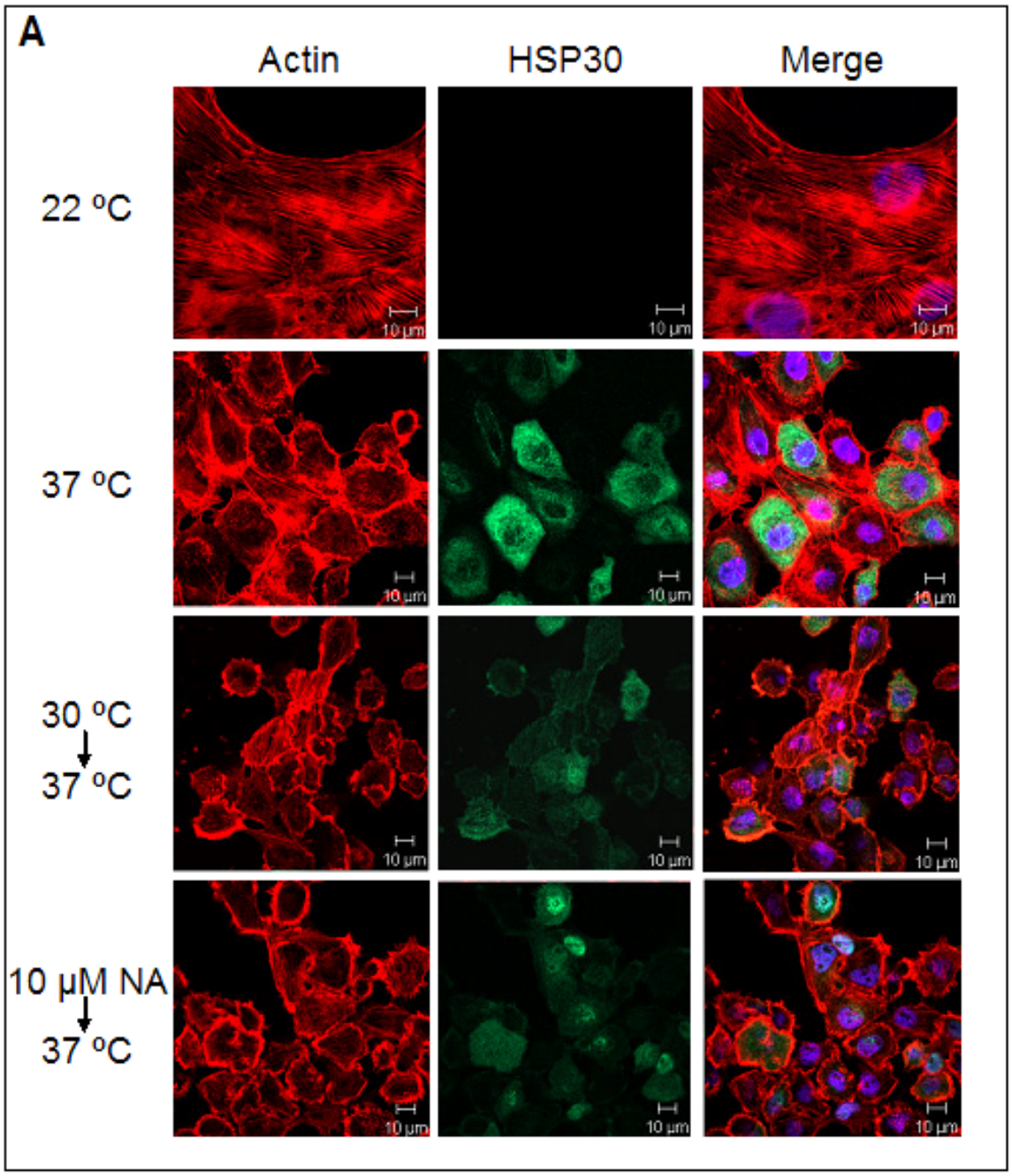
A
Actin
HSP30
Merge
22 °C
37 °C
30 °C
37 °C
10 µM NA
37 °C
10 µm

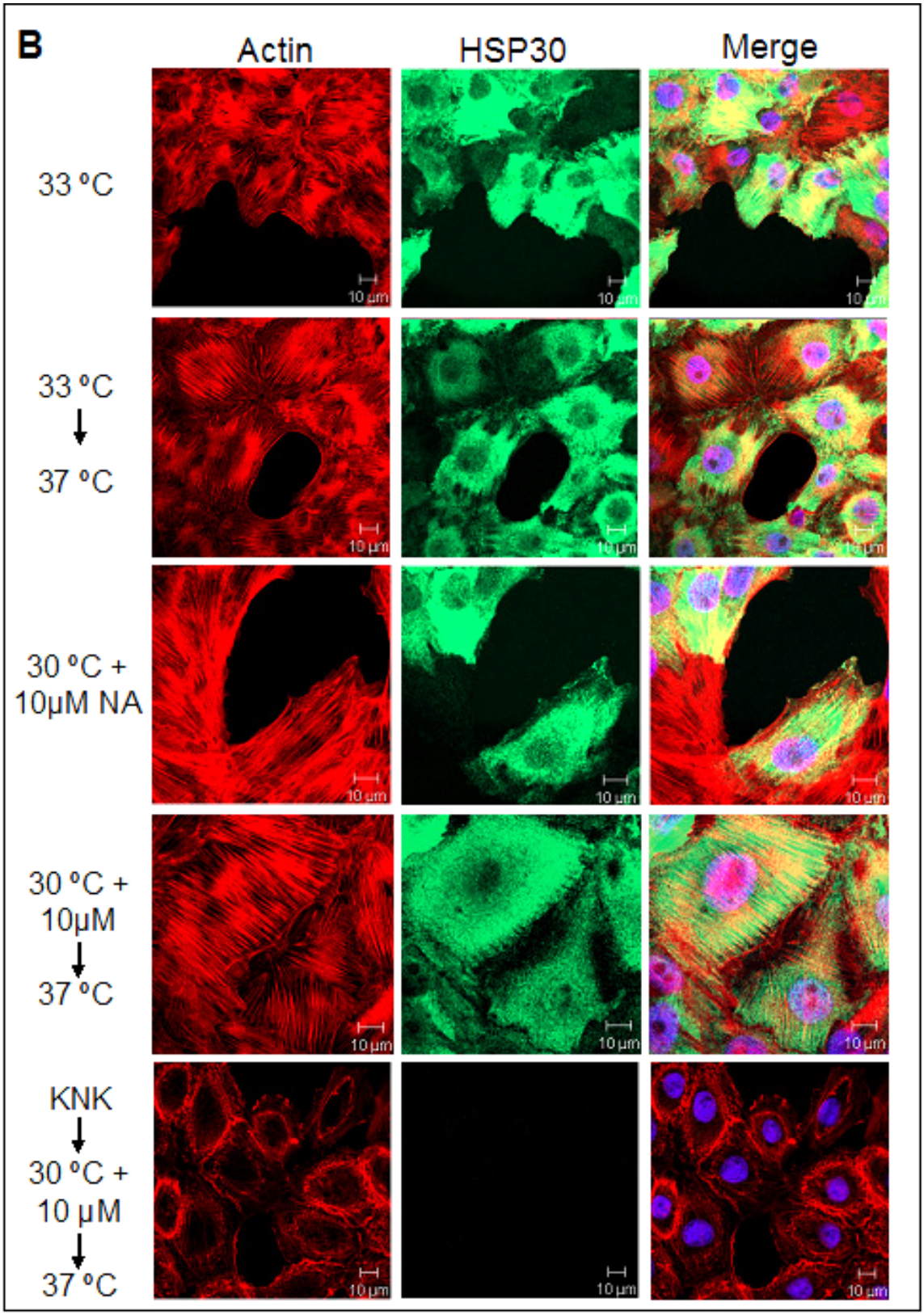
B
Actin
HSP30
Merge
33 °C
33 °C
37 °C
30 °C +
10µM NA
30 °C +
10µM
37 °C
KNK
30 °C +
10 µM
37 °C
10 µm

However, 80% of cells pretreated with a 33 ºC heat shock prior to the thermal challenge exhibited a normal actin cytoskeleton with intact stress fibers (Fig. 14B). Furthermore, pre-treatment with sodium arsenite plus mild heat shock before the thermal challenge resulted in 90% of cells displaying intact stress fibers and no cytoskeletal collapse. Thus, sodium arsenite plus mild heat shock pre-treatment was effective at conferring thermotolerance in A6 cells. The accumulation of HSPs in A6 cells was responsible for this acquired state of thermotolerance by the combined stressors since KNK437 pre-treatment, which inhibited the accumulation of HSP30 and HSP70, also resulted in cytoskeletal collapse (Fig. 14B; last row).

3.2 The effect of proteasomal inhibition on the expression of *Xenopus laevis hsp* genes

3.2.1 Examination of ubiquitinated protein accumulation in A6 cells exposed to different stressors

In order to determine the effectiveness of the proteasome inhibitors MG132 (a peptide aldehyde) and lactacystin in A6 cells, I conducted western blot analysis, employing a mouse anti-ubiquitin monoclonal antibody, to measure the relative accumulation of cellular proteins conjugated to ubiquitin. Increased levels of ubiquitinated proteins within the cell has been used in other studies as a method to confirm efficient proteasome inhibition (Mimnaugh *et al.*, 1997; Melikova *et al.*, 2006) The levels of ubiquitinated proteins in control and heat shocked cells were relatively low (Fig. 15). However, cells exposed to 20 μM sodium arsenite for 16 h had an increased accumulation of cellular proteins conjugated to ubiquitin. The relative accumulation of ubiquitinated proteins was much higher in proteasome inhibitor treated cells than found

Figure 15. Analysis of ubiquitinated protein accumulation in A6 cells treated with heat shock, sodium arsenite, MG132 or lactacystin. A6 cells were either maintained at 22 ºC (C), heat shocked at 33 ºC for 2 h followed by a 2 h recovery period at 22 ºC (1), exposed to 20 μM sodium arsenite for 16 h (2), treated with 30 μM MG132 for either 15 h (3) or 24 h (4), or treated with 15 μM lactacystin for 15 h (5). Total protein was isolated and analysed by immunoblotting using a mouse anti-ubiquitin monoclonal antibody (Zymed) as described in the legend of figure 7.

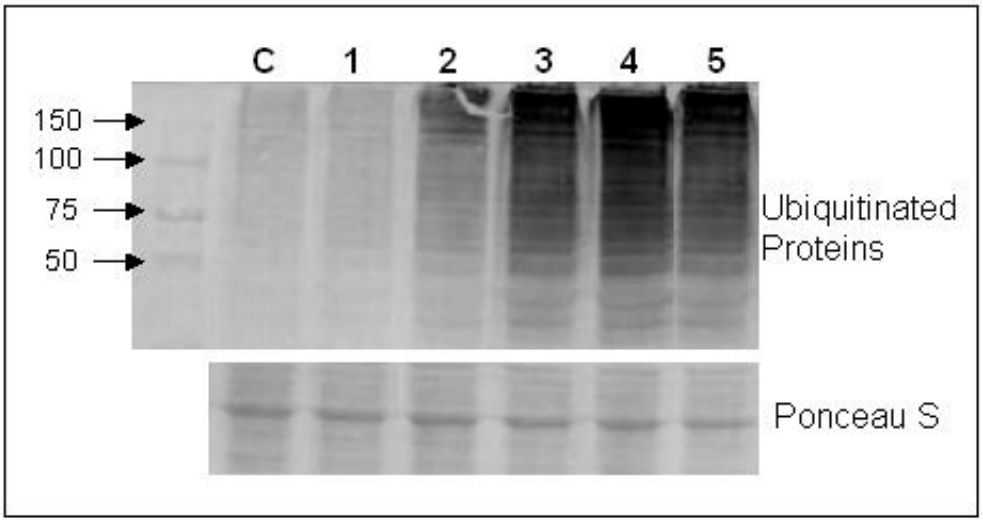
C
1
2
3
4
5
150
100
75
50
Ubiquitinated Proteins
Ponceau S

with control, heat shock or sodium arsenite. The level of cellular proteins conjugated to ubiquitin increased slightly in A6 cells treated with 30 μM MG132 for 24 h, compared to those treated for 15 h. The accumulation of ubiquitinated proteins was also relatively high in cells treated with 15 μM lactacystin for 15 h.

3.2.2 Analysis of the expression of *hsp30* and *hsp70* genes in A6 cells exposed to MG132

The next phase of this study examined the effect of MG132 on the accumulation of *hsp30* and *hsp70* mRNA in A6 cells by Northern hybridization analysis. As shown in Figure 16, A6 cells were exposed to concentrations of MG132 ranging from 1 to 50 μM for 24 h. *Hsp30* and *hsp70* mRNA accumulation were detectable at 1 μM MG132 with relatively higher amounts observed in cells treated with 5 to 20 μM. The highest relative levels of *hsp30* message accumulation were detected from 30 to 50 μM MG132 for 24 h. Similarly, *hsp70* mRNA levels increased with increasing MG132 concentration, attaining maximal levels at 20 to 50 μM.

Additionally, I have examined the effect of MG132 exposure on the accumulation of HSP30, HSP70 and actin protein in A6 cells. Relative protein levels were determined by western blot analysis after A6 cells were treated with MG132 concentrations ranging from 1 to 50 μM for 24 h (Fig. 17). There was no detectable HSP30 accumulation in cells treated with 1 μM MG132. However, there was a gradual increase in the relative levels of HSP30 from 5 to 20 μM MG132. The highest accumulation of HSP30 protein was detected in A6 cells treated with 20 to 50 μM MG132. A6 cells exposed to 1 μM MG132 had detectable HSP70 protein accumulation which increased when the concentration of MG132 was raised to 5 μM. A relatively constant level of accumulation of this protein

Figure 16. The accumulation of *hsp30* and *hsp70* mRNA in A6 cells treated with different concentrations of the proteasome inhibitor, MG132. A6 cells were either maintained at 22 ºC or exposed to numerous concentrations of MG132, ranging from 1 to 50 μM for 24 h in duration. Total RNA was isolated and utilized in Northern hybridization analysis as described in the legend of figure 6.

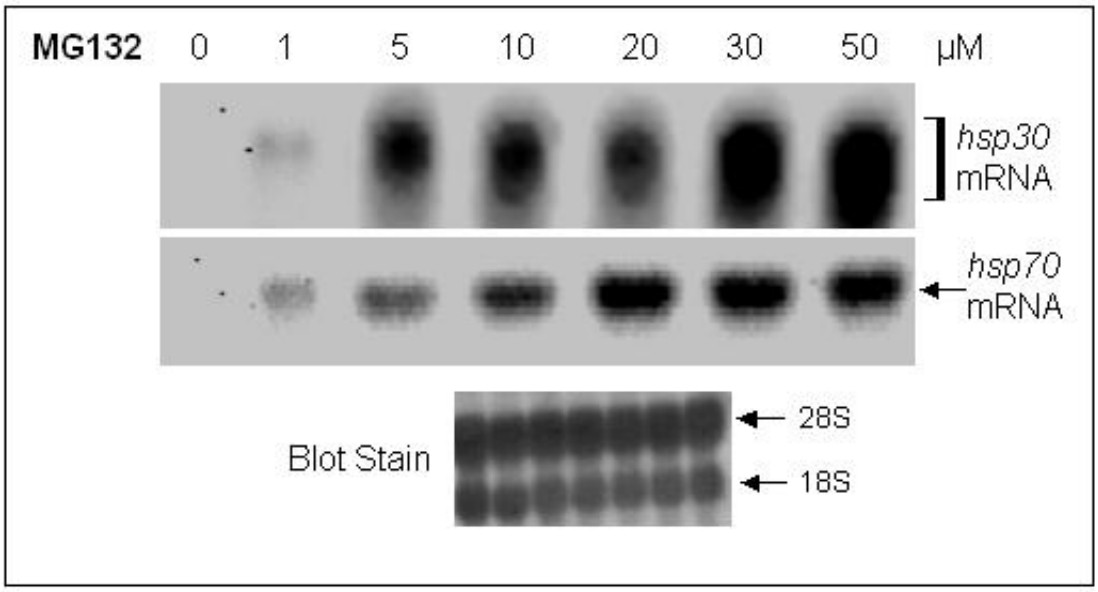
MG132
0
1
5
10
20
30
50
μM
hsp30
mRNA
hsp70
mRNA
Blot Stain
28S
18S

Figure 17. The accumulation of HSP30, HSP70 and actin protein in A6 cells exposed to different concentrations of MG132. A6 cells were either left at 22 ºC or treated with various concentrations of MG132, ranging from 1 to 50 μM for 24 h. Total protein was isolated and analysed by immunoblotting as detailed in the legend of figure 7.

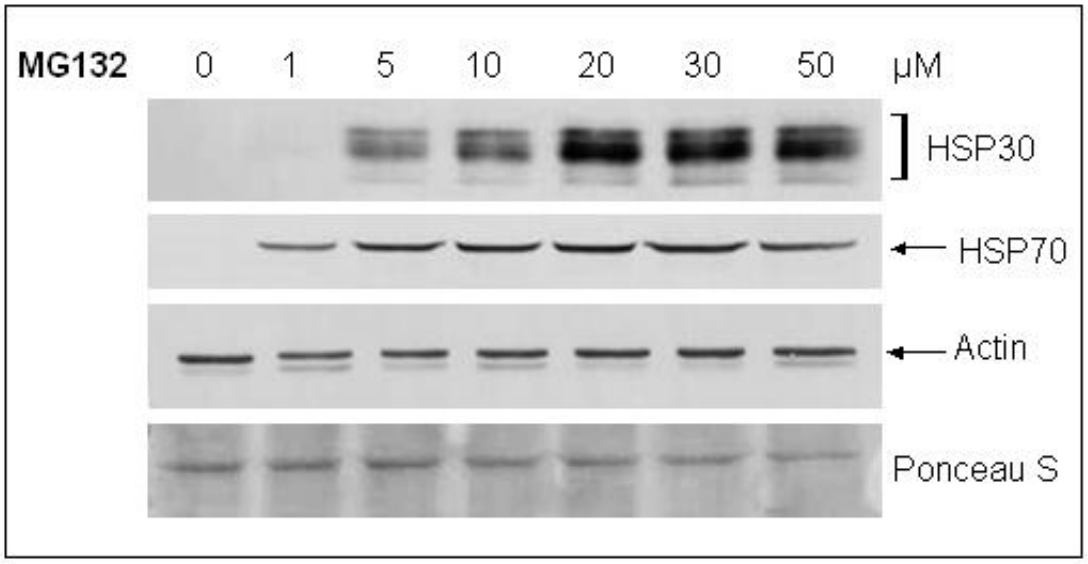
MG132
0
1
5
10
20
30
50
μM
HSP30
HSP70
Actin
Ponceau S

occurred from 5 to 30 μM MG132 with a slight decrease detected at 50 μM. The relative levels of actin were not affected by MG132 treatment as there were no detectable changes in its accumulation.

In time course studies, A6 cells were treated with either 50 μM or 10 μM MG132 for time periods ranging from 2 to 24 h (Fig. 18). In A6 cells treated with 50 μM MG132 the accumulation of HSP30 and HSP70 were first detectable at 8 and 4 h, respectively (Fig. 18A). The relative levels of both of these HSPs then increased from 12 to 24 h. As previously observed, the relative levels of actin were not affected by MG132 treatment. In A6 cells treated with 10 μM MG132 (Fig. 18B), HSP30 and HSP70 accumulation were first detected at 12 h of treatment. There was a gradual increase in the levels of these HSPs, with the highest accumulations observed at 24 h.

3.2.3 The effect of MG132 on the localization of HSP30 in A6 cells

The localization of HSP30 in A6 cells treated with MG132 was analyzed by immunocytochemistry and LSCM. A6 cells were grown on glass coverslips and maintained at 22 ºC or treated with different concentrations of MG132, ranging from 1 to 50 μM, for 24 h (Fig. 19A and B). There was no detectable HSP30 accumulation in A6 cells maintained at 22 ºC. However, there was a gradual increase in the accumulation of HSP30 in A6 cells treated with MG132 from 1 to 50 μM. The highest relative level of this protein was observed from 30 to 50 μM MG132. HSP30 accumulated in a granular or punctate pattern and was localized primarily in the cytoplasm, with a small amount of staining in the nucleus. Furthermore, there was no detectable HSP30 accumulation in the nucleolus. There were a few interesting intracellular HSP30 accumulation patterns uncovered in this study (Fig. 19C). First, approximately 70% of cells treated with 30 to

Figure 18. Time course of HSP30, HSP70 and actin protein accumulation in A6 cells treated with MG132. A6 cells were maintained at 22 ºC or treated with either A) 50 μM or B) 10 μM MG132 for different time intervals ranging from 2 to 24 h in duration. Total protein was isolated and analysed by immunoblotting as detailed in the legend of figure 7.

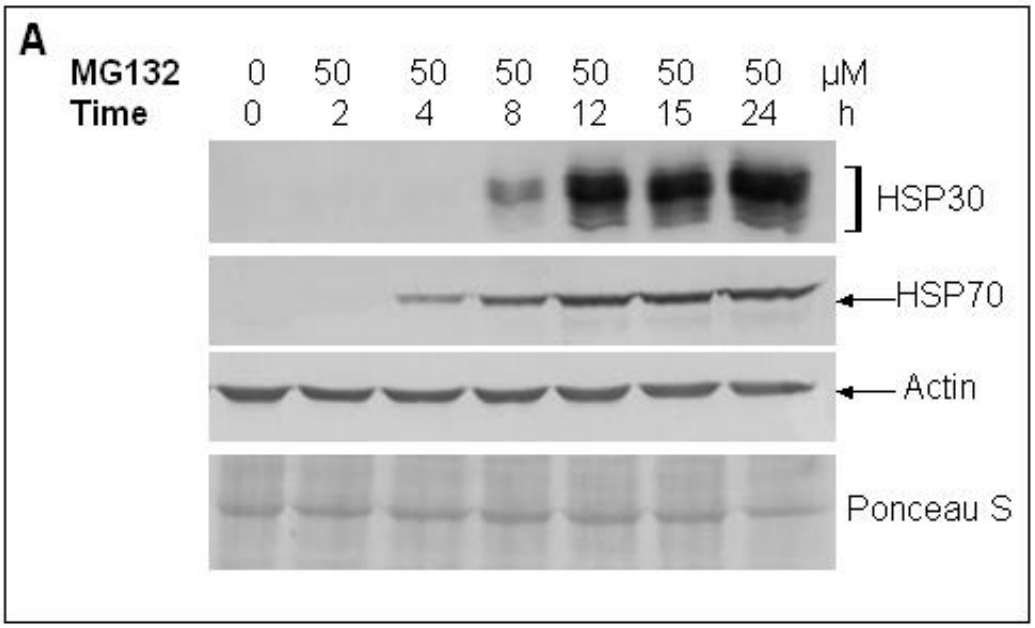
A
MG132 0 50 50 50 50 50 50 μM
Time 0 0 2 4 8 12 15 24 h
HSP30
HSP70
Actin
Ponceau S

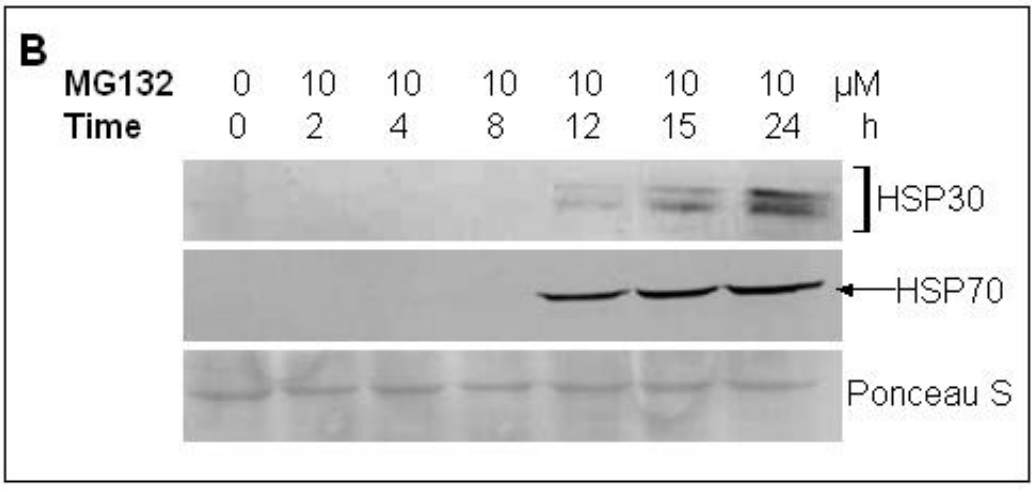
B
MG132 0 10 10 10 10 10 10 μM
Time 0 0 2 4 8 12 15 24 h
HSP30
HSP70
Ponceau S

Figure 19. Detection of HSP30 localization in A6 cells exposed to different MG132 concentrations by LSCM. A) A6 cells were grown on glass coverslips and were maintained at 22 ºC or treated with different MG132 concentrations ranging from 1 to 10 μM for 24 h. An example of intact actin stress fibers, observed in control cells, are indicated by the white arrows. B) A6 cells exposed to different MG132 concentrations ranging from 20 to 50 μM for 24 h. C) Enlargements of the HSP30 localization patterns observed in A6 cells treated with MG132. The bottom two images are magnifications of the areas within the red boxes. The white arrows indicate large circular cytoplasmic foci of HSP30 accumulation and the yellow arrows point to distinct areas within the cytoplasm where HSP30 accumulation was not detected. Actin and nuclei were stained directly with phalloiden conjugated to TRITC (red) and DAPI (blue), respectively. HSP30 was indirectly detected with an anti-HSP30 antibody and a secondary antibody conjugated to Alexa-488 (green).

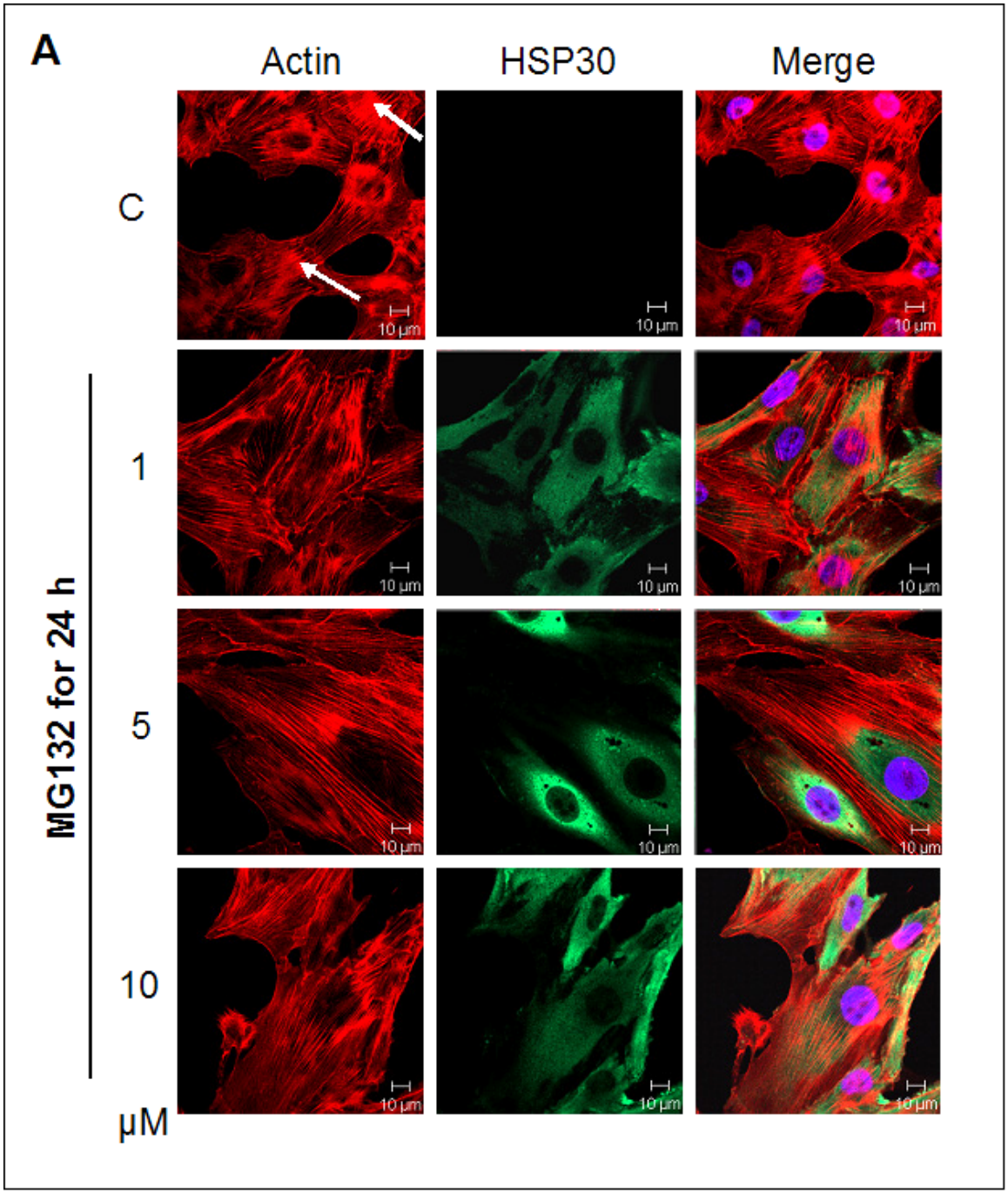
A
Actin
HSP30
Merge
C
1
5
10
μM
MG132 for 24 h
10 μm

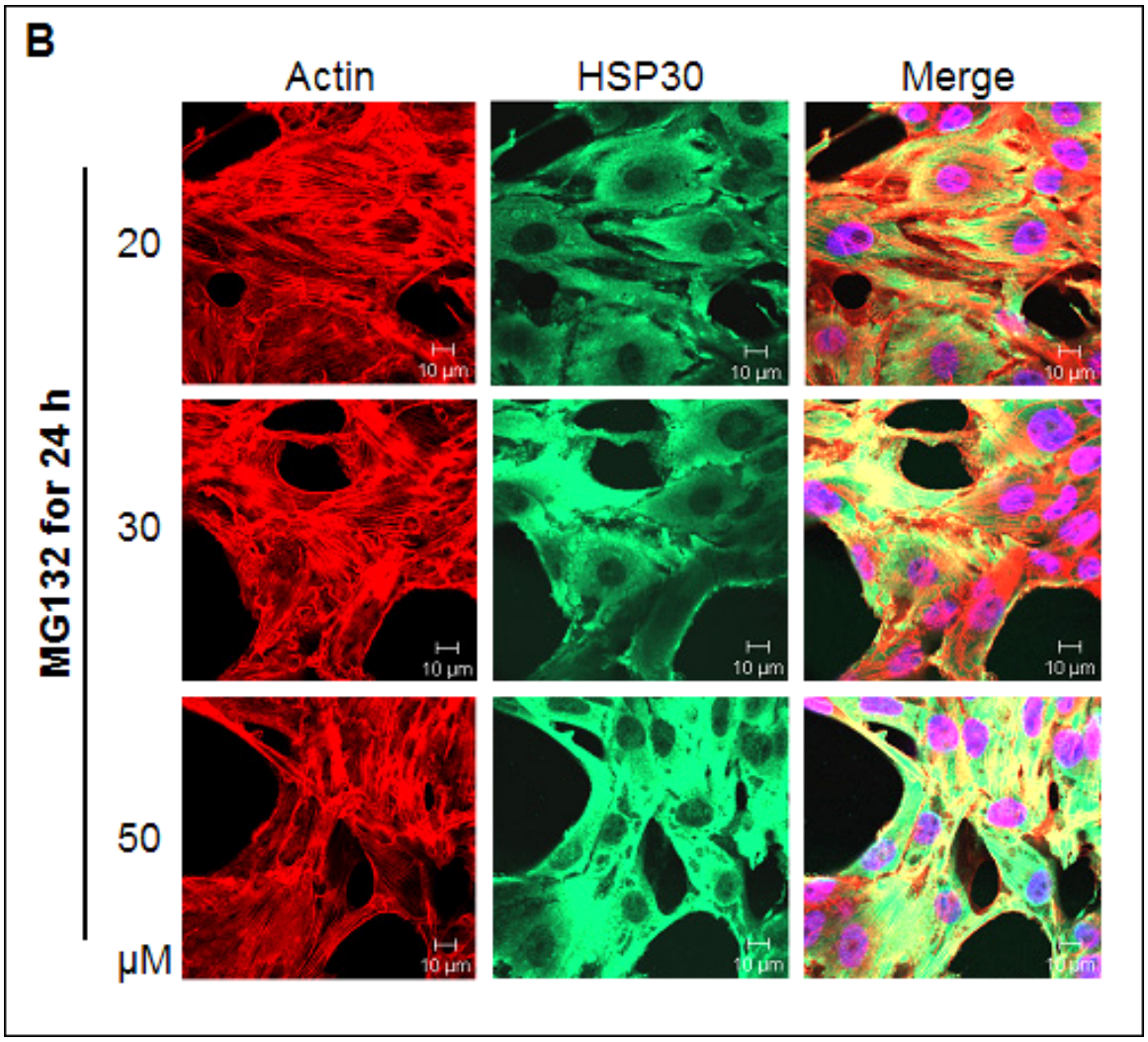
B
Actin
HSP30
Merge
MG132 for 24 h
20
30
50
μM
10 μm

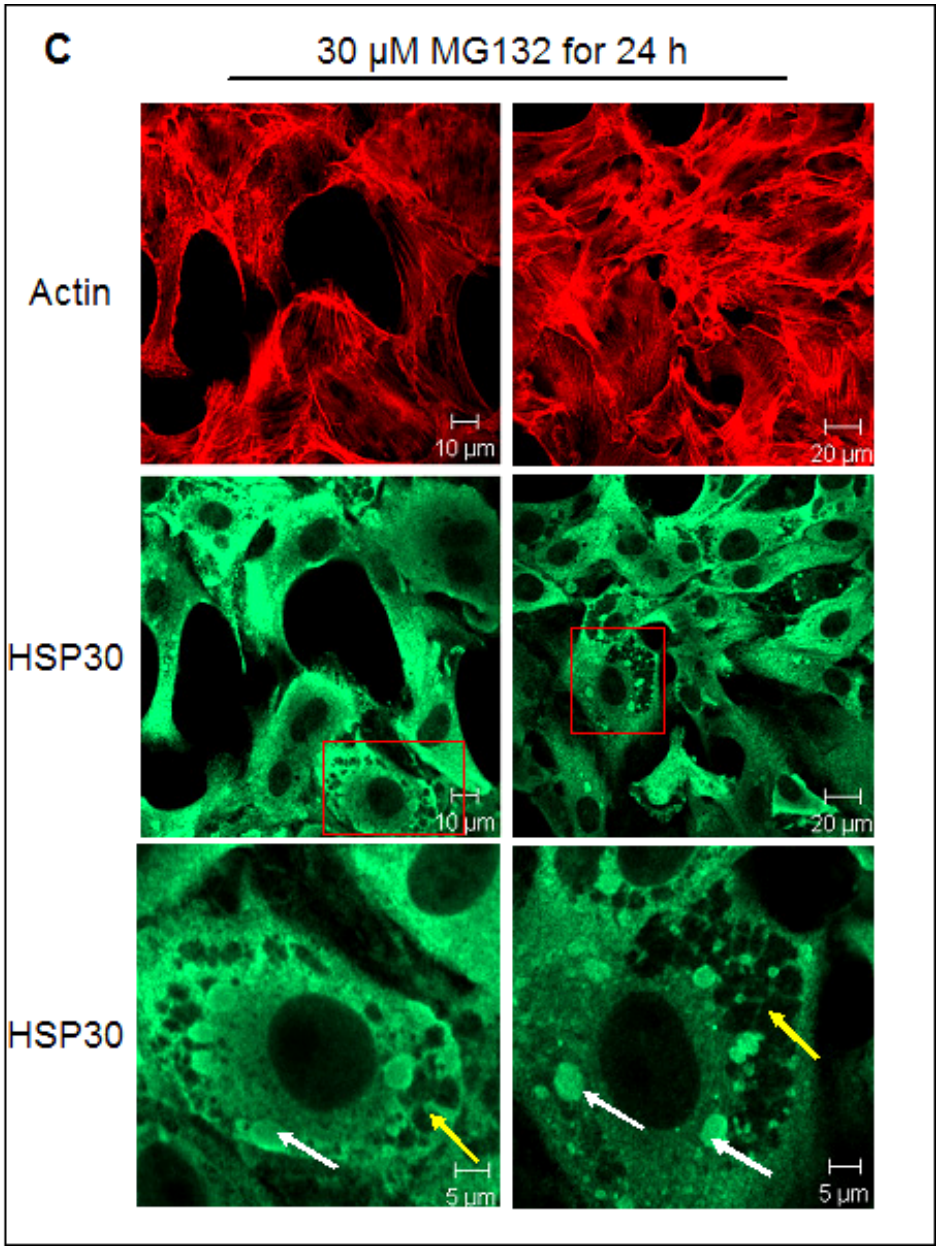
C
30 μM MG132 for 24 h
Actin
HSP30
HSP30
10 μm
20 μm
10 μm
20 μm
5 μm
5 μm

50 μM MG132 for 24 h contained relatively large circular HSP30 staining structures in the cytoplasm (Fig. 19C; white arrows). Secondly, approximately 50% of A6 cells treated with 30 to 50 μM MG132 for 24 h contained large areas within the cytoplasm where HSP30 was not detected (Fig. 19C; yellow arrows). Higher concentrations of MG132 also had an adverse effect on the actin cytoskeleton. In control cells, actin stress fibers transverse the cell in axial bundles and can be a good indicator of cellular viability and health (Fig. 19A; white arrows). When A6 cells were treated with 20 to 50 μM MG132 for 24 h there were fewer actin stress fibers and more actin disorganization. Furthermore, the general shape or morphology of A6 kidney epithelial cells changed after 30 to 50 μM MG132 treatment (Fig. 19B). In control cells, the general shape was cuboidal or short columnar, similar to other epithelial cells. However, after treatment with 30 to 50 μM MG132 the cellular width decreased and the cells became long columnar in terms of morphology.

3.2.4 Analysis of HSP30 and HSP70 accumulation in A6 cells recovering from MG132 treatment

In the present study, A6 cells were treated with 30 μM MG132 for 24 h and were then allowed to recover in fresh (L)-15 media for different time periods ranging from 8 to 48 h. The relative levels of both HSP30 and HSP70 protein were assessed by western blot analysis (Fig. 20A) and densitometry (Fig. 20B). The accumulation of HSP30 significantly ($p < 0.01$) decreased after 8 h of recovery and remained relatively constant from 8 to 24 h of recovery. After 48 h of recovery from MG132 exposure, the relative levels of HSP30 decreased dramatically. The accumulation of HSP30 after 24 h of recovery was 4-fold higher than after 48 h as determined by densitometric analysis. The

Figure 20. HSP30 and HSP70 protein accumulation in A6 cells recovering from MG132 treatment. A) A6 cells were either maintained at 22 ºC or exposed to 30 μM MG132 for 24 h followed by different recovery intervals in fresh (L)-15 media ranging from 8 to 48 h. Total protein was isolated and analysed by immunoblotting as described in the legend of figure 7. B) Image J (Version 1.38) software was used to perform densitometric analysis as outlined in the legend of figure 6. Significant differences between 0 h of recovery and the longer recovery times are indicated as * ($p < 0.05$) or Δ ($p < 0.01$).

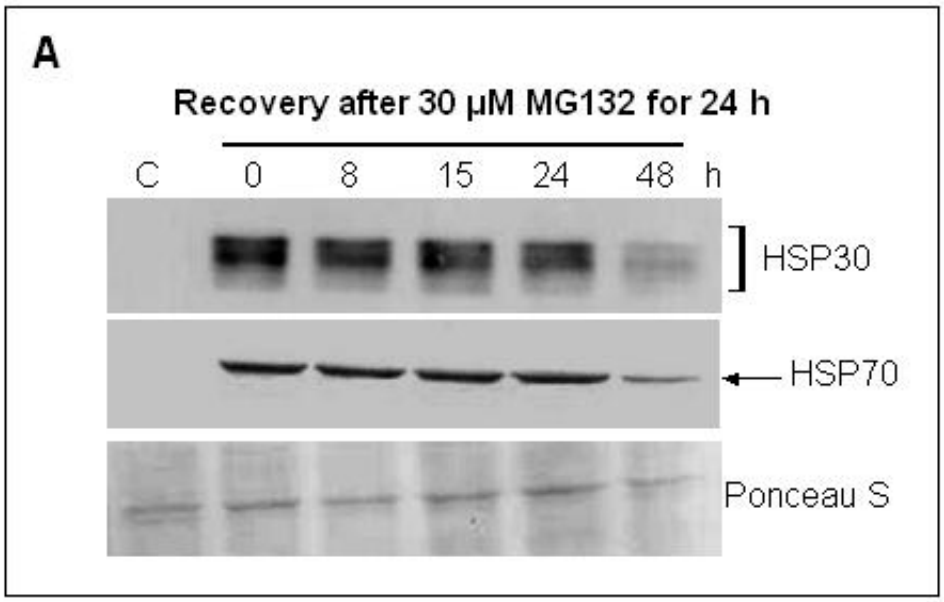
A
Recovery after 30 μM MG132 for 24 h
C
0
8
15
24
48
h
HSP30
HSP70
Ponceau S

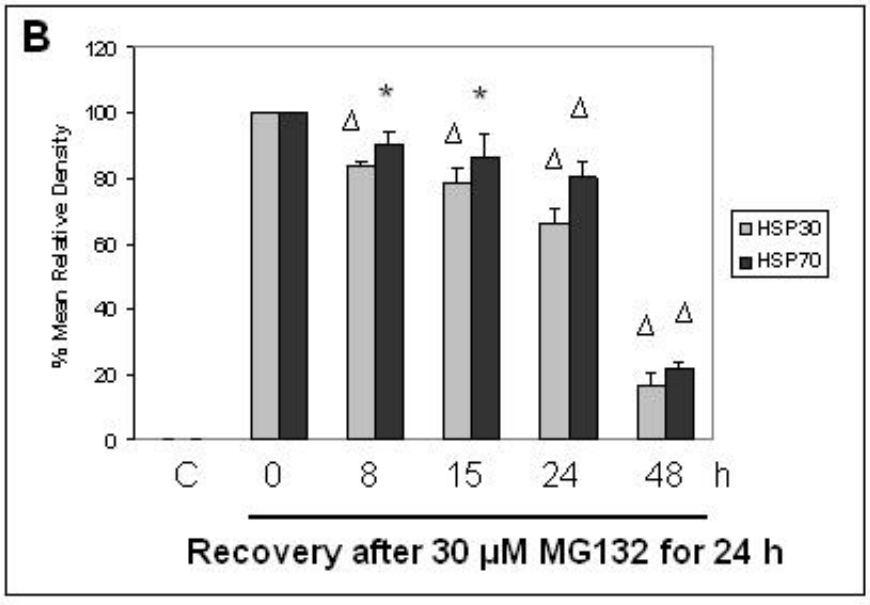
B
% Mean Relative Density
120
100
80
60
40
20
0
HSP30
HSP70
C
0
8
15
24
48
h
Recovery after 30 μM MG132 for 24 h

accumulation of HSP70 also decreased significantly ($p < 0.05$) after 8 h of recovery and remained relatively constant from 8 to 24 h. Between 24 h and 48 h of recovery the relative accumulation of HSP70 also decreased by 4-fold.

The examination of HSP30 accumulation in A6 cells recovering from MG132 treatment was also carried out using immunocytochemistry and LSCM. A6 cells were grown on glass coverslips and then exposed to 30 μM MG132 for 24 h followed by recovery periods in fresh media for 8 to 48 h in duration (Fig. 21). A large amount of HSP30 accumulation was observed in A6 cells treated with 30 μM MG132 for 24 h with no recovery period. Compared to control cells, they had fewer actin stress fibers and obvious actin cytoskeletal disorganization. Similar to the immunoblot analysis (Fig. 20), the accumulation of HSP30 decreased after 8 h of recovery and then remained relatively constant from 8 to 24 h followed by a decrease at 48 h. Interestingly, the actin cytoskeleton displayed a gradual increase in the amount of stress fibers and a decrease in the disorganization as the recovery periods became longer. After 24 h of recovery from MG132 treatment the accumulation of HSP30 was still relatively high but the actin stress fiber pattern was similar to control cells.

3.2.5 The effect of concurrent MG132 and mild heat shock on the accumulation of HSP30 and HSP70 in A6 cells

The effect of treating A6 cells simultaneously with combined MG132 plus heat shock on the accumulation of HSP30 and HSP70 was determined by western blot analysis. First, A6 cells were treated with 30 μM MG132 for 8 h plus different heat shock temperatures, ranging from 24 to 30 ºC (Fig. 22A). In A6 cells exposed to a 30 ºC heat shock for 8 h or 30 μM MG132 for 8 h at 22 ºC, a relatively low level of HSP30 and

Figure 21. HSP30 localization in A6 cells recovering from MG132 exposure. A) A6 cells were grown on glass coverslips and maintained at 22 ºC (image not shown) or treated with 30 μM MG132 for 24 h followed by different recovery times ranging from 0 to 48 h. Actin and nuclei were stained directly with phalloiden conjugated to TRITC (red) and DAPI (blue), respectively. HSP30 was indirectly detected with an anti-HSP30 antibody and a secondary antibody conjugated to Alexa-488 (green).

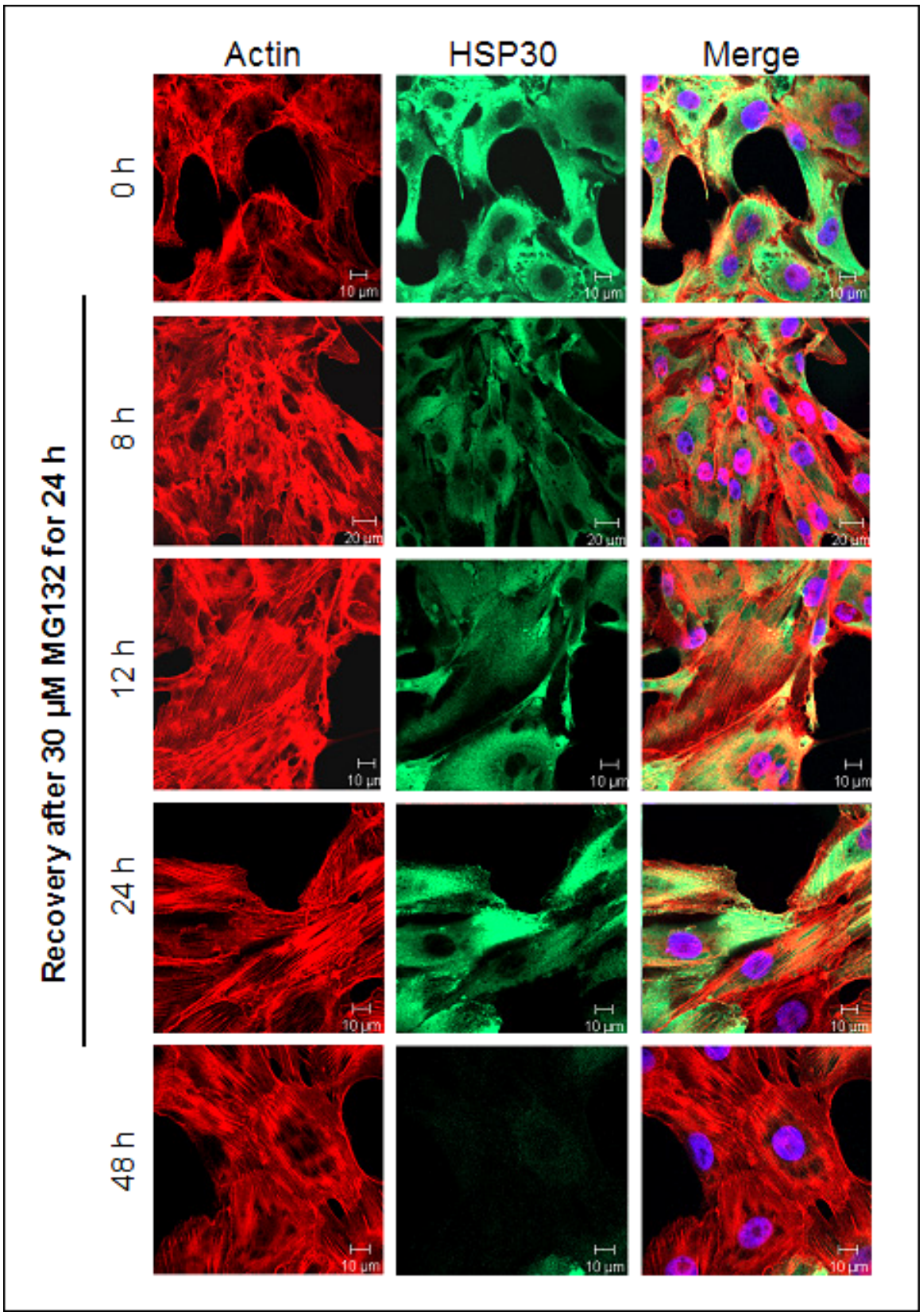
Actin
HSP30
Merge
0 h
8 h
12 h
24 h
48 h
Recovery after 30 μM MG132 for 24 h
10 μm
20 μm

Figure 22. Analysis of HSP30 and HSP70 protein accumulation in A6 cells exposed to elevated temperatures plus MG132. A) A6 cells were maintained at 22 ºC or treated concurrently with 30 μM MG132 plus different temperatures ranging from 22 to 30 ºC for 8 h. Total protein was isolated and analysed by immunoblotting as outlined in the legend of figure 7. B) Image J (Version 1.38) software was used to perform densitometric analysis as outlined in the legend of figure 6. Significant differences between the maximum signal and other treatments are indicated as * ($p < 0.05$) or Δ ($p < 0.01$).

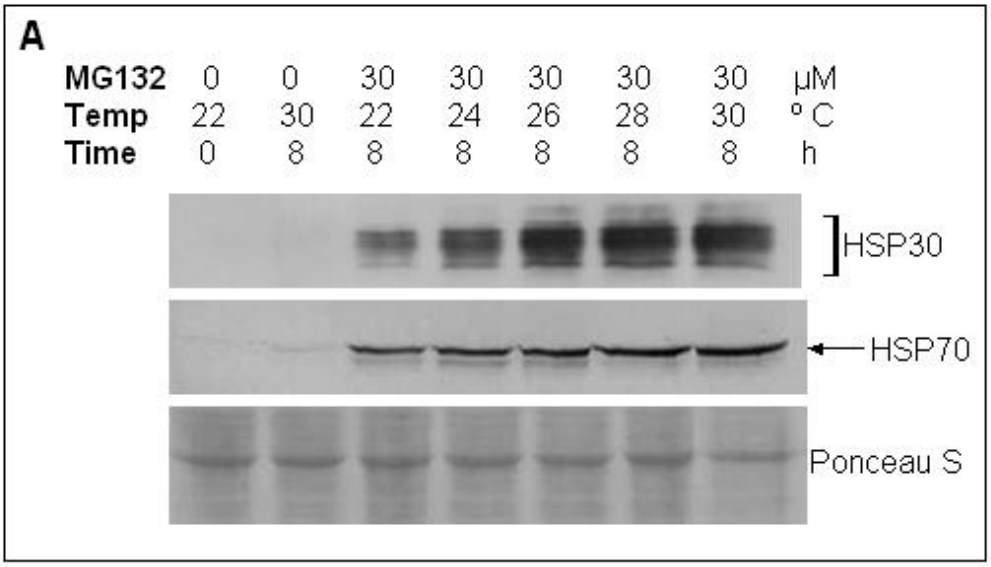
A
MG132 0 0 30 30 30 30 30 µM
Temp 22 30 22 24 26 28 30 ° C
Time 0 8 8 8 8 8 8 h
HSP30
HSP70
Ponceau S

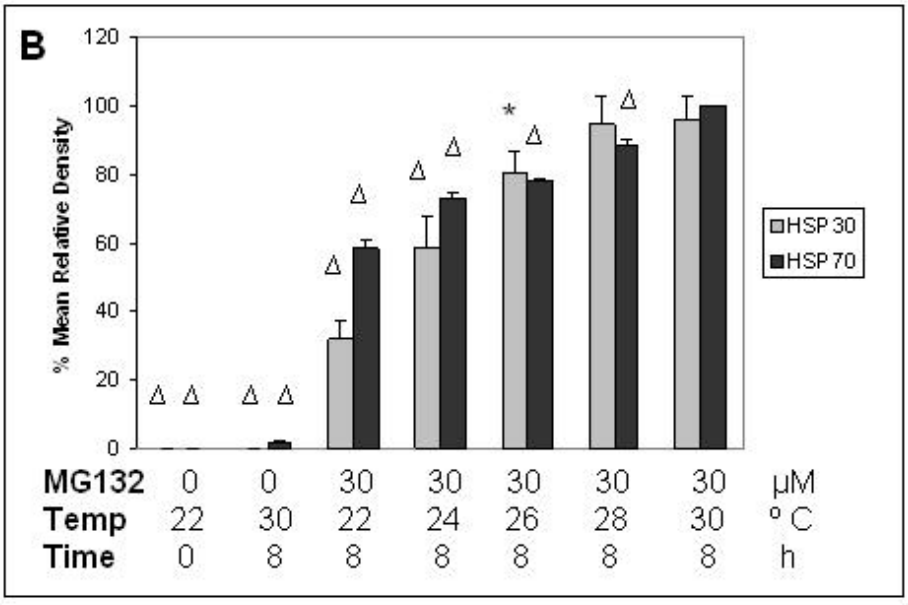
B
% Mean Relative Density
120
100
80
60
40
20
0
HSP 30
HSP 70
MG132 0 0 30 30 30 30 30 µM
Temp 22 30 22 24 26 28 30 ° C
Time 0 8 8 8 8 8 8 h

HSP70 accumulation was detected. However, when these two stressors were applied concurrently for 8 h, the accumulation was higher then the sum of the accumulation of each stressor alone as determined by densitometric analysis (Fig. 22B). In A6 cells treated with 30 μM MG132 for 8 h, the relative accumulation of HSP30 and HSP70 gradually increased as the temperature was elevated from 22 to 30 ºC. The highest accumulation was observed at 30 μM MG132 plus 28 or 30 ºC heat shock for 8 h.

A time course of HSP30 and HSP70 accumulation in A6 cells exposed to concurrent MG132 plus elevated temperature is shown in Figure 23. A6 cells were treated simultaneously with 30 μM MG132 plus a 30 ºC heat shock for time periods ranging from 2 to 8 h (Fig. 23A). In cells treated with concurrent MG132 and elevated temperature the accumulation of HSP30 and HSP70 gradually increased from 2 to 8 h of treatment, with the highest relative accumulation observed from 6 to 8 h. As found in previous experiments, when these stressors were applied concurrently for 8 h, the accumulation was higher then the sum of the accumulation of each stressor alone as determined by densitometry (Fig. 23B).

3.2.6 Involvement of HSF activation in the accumulation of HSP30 and HSP70 in A6 cells treated with MG132

In the present study, a HSF inhibitor, KNK437, was employed to determine if the accumulation of HSP30 and HSP70 in A6 cell was due to HSF activation. A6 cells were exposed to a 33 ºC heat shock for 2 h or 30 μM MG132 for 12 h either singly or after a 6 h pre-treatment with 100 μM KNK437 at 22 ºC (Fig. 24A). A6 cells exposed to a 33 ºC heat shock had a relatively high accumulation of HSP30 and HSP70. When A6 cells were pretreated with KNK437 prior to a heat shock there was an almost complete inhibition of

Figure 23. Time course of HSP30 and HSP70 protein accumulation in A6 cells treated with concurrent MG132 and mild heat shock. A) A6 cells were maintained at 22 ºC or exposed to 30 μM MG132 plus a 30 ºC heat shock for different time intervals ranging from 2 to 8 h in duration. Total protein was isolated and analysed by immunoblotting as outlined in the legend of figure 7. B) Image J (Version 1.38) software was used to perform densitometric analysis as outlined in the legend of figure 6. Significant differences between the maximum signal and other treatments are indicated as Δ ($p < 0.01$).

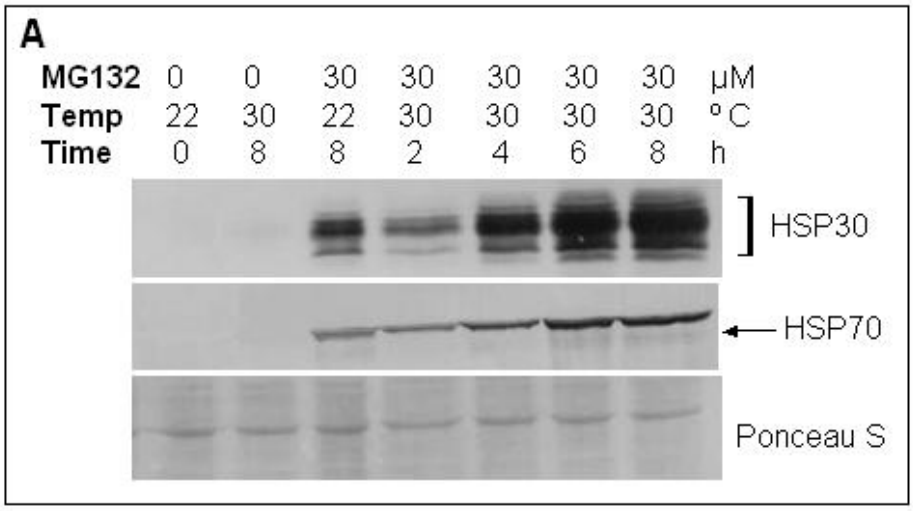
A
MG132 0 0 30 30 30 30 30 µM
Temp 22 30 22 30 30 30 30 °C
Time 0 8 8 2 4 6 8 h
HSP30
HSP70
Ponceau S

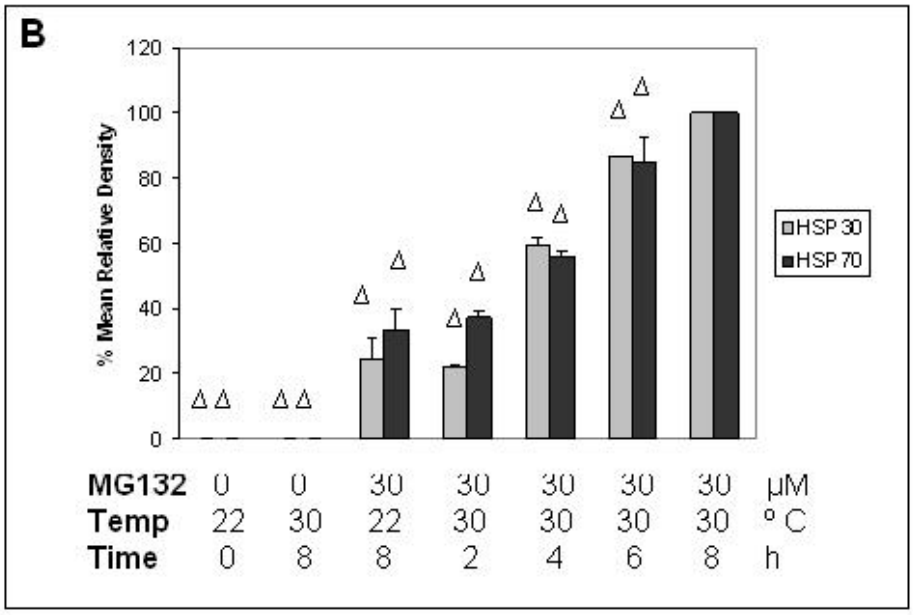
B
% Mean Relative Density
120
100
80
60
40
20
0
HSP 30
HSP 70
MG132 0 0 30 30 30 30 30 µM
Temp 22 30 22 30 30 30 30 °C
Time 0 8 8 2 4 6 8 h

Figure 24. Effect of KNK437 (KNK) on the accumulation of HSP30 and HSP70 protein in A6 cells treated with MG132. A) Cells were maintained at 22 ºC, pretreated with 100 μM KNK437 for 6 h, or pretreated and then exposed to 30 μM MG132 for 12 h. Total protein was isolated and analysed by immunoblotting as detailed in the legend of figure 7. B) Image J (Version 1.38) software was used to perform densitometric analysis as described in the legend of figure 6. Significant inhibition of HSP accumulation by KNK437 is indicated as Δ ($p < 0.01$).

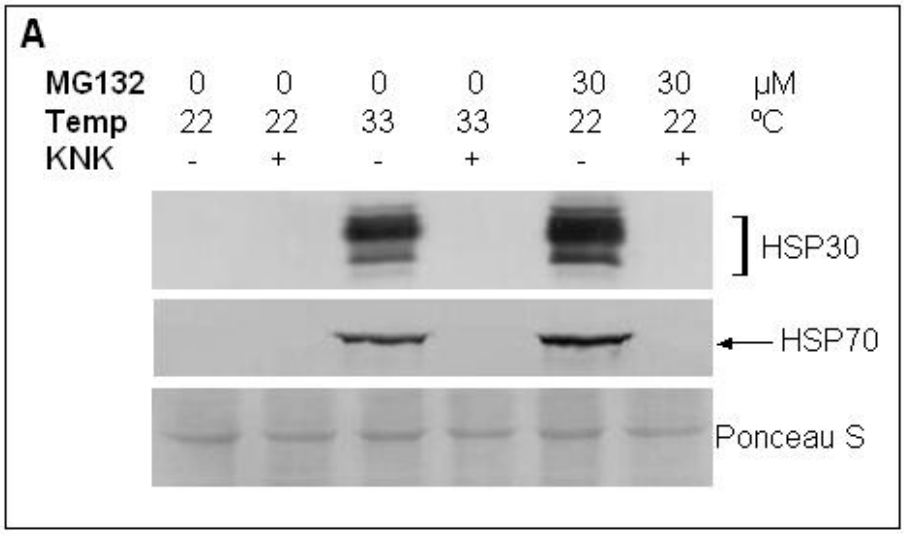
A
MG132 0 0 0 0 30 30 µM
Temp 22 22 33 33 22 22 ºC
KNK - + - + - +
HSP30
HSP70
Ponceau S

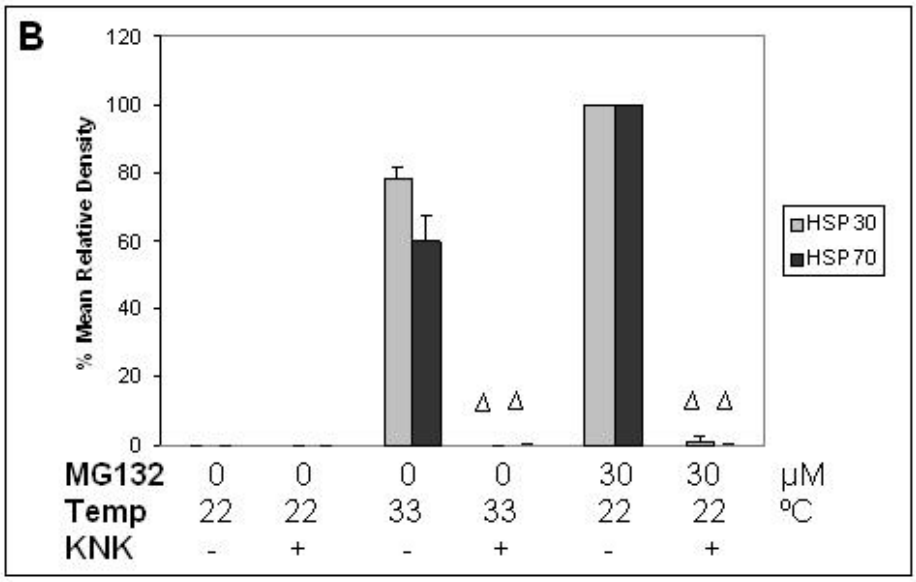
B
% Mean Relative Density
120
100
80
60
40
20
0
HSP 30
HSP 70
MG132 0 0 0 0 30 30 µM
Temp 22 22 33 33 22 22 ºC
KNK - + - + - +

HSP30 and HSP70 accumulation. Similarly, pre-treatment of A6 cells with KNK437 prior to MG132 exposure produced a nearly complete inhibition of HSP30 and HSP70 accumulation. Subsequent densitometric analysis demonstrated that KNK437 caused inhibition of MG132-induced HSP30 and HSP70 accumulation by 99.1% and 99.8%, respectively (Fig. 24B).

The effect of KNK437 on MG132-induced HSP accumulation was also examined by immunocytochemistry and LSCM. A6 cells were grown on glass coverslips and then treated with a 33 ºC heat shock or MG132 either singly or after a 6 h 100 μM KNK437 pre-treatment. After a 33 ºC heat shock or a 30 μM MG132 treatment for 8 or 12 h, A6 cells displayed relatively high levels of HSP30 accumulation (Fig. 25A). Like control cells, those treated with 30 μM MG132 for 8 or 12 h had intact stress fibers as well as little disorganization of the actin cytoskeleton. As shown in Figure 25B, when A6 cells were pretreated with KNK437 prior to a 33 ºC heat shock or 30 μM MG132 for 8 h there was an almost complete inhibition of HSP30 accumulation. The inhibition was less, but still profound, in A6 cells exposed to 30 μM MG132 for 12 h after a KNK437 pre-treatment. The actin cytoskeleton of A6 cells pretreated with KNK437 prior to exposure to 30 μM MG132 for 8 or 12 h had increased cytoskeletal disorganization compared to control.

3.2.7 The effect of MG132 on the acquisition of thermotolerance in A6 cells

A6 cells were pretreated with MG132 prior to a thermal challenge at 37 ºC to assess whether this agent can produce thermotolerance. Shifting the incubation temperature of A6 cells from 22 ºC directly to a 37 ºC thermal challenge for 1 h resulted in the collapse of the actin cytoskeleton (Fig. 26A). It was established that pre-treatment

Figure 25. Effect of KNK437 (KNK) on the localization of HSP30 in A6 cells exposed to MG132. A) A6 cells were grown on glass coverslips and either maintained at 22 ºC, pretreated with 100 μM KNK437 for 6 h, or treated with 30 μM MG132 for either 8 or 12 h. B) A6 cells pretreated with 100 μM KNK437 for 6 h followed by exposure to 30 μM MG132 for either 8 or 12 h. Actin and nuclei were stained directly with phalloiden conjugated to TRITC (red) and DAPI (blue), respectively. HSP30 was indirectly detected with an anti-HSP30 antibody and a secondary antibody conjugated to Alexa-488 (green).

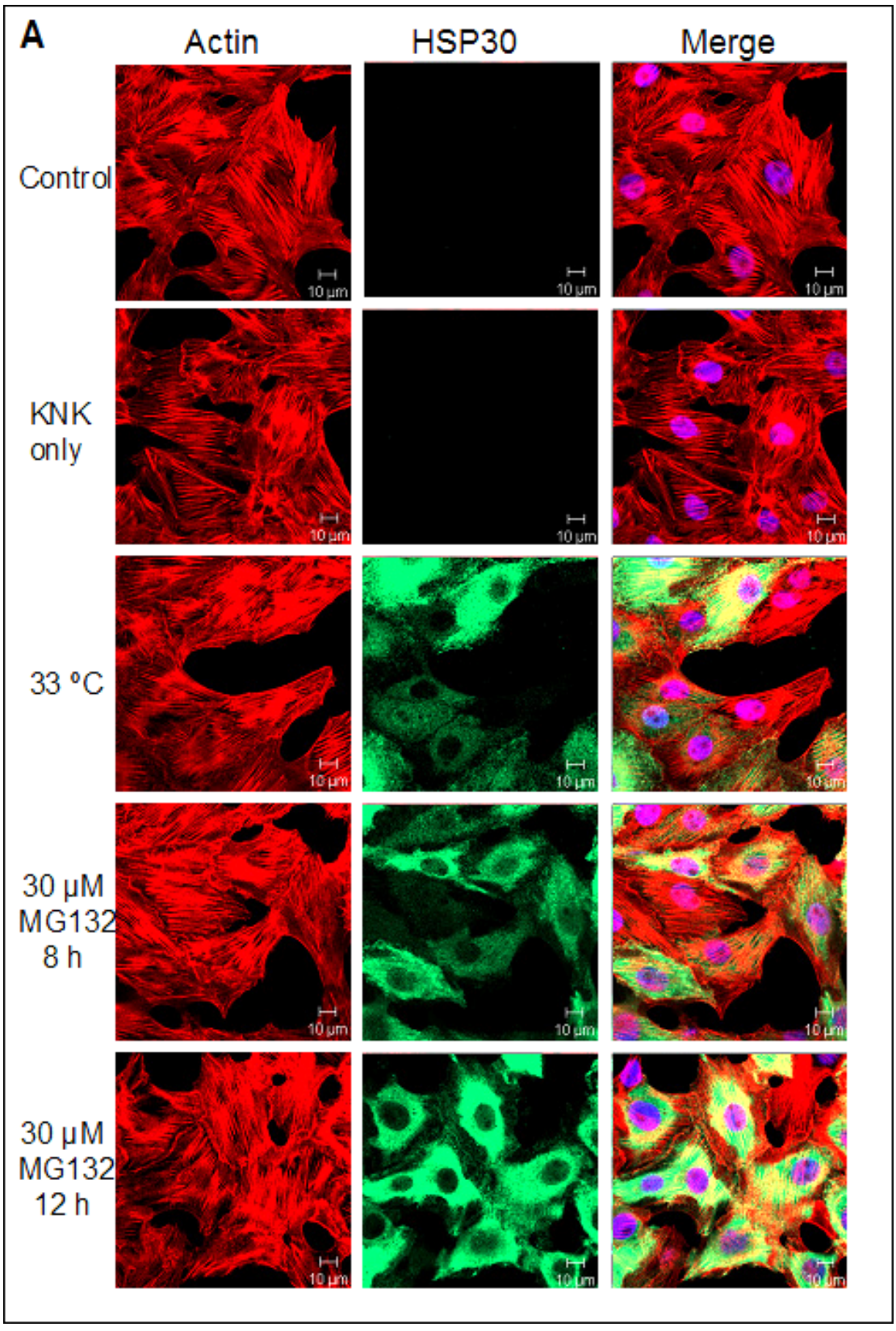
A
Actin
HSP30
Merge
Control
KNK only
33 °C
30 µM MG132 8 h
30 µM MG132 12 h
10 µm

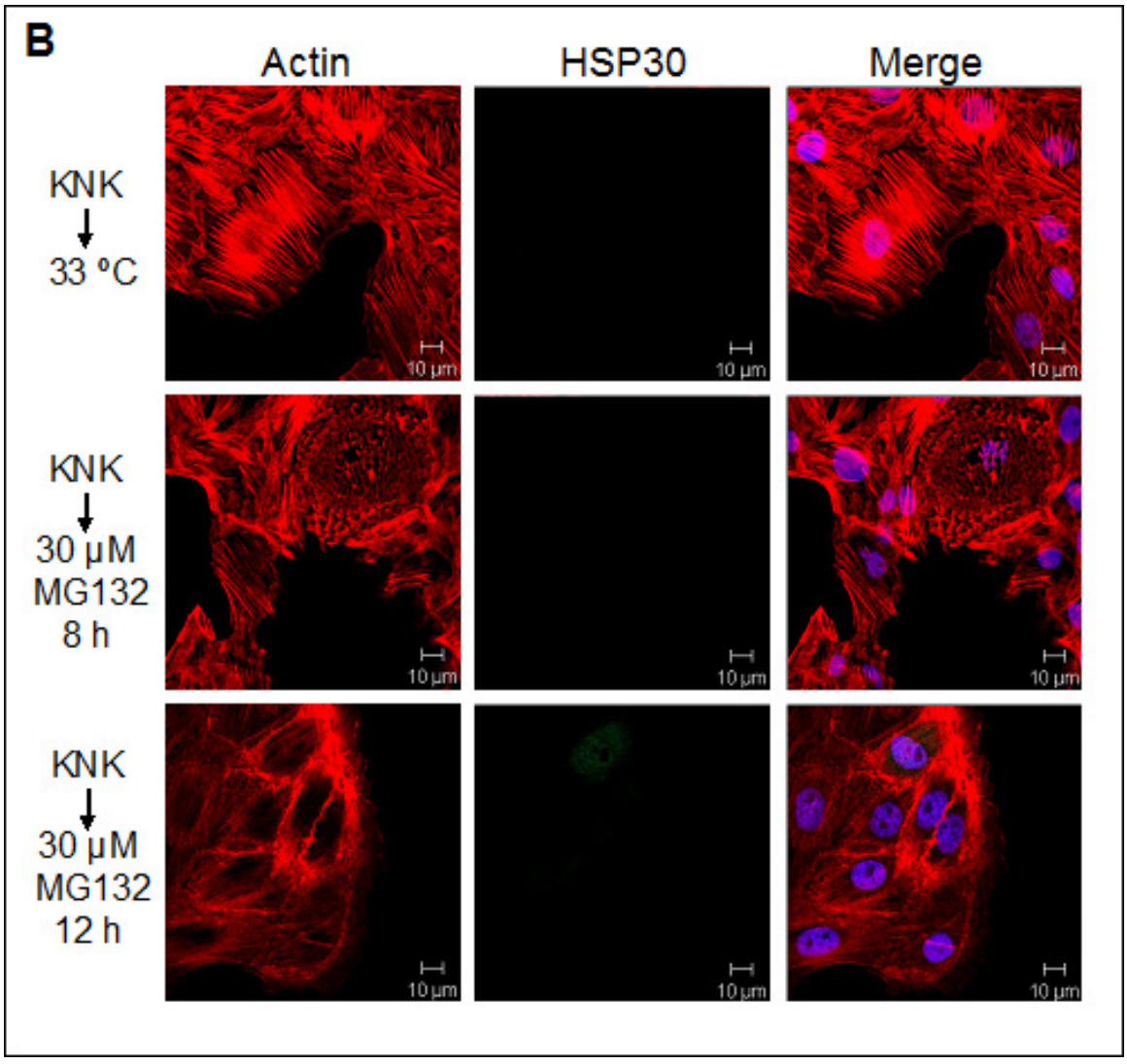
B
Actin
HSP30
Merge
KNK
33 °C
KNK
30 µM
MG132
8 h
KNK
30 µM
MG132
12 h
10 µm

Figure 26. Cytoprotective effects of pre-treating A6 cells with MG132 prior to a 37 ºC thermal challenge. A) A6 cells were grown on glass coverslips and were maintained at 22 ºC, subjected to a 37 ºC thermal challenge, heat shocked at 33 ºC, or exposed to 30 μM MG132 for either 8 or 12 h. B) A6 cells were subjected to a 33 ºC heat shock or 30 μM MG132 for either 8 or 12 h prior to a 37 ºC thermal challenge for 1 h. In the last row, cells were pretreated with 100 μM KNK437 for 6h before exposure to 30 μM MG132 for 12 h and subsequence thermal challenge. Heat shocks and thermal challenges were followed by a 2 h recovery period at 22 ºC. Actin and nuclei were stained directly with phalloiden conjugated to TRITC (red) and DAPI (blue), respectively. HSP30 was indirectly detected with an anti-HSP30 antibody and a secondary antibody conjugated to Alexa-488 (green).

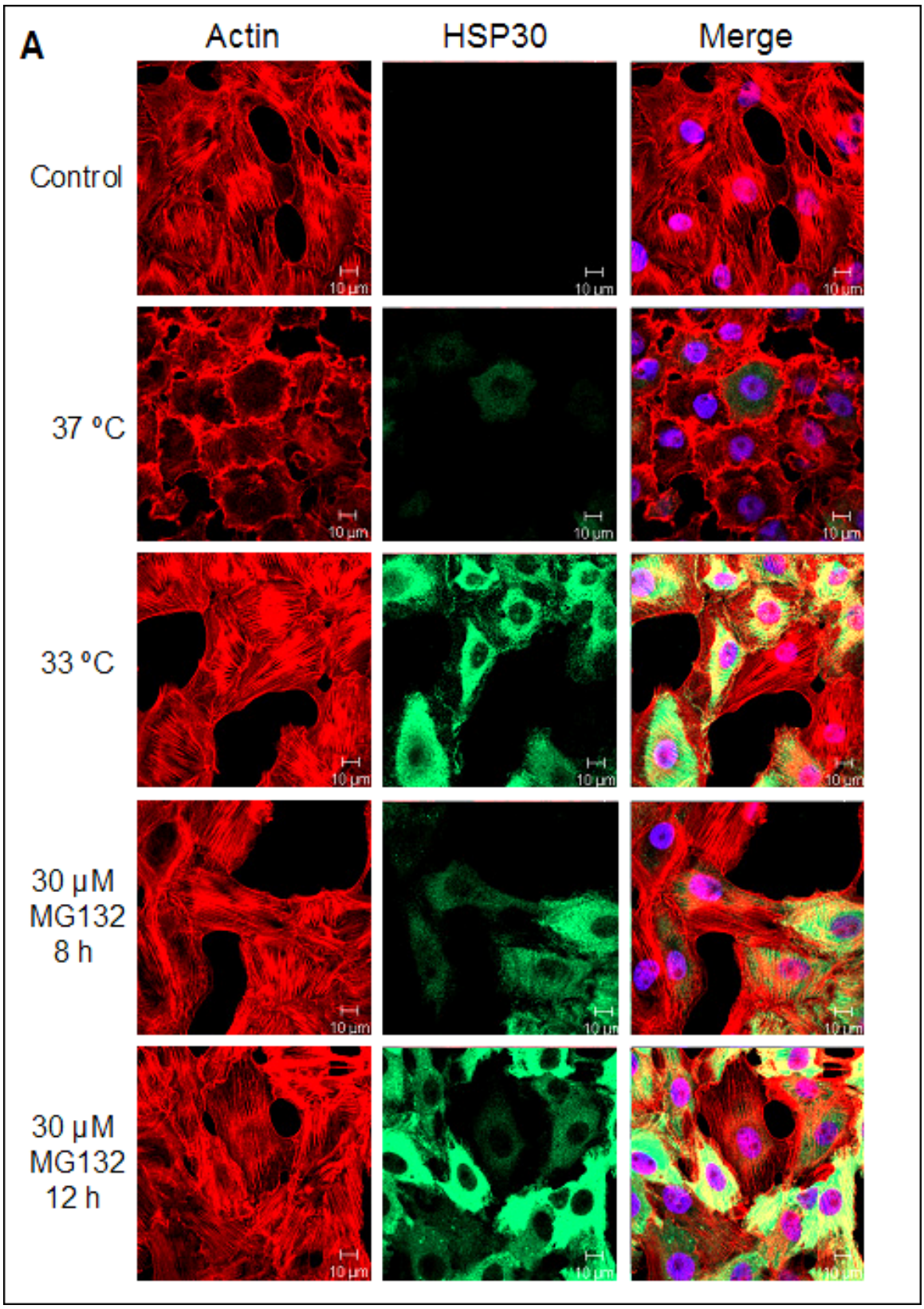
A
Actin
HSP30
Merge
Control
37 °C
33 °C
30 µM MG132 8 h
30 µM MG132 12 h
10 µm

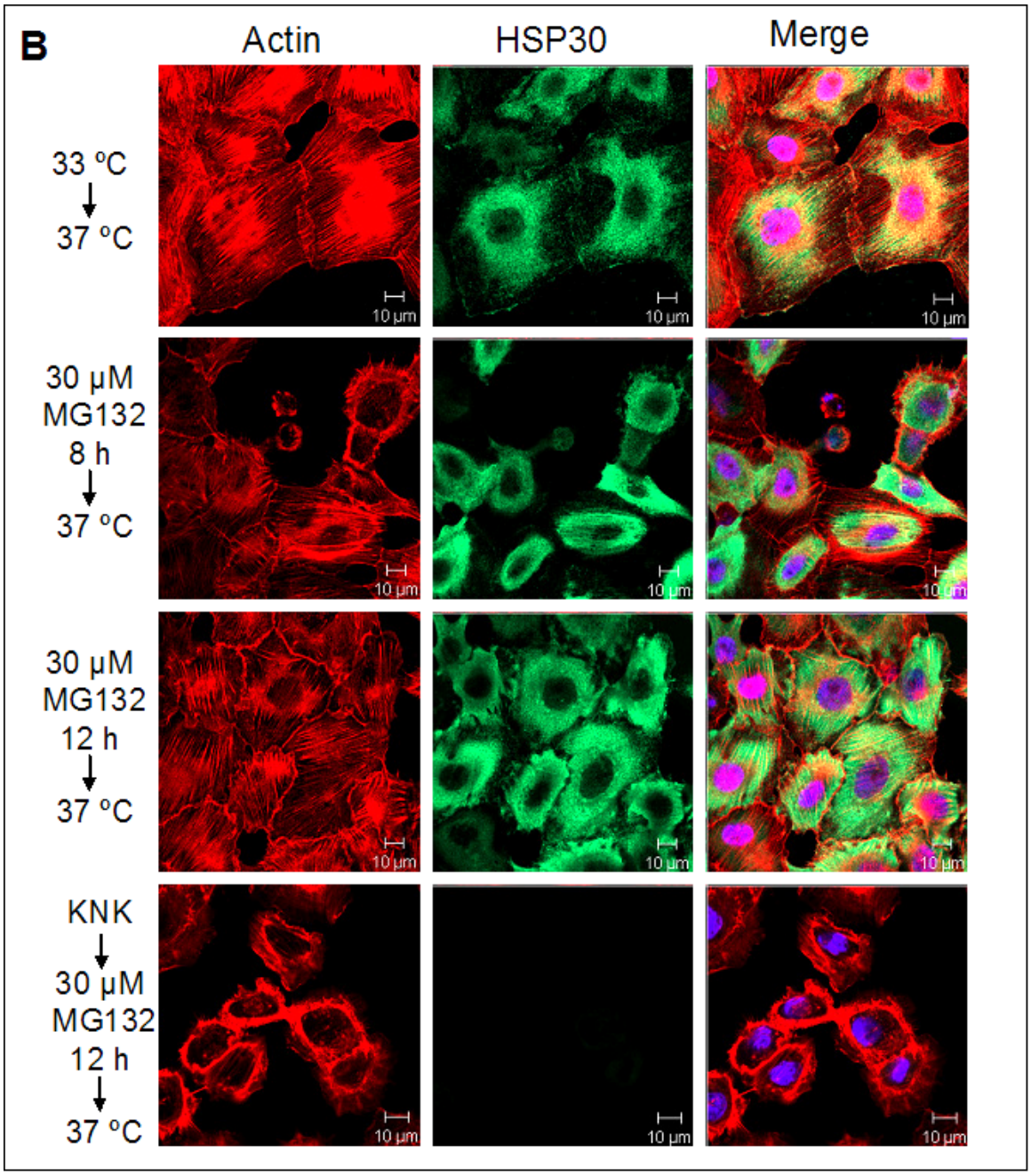
B
Actin
HSP30
Merge
33 °C
37 °C
30 μM
MG132
8 h
37 °C
30 μM
MG132
12 h
37 °C
KNK
30 μM
MG132
12 h
37 °C
10 μm

of A6 cells with a 33 ºC heat shock resulted in the accumulation of HSPs and an acquired state of thermotolerance (Manwell and Heikkila, 2007). Similarly in the present study, A6 cells pretreated with a 33 ºC heat shock prior to a thermal challenge at 37 ºC for 1 h acquired thermotolerance as evidenced by a normal actin cytoskeleton (Fig. 26B). As noted previously, A6 cells treated with 30 μM MG132 for 8 or 12 h had a relatively high accumulation of HSP30. Therefore these conditions were employed in the present thermotolerance studies. As shown in Figure 26B, approximately 50% of A6 cells pretreated with 30 μM MG132 for 8 h prior to a thermal challenge did not have a collapsed actin cytoskeleton and displayed intact stress fibers. However, that number increased to 95% when A6 cells were exposed to 30 μM MG132 for 12 h prior to the thermal challenge. Thus, MG132 pre-treatment was effective at conferring thermotolerance in A6 cells. The accumulation of HSPs in A6 cells maybe responsible for this acquired state of thermotolerance by MG132 since KNK437 pre-treatment, which inhibited the accumulation of HSP30 and HSP70, also resulted in cytoskeletal collapse (Fig. 26B; last row). This suggests an involvement of HSPs in the acquisition of thermotolerance in A6 cells exposed to MG132.

3.2.8 The effect of MG132 treatment on the accumulation of HSP30 and HSP70 in *Xenopus laevis* tadpoles

The next step of this study was to determine the effect of MG132 on the accumulation of HSP30 and HSP70 *in vivo* using *Xenopus laevis* tadpoles. *Xenopus* eggs were collected, fertilized and then allowed to develop until the tadpole stage (approximately stage 45). Tadpoles were then exposed to different concentrations of MG132 ranging from 20 to 70 μM for time periods of 6 to 48 h. Protein was then isolated

and analysed by western blotting. No HSP30 or HSP70 accumulation was detected in tadpoles treated with 20 to 30 μM MG132 for 6 to 48 h (data not shown). As shown in Figure 27, tadpoles exposed to a 33 ºC heat shock for 2 h followed by a 2 h recovery period at 22 ºC had a relatively high accumulation of HSP30 and HSP70. HSP30 accumulation was not detected in *Xenopus laevis* tadpoles until 48 h of 70 μM MG132 treatment. In tadpoles treated with either 50 or 70 μM MG132 there was a gradual increase in the accumulation of HSP70 from 24 to 48 h. The highest HSP70 accumulation was observed in tadpoles exposed to 70 μM MG132 for 48 h. Furthermore, there was no difference in the appearance or morphology of MG132-treated tadpoles compared to control tadpoles (data not shown).

3.2.9 The effect of lactacystin on *hsp30* and *hsp70* gene expression in A6 cells

Although most of this study has focused on MG132, another potent proteasome inhibitor, lactacystin (lacta), was employed to analyze its effect on *hsp30* and *hsp70* gene expression. First, the effect of lactacystin on the accumulation of *hsp30* and *hsp70* message was determined by Northern hybridization analysis (Fig. 28). A6 cells were either maintained at 22 ºC or exposed to different concentrations of lactacystin, ranging from 1 to 20 μM, for 15 h. *Hsp30* mRNA accumulation was not detected at 1 μM lactacystin but from 5 to 20 μM the relative level of this message began to gradually increase. The highest accumulation of *hsp30* mRNA was detected at 20 μM lactacystin for 15 h. Additionally, *hsp70* mRNA accumulation was detected at 1 μM lactacystin and its relative level increased when cells were exposed from 5 to 20 μM.

Figure 27. HSP30 and HSP70 protein accumulation in *Xenopus laevis* tadpoles treated with MG132. Tadpoles were either maintained at 22 ºC, heat shocked at 33 ºC for 2 h followed by a 2 h recovery period at 22 ºC, or treated with 50 or 70 μM MG132 for 6 to 48 h in duration. Total protein was isolated and analysed by immunoblotting as detailed in the legend of figure 7.

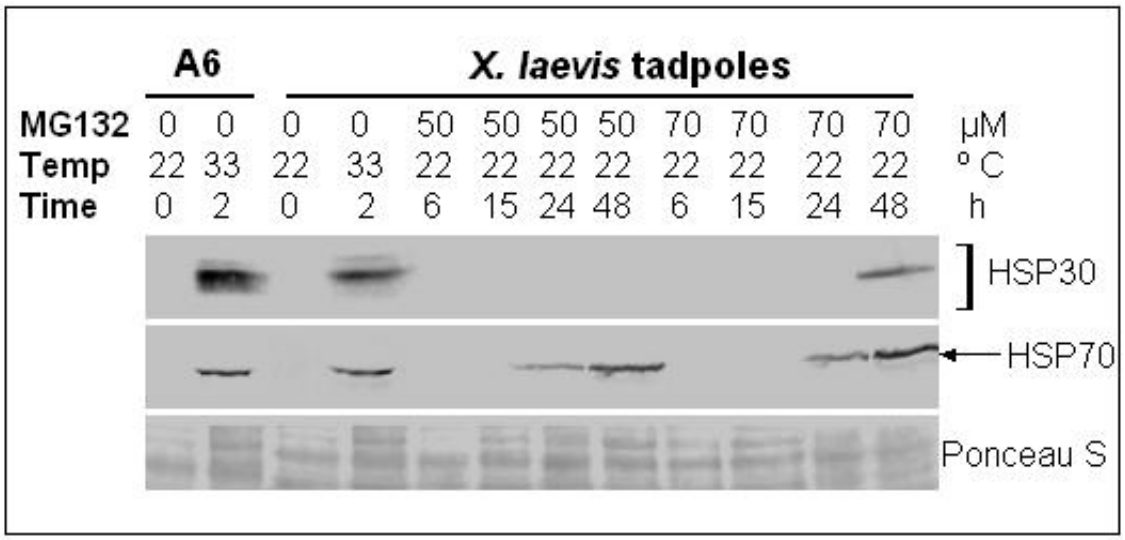
A6
X. laevis tadpoles
MG132 0 0 0 0 50 50 50 50 70 70 70 70 µM
Temp 22 33 22 33 22 22 22 22 22 22 22 22 ° C
Time 0 2 0 2 6 15 24 48 6 15 24 48 h
HSP30
HSP70
Ponceau S

Figure 28. The accumulation of *hsp30* and *hsp70* mRNA in A6 cells treated with different concentrations of the proteasome inhibitor, lactacystin (lacta). A6 cells were either maintained at 22 ºC or exposed to numerous concentrations of lactacystin, ranging from 1 to 20 μM for 15 h in duration. Total RNA was isolated and utilized in Northern hybridization analysis as described in the legend of figure 6.

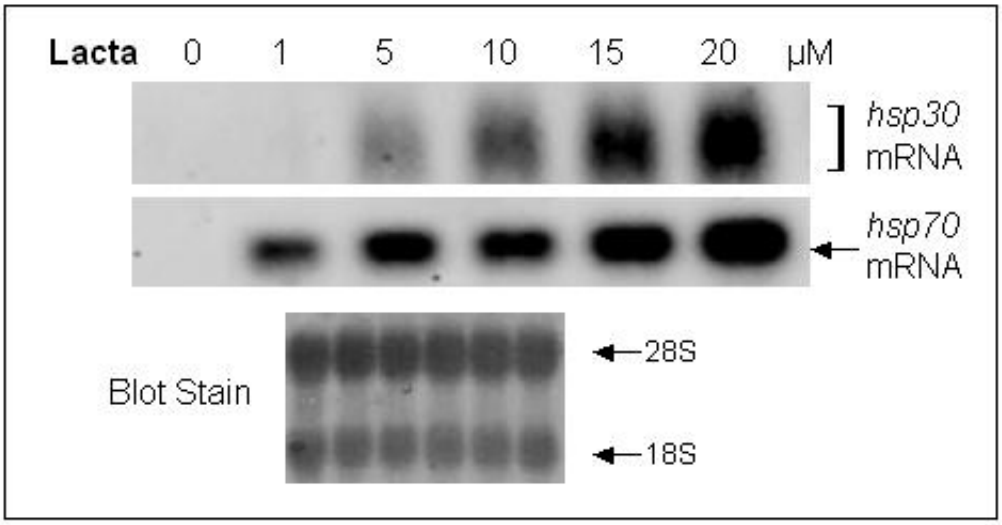
Lacta 0 1 5 10 15 20 µM
hsp30 mRNA
hsp70 mRNA
Blot Stain
28S
18S

The next stage of this study was to analyze the effect of different lactacystin concentrations on the accumulation of HSP30, HSP70 and actin protein in A6 cells by western blot analysis (Fig. 29). A6 cells were either maintained at 22 ºC or treated with different concentrations of lactacystin, ranging from 1 to 20 μM, for 15 h. A very small accumulation of HSP30 was detected in A6 cells treated with 1 μM lactacystin. The accumulation of HSP30 gradually increased in A6 cells treated with 1 to 10 μM lactacystin and the highest levels of this protein occurred from 10 to 20 μM. The accumulation pattern of HSP70 was similar, except that it was more easily detected in cells treated with 1 μM lactacystin. As with MG132, treatment with lactacystin had no effect on the accumulation of actin in A6 cells.

A time course of HSP30, HSP70 and actin accumulation in A6 cells exposed to lactacystin was carried out. A6 cells were either maintained at 22 ºC or treated with 10 μM lactacystin for time periods ranging from 6 to 24 h (Fig. 30). Low levels of HSP30 and HSP70 accumulation were first detected in A6 cells treated with 10 μM lactacystin for 8 h. The accumulation of these proteins increased between 8 and 24 h. Again, lactacystin treatment did not affect the accumulation of actin in A6 cells, as its levels remained constant in each sample.

3.2.10 The effect of lactacystin on the localization of HSP30 in A6 cells

The effect of lactacystin on the localization of HSP30 in A6 cells was determined by immunocytochemistry and LSCM. A6 cells were treated with different concentrations of lactacystin, ranging from 1 to 20 μM, for 15 h (Fig. 31A). A low amount of HSP30 accumulation, in only 30% of cells, was detected at 1 μM lactacystin for 15 h. The accumulation of this protein gradually increased as the concentration of lactacystin

Figure 29. The accumulation of HSP30, HSP70 and actin protein in A6 cells exposed to different concentrations of lactacystin. A6 cells were either left at 22 ºC or treated with various concentrations of lactacystin, ranging from 1 to 20 μM for 15 h. Total protein was isolated and analysed by immunoblotting as detailed in the legend of figure 7.

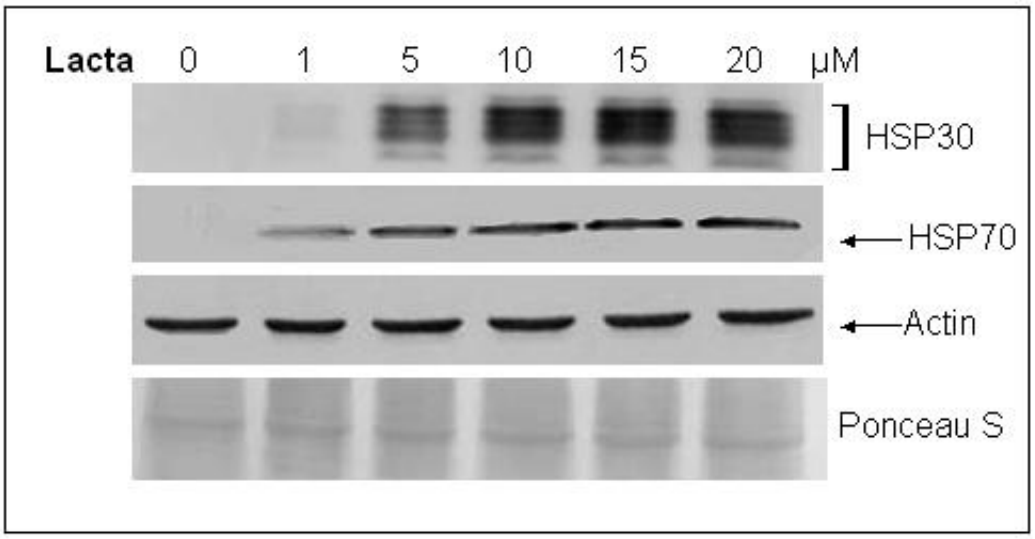
Lacta
0
1
5
10
15
20
μM
HSP30
HSP70
Actin
Ponceau S

Figure 30. Time course of HSP30, HSP70 and actin protein accumulation in A6 cells treated with lactacystin. A6 cells were either maintained at 22 ºC or treated with 10 μM lactacystin for different time intervals ranging from 6 to 24 h in duration. Total protein was isolated and analysed by immunoblotting as detailed in the legend of figure 7.

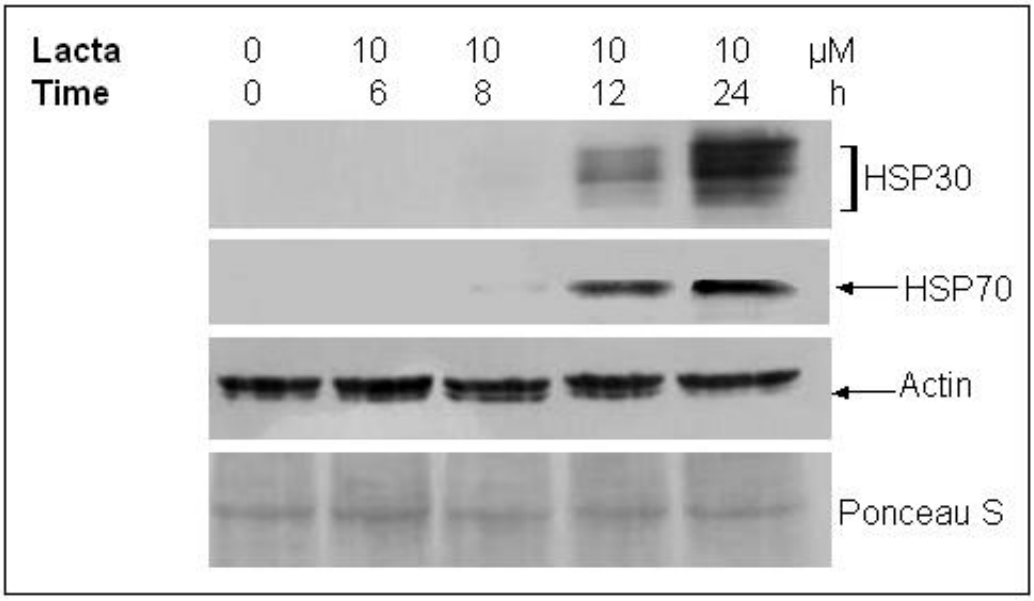
Lacta
Time
0
0
10
6
10
8
10
12
10
24
μM
h
HSP30
HSP70
Actin
Ponceau S

Figure 31. HSP30 localization in A6 cells exposed to different lactacystin concentrations by LSCM. A) A6 cells were grown on glass coverslips and were maintained at 22 ºC or treated with different lactacystin concentrations ranging from 1 to 20 μM for 15 h. B) Interesting HSP30 accumulation patterns observed in A6 cells treated with 15 or 20 μM lactacystin for 15 h. The white arrows indicate large circular cytoplasmic foci of HSP30 accumulation. Actin and nuclei were stained directly with phalloiden conjugated to TRITC (red) and DAPI (blue), respectively. HSP30 was indirectly detected with an anti-HSP30 antibody and a secondary antibody conjugated to Alexa-488 (green).

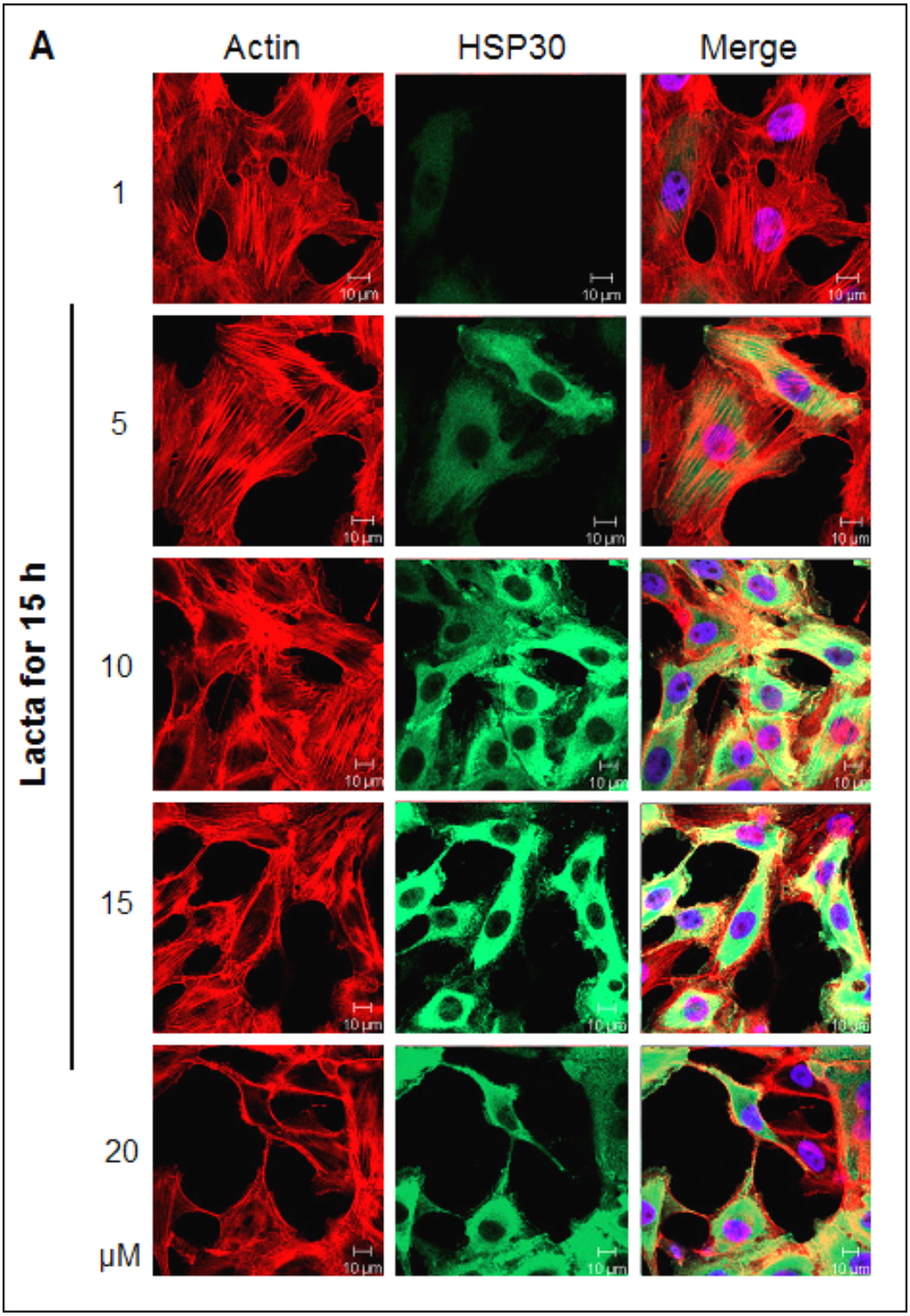
A
Actin
HSP30
Merge
1
5
10
15
20
μM
Lacta for 15 h
10 μm

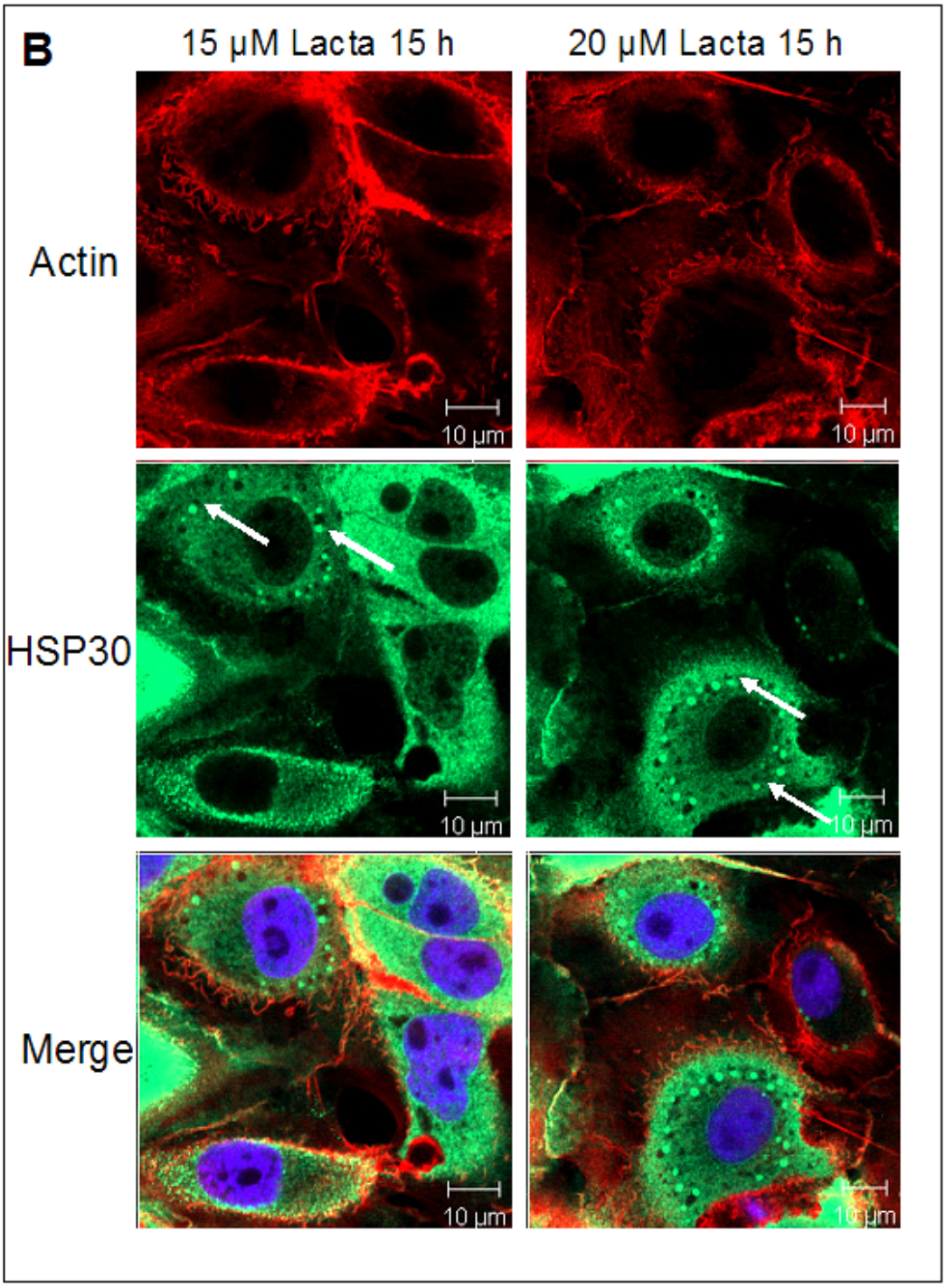
B
15 µM Lacta 15 h
20 µM Lacta 15 h
Actin
HSP30
Merge
10 µm
10 µm
10 µm
10 µm
10 µm
10 µm

increased from 1 to 20 μM. The highest accumulation of HSP30 was observed in A6 cells treated with 20 μM lactacystin for 15 h. In A6 cells treated with lactacystin, HSP30 was localized primarily in the cytoplasm, with a small amount of staining in the nucleus. Relatively large circular HSP30 staining structures were observed in the cytoplasm of 50% of cells treated with 15 to 20 μM lactacystin for 15 h (Fig. 31B; white arrows). As described in section 3.2.2, this pattern of HSP30 accumulation was also observed in MG132-treated A6 cells. As the concentration of lactacystin increased, the disorganization of the actin cytoskeleton became more apparent (Fig. 31A). Moreover, the disorganization of actin stress fibers gradually increased with the concentration of lactacystin. Similar to MG132, A6 cells treated with lactacystin also displayed a change in general shape or morphology from cuboidal or short columnar to long columnar.

4.0 Discussion

The present study has characterized the expression of *Xenopus laevis hsp30* and *hsp70* genes in response to concurrent stressors as well as proteasomal inhibition. In this study, A6 cells treated with sodium arsenite and mild heat shock had an enhanced accumulation of HSP30 and HSP70 compared to cells exposed to the stressors individually. Furthermore, proteasomal inhibition by MG132 and lactacystin also induced the expression of *Xenopus hsp30* and *hsp70* genes. Immunocytochemistry and LSCM verified the accumulation of HSP30 in A6 cells exposed to combined stressors and proteasome inhibitors. However, the intracellular pattern of HSP30 localization induced by the two types of stressors displayed unique features. Finally, both combined stressors and MG132 treatment conferred a state of thermotolerance in A6 cells such that they were able to survive a subsequent thermal challenge.

4.1 The effect of concurrent sodium arsenite and heat shock treatment on the expression of *hsp* genes in A6 cells

Most stress response studies have focused on the effect of individual stressors *in vitro*. However, aquatic organisms, like *Xenopus*, can encounter multiple stressors *in vivo* and usually at low magnitudes. Consequently, in the present study, I characterized the expression of *hsp30* and *hsp70* genes in *Xenopus laevis* A6 kidney epithelial cells in response to simultaneous exposure of low doses of sodium arsenite plus mild heat shock. Exposure of A6 cells to both sodium arsenite (1-10 μM) and a mild heat shock (30 ºC) resulted in enhanced HSP30 and HSP70 accumulation as well as their respective mRNAs. In fact, the relative levels of accumulation induced by the concurrent stresses were greater than the sum of the levels found with each stress individually. An enhanced level

of *hsp* gene expression was also observed when cells were incubated with 10 μM sodium arsenite at relatively mild heat shock temperatures of 26, 28 or 30 ºC. In other studies, relatively mild heat shock temperatures enhanced the induction of *hsp* gene expression in *Xenopus* A6 kidney epithelial cells by simultaneous treatment with relatively low concentrations of herbimycin A, hydrogen peroxide or cadmium chloride (Briant *et al.*, 1997; Muller *et al.*, 2004; Woolfson and Heikkila, 2009). In the rat kidney cell line, NRK-52E, low doses of arsenite or cadmium alone resulted in normal expression of *hsp60*, *hsp70* and *hsp90* genes (Madden *et al.*, 2002). When these low doses were added concurrently the expression of these *hsp* genes was significantly enhanced.

The mechanism for the enhanced expression of *hsp30* and *hsp70* genes induced by concurrent sodium arsenite and heat shock in A6 cells is not known. However, it is likely that the activation of HSF1 is involved since pre-treatment of A6 cells with KNK437, an HSF1 activation inhibitor, repressed the combined stress-induced accumulation of HSP30 and HSP70. As mentioned previously, the signal for HSF1 activation appears to be an accumulation of unfolded protein (Voellmy, 2004; Morimoto, 2008). This signal for HSF1 activation has been described for cells treated with either heat shock or sodium arsenite alone (Zou *et al.*, 1998; Voellmy *et al.*, 2004). Therefore, it is possible that exposure of *Xenopus* A6 cells with the concurrent mild stresses induced the accumulation of unfolded protein to a level that exceeded a set point or threshold level, such that there was a strong activation of HSF1 resulting in the enhanced expression of *hsp* genes. Research supporting a set point or threshold level for HSF1 activation has been demonstrated in a number of organisms including mouse T-

lymphocytes and testis, intertidal mussels, human HeLa cells and *Xenopus* heart (Sarge *et al.*, 1995; Lee *et al.*, 1995; Ali *et al.*, 1997; Buckley *et al.*, 2001; Gothard *et al.*, 2003).

In time course experiments, A6 cells treated with simultaneous mild heat shock and low sodium arsenite concentrations exhibited maximal accumulation of HSP30 and HSP70 at 12 and 15 h. Intriguingly, this pattern of HSP accumulation was similar to the results obtained with higher concentrations of sodium arsenite (20-50 μM) at 22 ºC (Darasch *et al.*, 1988; Gauley and Heikkila, 2006; Voyer and Heikkila, 2008). In contrast, it has been shown that A6 cells exposed to higher heat shock temperatures (e.g. 33 ºC), displayed a transient accumulation of *hsp* mRNA or protein reaching maximal levels after only 2-4 h. In the present study, A6 cells recovering from concurrent stress treatment displayed elevated levels of HSPs for at least 15 h after removal of the stressors. Again, this pattern of HSP accumulation was parallel to recovery of A6 cells from treatment with higher concentrations of sodium arsenite rather than from heat shock, which displayed a more rapid decline in the relative levels of HSPs (Darasch *et al.*, 1988). In the present study, the reason for the similarity between the extended pattern of *hsp* gene expression during time course and recovery experiments induced by combined stress or higher sodium arsenite concentrations is not known. Since sodium arsenite can cause oxidative damage of cellular protein (Del Razo *et al.*, 2001), it is possible that this phenomenon was elicited when A6 cells were treated concurrently with both stresses. This could lead to a prolonged accumulation of unfolded proteins that would result in an extended pattern of HSF1-mediated *hsp* gene expression.

Immunocytochemistry and LSCM verified the enhanced accumulation of HSP30 in A6 cells treated concurrently with low sodium arsenite concentrations and a mild heat

shock compared to the stresses individually. HSP30 accumulation occurred primarily in the cytoplasm in a punctate pattern with a lesser amount in the nucleus. This pattern, which was readily detected in cells treated with 5-10 μM sodium arsenite at 30 ºC, was similar to our previous findings in A6 cells subjected to heat shock or sodium arsenite treatment alone (Gellalchew and Heikkila, 2005; Voyer and Heikkila, 2008). The punctate pattern of HSP30 accumulation in A6 cells may be due to the stress-induced formation of HSP30 multimeric structures (Ohan *et al.*, 1998b), which appears to be necessary for sHSP function (MacRae, 2000; Van Montfort *et al.*, 2002). In the present study, the combined stress conditions did not cause detectable disruptions in the actin cytoskeleton, which has been used an indicator of cellular viability and health (Wiegant *et al.*, 1987; Ohtsuka *et al.*, 1993). This is in contrast to treatment of A6 cells with higher concentrations of sodium arsenite, which resulted in a disruption or even a total collapse of the actin cytoskeleton (Gellalchew and Heikkila, 2005).

Finally, this study determined that treatment of A6 cells with concurrent sodium aresenite and heat shock not only induced the accumulation of HSPs but also conferred thermotolerance. This was not observed when the cells were treated with the stresses individually. Previous studies in A6 cells found that a 33 ºC heat shock resulted in the production of HSPs and the acquisition of thermotolerance (Phang *et al.*, 1999; Manwell and Heikkila, 2007). In the present study, the acquisition of thermotolerance by simultaneous sodium arsenite and heat shock treatments required *hsp* gene expression since it was repressed by KNK437. The ability of A6 kidney epithelial cells to respond to two relatively mild stresses and produce an enhanced accumulation of HSPs that can protect them from a subsequent potentially lethal stress is certainly advantageous for

survival. This is advantageous because HSPs are synthesized to prevent or ameliorate the deleterious effects of stress-induced misfolded, damaged or aggregated protein. The current analysis in kidney cells is of importance given arsenite-induced nephrotoxicity in febrile mammals or poikilothermic animals subjected to elevated environmental temperatures. Additionally, the concept of using two relatively mild stressors to induce an enhanced level of *hsp* gene expression may be a strategic method to elevate HSP levels with minimal cellular damage. This is of importance given that upregulation of cellular HSPs has been proposed as a possible therapeutic strategy for protein conformational diseases (Westerheide and Morimoto, 2005).

Future experiments studying the expression of *hsp* genes in response to concurrent sodium arsenite and heat shock may involve an analysis of expression during *Xenopus* embryogenesis. Furthermore, providing additional evidence for the mechanism of *hsp* gene expression in response to this combined treatment would be beneficial. For example, the utilization of HSF1 antisense morpholino oligonucleotides could theoretically inhibit the accumulation of HSF1 and therefore the heat shock response in *Xenopus* A6 cells and embryos treated with combined stressors. Also, microinjection of HSF1 antibody, to inactive HSF1 function, could be a viable approach in *Xenopus* embryos.

4.2 The effect of proteasomal inhibition on the expression of *hsp* genes in *Xenopus laevis*

Previous studies have shown that inhibiting the activity of the proteasome leads to the accumulation of damaged or unfolded proteins within the cell (Lee and Goldberg, 1998b; Johnston *et al.*, 1998). Under stress conditions, unfolded protein is thought to be

the signal for the activation of *hsp* gene expression (Voellmy *et al.*, 2004). Therefore, in the present study, my goal was to determine whether inhibitors of the proteasome could elicit the expression of stress-inducible *hsp* genes in *Xenopus laevis.* In initial experiments, A6 cells treated with the proteasome inhibitors, MG132 and lactacystin, exhibited an increased accumulation of cellular proteins conjugated to ubiqutin. Increased levels of ubiquitinated proteins within the cell was used in other studies as a method to confirm efficient proteasome inhibition (Mimnaugh *et al.*, 1997; Melikova *et al.*, 2005). My findings suggest that A6 cells exposed to MG132 and lactacystin had decreased proteasomal activity. This study has shown, for the first time in amphibians, that exposure to MG132 and lactacystin resulted in detectable levels of HSP30 and HSP70 protein as well as their respective mRNAs. Moreover, this accumulation occurred in a dose- and time-dependent manner. *Hsp* gene expression in response to proteasome inhibition has also been described in other organisms. In yeast, inhibition of protein degradation by MG132 caused a coordinate induction of many HSPs, including HSP70 and HSP104 (Lee and Goldberg, 1998b). In several *Drosophila* cell lines, genome microarrays uncovered that proteasomal inhibition by MG132 caused an enhanced expression of HSP27 and HSC70 (Lundgren *et al.*, 2005). Furthermore, in rainbow trout liver cells (RTLW) exposed to MG132 there was an increase in the accumulation of HSP70 as well as a drastic elevation in HSF2 activation and nuclear localization (Le Goff *et al.*, 2004). Proteasomal inhibition has also been shown to induce or enhance *hsp* gene expression in mammalian systems: HSP70 and BiP in Madin-Darby canine kidney cells; HSP27, HSP60, HSP70 and HSP90 in neonatal rat cardiomyocytes; HSP72 in Caco-2 human intestinal epithelial cells and HSP27 and αB-crystallin in αTN4-1 murine lens

epithelial cells (Bush *et al.*, 1997; Stangl *et al.*, 2002; Pritts *et al.*, 2002; Awasthi and Wagner, 2005).

The present study has also demonstrated that MG132 induced the accumulation of HSP30 and HSP70 in *Xenopus laevis* tadpoles. In mouse embryos, McMillan *et al.* (2002) demonstrated an increase in the expression and activation of HSF2 by lactacystin treatment. Compared to A6 cells, a higher dose of MG132 as well as increased time of exposure was necessary to detect HSP30 and HSP70 in tadpoles. Similarly, in a study examining the effect of proteasome dysfunction on development it was revealed that a high concentration of MG132 (200 μM) was necessary to completely inhibit the proteasome in *Xenopus* embryos (Iijima *et al.*, 2003). These results may be a consequence of slower uptake of MG132 into embryonic tissues. Decreased uptake of cadmium into early *Xenopus* embryos was suggested to be a consequence of the protective vitelline membrane and cortex (Herkovits *et al.*, 1998).

The molecular and cellular mechanisms that lead to stress-inducible *hsp* gene expression during proteasomal inhibition are unclear. Since the proteasome degrades about 80-90% of all proteins, inhibition of this process results in a substantial increase in the concentration of total cellular protein (Lee and Goldberg, 1998a). Damaged or aged proteins, normally degraded by the proteasome, are prone to misfolding which can result in the exposure of their hydrophobic amino acid residues and subsequent aggregation. The accumulation of unfolded cellular protein by proteasomal inhibition may therefore trigger the activation of HSF. In the present study, KNK437 inhibited HSP30 and HSP70 accumulation suggesting that the activation of HSF1 was associated with MG132-induced *hsp* gene expression. In other studies, HSF activation in response to MG132 was

reported in the chicken erythroblast cell line, HD6, where the activities of HSF1, HSF2 and HSF3 were up-regulated (Kawazoe *et al.*, 1998). Moreover, in mouse embryonic fibroblast (MEF) cells, both MG132 and lactacystin induced hyperphosphorylation, trimerization and HSE-binding activity of HSF1 (Kim *et al.*, 1999).

The present study also investigated the pattern of *hsp* gene expression in A6 cells recovering from MG132 treatment. A6 cells treated with 30 μM MG132 for 24 h had a relatively high accumulation of HSP30 and HSP70 and it remained elevated for up to 24 h after the removal of MG132. At 48 h post-treatment, the relative levels of these HSPs decreased substantially. A prolonged accumulation of HSPs in cells following proteasomal inhibition was also documented in rat neonatal cardiomyocytes and Chinese hamster ovary (CHO) cells (Stangl *et al.*, 2002; Kovacs *et al.*, 2006). However, there is no experimental evidence to explain this pattern of HSP accumulation. This pattern could be present because MG132 has a long half-life (Lee and Goldberg, 1998a) and continues to inhibit proteasome function after its removal from the media. Furthermore, it may take the cell time to degrade all of the ubiquitinated cellular proteins that have accumulated during proteasomal inhibition. The combination of these two possibilities may explain the prolonged accumulation of HSP30 and HSP70 in A6 cells recovering from MG132 exposure.

Immunocytochemistry and LSCM was employed to determine the localization of HSP30 in A6 cells exposed to MG132 or lactacystin. In both instances, HSP30 accumulation occurred primarily in the cytoplasm in a punctate pattern with a lesser amount in the nucleus. As stated previously, the punctate pattern of HSP30 accumulation in A6 cells may be due to the stress-induced formation of HSP30 multimeric structures

(Ohan *et al.*, 1998b). Some A6 cells treated with higher concentrations of MG132 and lactacystin displayed relatively large cytoplasmic foci containing HSP30 accumulation. This localization pattern may be due to the formation of cellular aggregates of unfolded protein. As a molecular chaperone, HSP30 could localize to these aggregates in an attempt to render them soluble. These HSP30-containing cytoplasmic foci could also be stress granules. A study by Mazroui *et al.* (2007) observed the formation of cytoplasmic foci called stress granules in response to proteasomal inhibition by MG132. Decreased proteasome activity has been shown to reduce translation initiation (Vabulas and Hartl, 2005). It was reported that interfering with proteasome function prevented the rapid decay of a reporter mRNA containing AU-rich elements (AREs) in its 3' UTR region (Laroia *et al.*, 1999). The rapid decay of messages containing AREs also involves regulatory factors called AU-binding proteins (AUBPs) that can positively or negatively effect this process (Fan and Steitz, 1998). Some AUBPs, such as HuR, can protect these ARE mRNAs from the decay machinery. It has been well established that under stress conditions the stabilization of ARE-containing mRNAs correlates with the recruitment of some of the AUBPs, such as HuR, to cytoplasmic stress granules. Interestingly, in HeLa cells, HSP70 has been found to localize to stress granules upon proteasome inhibition (Mazroui *et al.*, 2007). Therefore, in the present study, it is possible that HSP30 could be localizing to stress granules in response to MG132 treatment. Also, a study by Johnston *et al.* (1998) discovered that exposure of human embryonic kidney (HEK) or CHO cells with proteasome inhibitors caused aggregated cellular protein to accumulate in a distinct region within the cell that was termed the aggresome. Unfolded proteins that are beginning to aggregate first form large cytoplasmic inclusion bodies which are then

delivered to the aggresome by a dynein-based retrograde transport on microtubules (Garcua-Mata *et al.*, 1999). Aggresome formation is accompanied by redistribution of the intermediate filament protein vimentin to form a cage surrounding a pericentriolar core of aggregated protein. In the present study, the large cytoplasmic foci containing HSP30 could potentially be inclusion bodies prior to their delivery to the aggresome by microtubules. HSP30 oligomeric structures could be present within inclusion bodies in an attempt to keep these cellular proteins in a folding competent state. This is supported by experiments in human glioma cells where HSP27 and αB-crystallin co-localized with inclusion bodies and the aggresome in response to proteasome inhibition (Ito *et al.*, 2002). I attempted to examine whether these cytoplasmic foci containing HSP30 co-localized with vimentin in A6 cells. However, after attempts with several antibodies, I was unable to detect vimentin by immunocytochemistry and LSCM in *Xenopus* A6 cells (data not shown). Another unique HSP30 accumulation pattern observed in some A6 cells treated with high concentrations of MG132 was the presence of distinct regions within the cytoplasm where HSP30 did not accumulate. The identity and the mechanism involved in the formation of this accumulation pattern is not known. One possibility is that unfolded proteins localize to the large cytoplasmic HSP30-containing foci. Therefore, the surrounding areas, which contain very little unfolded protein, would have a very low level of HSP30 since it is not required. In support of this possibility a study by Johnston *et al.* (1998) showed that the green fluorescent protein (GFP)-tagged cystic fibrosis transmembrane conductance regulator (CFTR) accumulated within inclusion bodies and the aggresome in response to proteasomal inhibition and was substantially depleted elsewhere in the cytoplasm.

The present study also determined that treatment of A6 cells with higher concentrations of MG132 and lactacystin caused a disruption in the organization of the actin cytoskeleton. This cytoskeletal disruption in response to proteasomal inhibition was reported in both mammals and plants (Verschuure *et al.*, 2002; Sheng *et al.*, 2006; Csizmadia *et al.*, 2008). In A6 cells recovering from MG132, the organization of the actin cytoskeleton began to gradually return to normal 12 h after MG132 removal. By 48 h of recovery the organization was comparable to control cells. The present results are not surprising since numerous studies have shown that proteasomal inhibition by MG132 is reversible after removal of the inhibitor (Rock *et al.*, 1994; Lee and Goldberg, 1998a).

The present study also determined that A6 cells acquired a state of thermotolerance when treated with MG132, such that they were able to survive a subsequent thermal challenge at 37 ˚C. Thermotolerance following proteasomal inhibition has been reported in yeast, rat cardiomyocytes, canine kidney cells and also human fibroblast cells (Bush *et al.*, 1997; Lee and Goldberg, 1998b; Luss *et al.*, 2002; Bonelli *et al.*, 2004). In the present study, *hsp* gene expression was required for this state of thermotolerance since it was repressed by KNK437. Together these findings suggest that MG132-induced HSP accumulation can protect cells from injury or other stresses.

This study has provided useful information regarding the expression of *hsp* genes in response to proteasomal inhibition in *Xenopus laevis*. Proteasome dysfunction and *hsp* gene expression have been implicated in numerous neuropathologies, including Alzheimer's disease (Morimoto, 2008). A consistent feauture of Alzheimer's disease is the presence of ubiquitinated tau-positive inclusion bodies containing HSPs in oligodendrocytes (Goldbaum and Richter-Landsberg, 2004). This suggests that the

proteasome and HSPs have an essential role in maintaining tau protein homeostasis and dysfunction of these processes could lead to pathology.

Future studies examining proteasome inhibitor-induced *hsp* gene expression in *Xenopus* may include an analysis of this phenomenon during early development. Also, a characterization of the expression of other *hsp* genes in *Xenopus*, such as *hsp47, hsp90, hsp110 and BiP* could be carried out. Future experiments could also analyse the mechanism of actin cytoskeletal disruption in A6 cells exposed to MG132 and lactacystin. Additionally, experimental evidence is needed to explain the large cytoplasmic foci containing HSP30 observed in A6 cells exposed to MG132 and lactacystin. For example, a test for co-localization of HuR and HSP30, utilizing immunocytochemistry and LSCM, would help to determine if these foci are stress granules. Also, additional experimentation would be useful to determine whether vimentin co-localizes to the foci, which would provide evidence that they are inclusion bodies or an aggresome.

References

Abdulle, R., Mohindra, A., Fernando, P. and Heikkila, J.J. 2002. *Xenopus* small heat shock proteins, Hsp30C and Hsp30D, maintain heat- and chemically-denatured luciferase in a folding-competent state. *Cell Stress and Chaperones* 7, 6-16.

Adhikari, A.S., Sridhar Rao, K., Rangaraj, N., Parnaik, V.K. and Mohan Rao, Ch. 2004. Heat stress-induced localization of small heat shock proteins in mouse myoblasts: intranuclear lamin A/C speckles as target for alphaB-crystallin and Hsp25. *Experimental Cell Research* 299, 393-403.

Alexandrov, P.N., Zhao, Y., Pogue, A.I., Tarr, M.A., Kruck, T.P.A., Percy M.E., Cui, J-E. and Lukiw, W.J. 2005. Synergistic effects of iron and aluminum on stress-related gene expression in primary human neural cells. *Journal of Alzheimer's Disease* 8, 117-127.

Ali, A., Krone, P. and Heikkila, J.J. 1993. Expression of endogenous and microinjected *hsp30* genes in early *Xenopus* tadpoles. *Development* 103, 59-67.

Ali, A., Salter-Cid, L., Flajnik, M.F. and Heikkila, J.J. 1996a. Isolation and characterization of a cDNA encoding a *Xenopus* 70 kDa heat shock protein, Hsc70.I. *Comparative Biochemistry and Physiology* B 113, 681-687.

Ali, A., Krone, P.H., Pearson, D.S. and Heikkila, J.J. 1996b. Evaluation of stress inducible *hsp90* gene expression as a potential biomarker in *Xenopus laevis*. *Cell Stress and Chaperones* 1, 62-69.

Ali, A., Fernando, P., Smith, W.L., Ovsenek, N., Lepock, J.R. and Heikkila, J.J. 1997. Preferential activation of HSF-binding activity and *hsp70* gene expression in *Xenopus* heart after mild hyperthermia. *Cell Stress and Chaperones* 2, 229-237.

Allen, S.P., Polazzi, J.O., Gierse, J.K. and Easton, A.M. 1992. Two novel heat shock genes encoding proteins produced in response to heterologous protein expression in *Escherichia coli*. *Journal of Bacteriology* 174, 6938-6947.

Arrigo, A.P. and Landry, J. 1994. Expression and function of the low-molecular weight heat shock proteins. In: The Biology of Heat Shock Proteins and Molecular Chaperones.

Aviel, S., Winberg, G., Massucci, M. and Ciechanover, A. 2000. Degradation of the Epstein-Barr virus latent membrane protein 1 (LMP1) by the ubiquitin-proteasome pathway. Targeting via ubiquitination of the N-terminal residue. *The Journal of Biological Chemistry* 275, 23491–23499.

Awasthi, N. and Wagner, B.J. 2005. Upregulation of heat shock protein expression by proteasome inhibition: an antiapoptotic mechanism in the lens. *Investigative Ophthalmology and Visual Science* 46, 2082-2091.

Azzoni, A.R., Tada, S.F.S., Rosselli, L.K., Paula, D.P., Catani, C.F., Sabino, A.A., Barbosa, J.A.R.G., Guimarães, B.G., Eberlin, M.N., Medrano, F.J. and Souza, A.P. 2004. Expression and purification of a small heat shock protein from the plant *Xylella fastidiosa*. *Protein Expression and Purification* 33, 297-303.

Ballinger, C.A., Connell, P., Wu,Y., Hu, Z., Thompson, L.J., Yin, L.Y. and Patterson, C. 1999. Identification of CHIP, a novel tetratricopeptide repeatcontaining protein that interacts with heat shock proteins and negatively regulates chaperone functions. *Molecular and Cellular Biology* 19, 4535– 4545.

Beaulieu, J.F., Arrigo, A.P. and Tanguay, R.M. 1989. Interaction of *Drosophila* 27,000 Mr heat-shock protein with the nucleus of heat-shocked and ecdysone-stimulated culture cells. *Journal of Cell Science* 92, 29-36.

Beere, H. M. 2001. Stressed to death: regulation of apoptotic signaling pathways by the heat shock proteins. *Science STKE* 93: RE1.

Bienz, M. 1984a. Developmental control of the heat shock response in *Xenopus*. *Proceedings of the National Academy of Sciences USA* 81, 3138-3142.

Bienz, M. 1984b. *Xenopus hsp70* genes are constitutively expressed in injected oocytes. *EMBO Journal* 3, 2477-2483.

Bjerregaard H. 2007. Effects of cadmium on differentiation and cell cycle progression in cultured *Xenopus* kidney distal epithelial (A6) cells. *Alternatives to Laboratory Animals* 35, 343-348.

Bode, A.M. and Dong, Z. 2002. The paradox of arsenic: molecular mechanisms of cell transformation and chemotherapeutic effects. *Critical Reviews in Oncology/Hematology* 42, 5-24.

Bonelli, M.A., Alfieri, R.R., Desenzani, S., Petronini, P.G. and Borghetti, A.F. 2004. Proteasome inhibition increases HuR level, restores heat-inducible HSP72 expression and thermotolerance in WI-38 senescent human fibroblasts. *Experimental Gerontology* 39, 423-432.

Boorstein, W. R., Ziegelhoffer, T. and Craig, E. A. 1994. Molecular evolution of the HSP70 multigene family. *Journal of Molecular Evolution* 38, 1-17.

Boston, R.S., Viitanen, P.V. and Vierling, E. 1996. Molecular chaperones and protein folding in plants. *Plant Molecular Biology* 32, 191-222.

Buchner, J., Ehrnsperger, M., Gaestel, M., and Walke, S. 1998. Purification and characterization of small heat shock proteins. *Methods in Enzymology* 290, 339-349.

Buckley, B.A., Owen, M-E., Hofmann, G.E. 2001. Adjusting the thermostat: the threshold induction temperature for the heat-shock response in intertidal mussels (genus *Mytilus*) changes as a function of thermal history. *Journal of Experimental Biology* 204, 3571-3579.

Bush, K.T., Goldberg, A.L. and Nigam, S.K. 1997. Proteasome inhibition leads to a heat-shock response, induction of endoplasmic reticulum chaperones, and thermotolerance. *The Journal of Biological Chemistry* 272, 9086-9092.

Breitschopf, K., Bengal, E., Ziv, T., Admon, A. and Ciechanover, A. 1998. A novel site for ubiquitination: the N-terminal residue, and not internal lysines of MyoD, is essential for conjugation and degradation of the protein. *EMBO Journal* 17, 5964–5973.

Briant, D., Ohan, N. and Heikkila, J.J. 1997. Effect of herbimycin A on *hsp30* and *hsp70* heat shock protein gene expression in *Xenopus* cultured cells. *Biochemistry and Cell Biology* 75, 777-782.

Brodsky, J.L. and Chiosis, G. 2006. Hsp70 molecular chaperones: emerging roles in human disease and identification of small molecule modulators. *Current Topics in Medicinal Chemistry* 6, 1215-1225.

Chen, C.J., Chiou, H.Y., Chiang, M.H., Lin, L.J., and Tai, T.Y. 1996. Dose-response relationship between ischemic heart disease mortality and long-term arsenic exposure. *Arteriosclerosis, Thrombosis and Vascular Biology* 16, 504-510.

Chou, I.N. 1989. Distinct cytoskeletal injuries induced by As, Cd, Co, Cr, and Ni compounds. *Biomedical and Environmental Sciences* 2, 358-365.

Ciechanover, A., Heller, H., Elias, S., Haas, A. L. and Hershko, A. 1980. ATP-dependent conjugation of reticulocyte proteins with the polypeptide required for protein degradation. *Proceedings for the National Academy of Sciences USA* 77, 1365–1368.

Ciocca, D.R., Oesterreich, S., Chamness, G.C., McGuire, W.L. and Fuqua, S.A.W. 1993. Biological and clinical implications of heat shock protein 27000 (Hsp27): a review. *Journal of the National Cancer Institute* 85, 1558-1570.

Connell, P., Ballinger, C.A., Jiang, J., Wu, Y., Thompson, L.J., Hohfeld, J. and Patterson, C. 2001. The co-chaperone CHIP regulates protein triage decisions mediated by heat-shock proteins. *Nature Cell Biology* 3, 93–96.

Csizmadia, V., Raczynski, A., Csizmadia, E., Fedyk, E.R., Rottman, J. and Alden, C.L. 2008. Effect of an experimental proteasome inhibitor on the cytoskeleton, cytosolic protein turnover, and induction in the neuronal cells *in vitro*. *Neurotoxicity* 29, 232-243.

Cyr, D.M., Hohfeld, J. and Patterson, C. 2002. Protein quality control: U-box containing E3 ubiquitin ligases join the fold. *Trends in Biochemical Sciences* 27, 368– 375.

Darasch, S., Mosser, D.D., Bols, N.C. and Heikkila, J.J. 1988. Heat shock gene expression in *Xenopus laevis* A6 cells in response to heat shock and sodium arsenite treatments. *Biochemistry and Cell Biology* 66, 862-870.

Daugaard, M., Rohde A. and Jäättelä, M. 2007. The heat shock protein 70 family: highly homologous proteins with overlapping and distinct functions. *FEBS Letters* 581, 3702-3710.

Del Razo, L.M., Quintanilla-Vega, B., Brambila-Colombres, E., Calderon-Aranda, E.S., Manno, M. and Albores, A. 2001. Stress proteins induced by arsenic. *Toxicology and Applied Pharmacology* 177, 132-148.

Deuchar, E. M. 1975. *Xenopus*: The South African Clawed Frog. John Wiley & Sons Ltd.: London.

Dick, L.R., Cruikshank, A.A., Grenier, L., Melandri, F.D., Nunes, S.L. and Stein, R.L. 1996. Mechanistic studies on the inactivation of the proteasome by lactacystin: a central role for clasto-lactacystin beta-lactone. *The Journal of Biological Chemistry* 271, 7273-7276.

Djabali, K., de Nechaud, B., Landon, F. and Portier, M.M. 1997. aB-crystallin interacts with intermediate filaments in response to stress. *Journal of Cell Science* 110, 2759-2769.

Eder, K.J., Kohler, H.R. and Werner, I. 2007. Pesticide and pathogen: heat shock protein expression and acetylcholinesterase inhibition in juvenile Chinook salmon in response to multiple stressors. *Environmental Toxicology and Chemistry* 26, 1233-1242.

Ehrnsperger, M., Graber, S., Gaestel, M., and J. Buchner. 1997. Binding of non-native protein to hsp25 during heat shock creates a reservoir of folding intermediates for reactivation. *EMBO Journal* 16, 221-229.

Fatica, A., Oeffinger, M., Tollervey, D. and Bozzoni, I. 2003. Cic1p/Nsa3p is required for synthesis and nuclear export of 60S ribosomal subunits. *RNA* 12, 1431-1436.

Feige, U., Morimoto, R. I., Yahara, I. and Polla, B. S. 1996. "Stress-inducible cellular responses," Birkhauser Verlag., Basel: Switzerland.

Fenteany, G., Standaert, R.F., Lane, W.S., Choi, S., Corey, E.J. and Schreiber S.L. 1995. Inhibition of proteasome activities and subunit-specific amino-terminal threonine modification by lactacystin. *Science* 268, 726-731.

Fernando, P. and Heikkila, J.J. 2000. Functional characterization of *Xenopus* small heat shock protein, Hsp30C: the carboxyl end is required for stability and chaperone activity. *Cell Stress and Chaperones* 5, 148-159.

Fernando, P., Megeney, L.A., and Heikkila, J.J. 2003. Phosphorylation-dependent structural alterations in the small hsp30 chaperone are associated with cellular recovery. *Experimental Cell Research* 286, 175-185.

Fan, X.C. and Steitz, J.A. 1998. HNS, a nuclear-cytoplasmic shuttling sequence in HuR. *Proceedings of the National Academy of Sciences USA* 95, 15293-15298.

Freeman, B.C. and Morimoto, R.I. 1996. The human cytosolic molecular chaperones hsp90, hsp70 (hsc70) and hdj-1 have distinct roles in recognition of a non-native protein and protein refolding. *EMBO Journal* 15, 2969-2979.

Freeman, B.C. and Yamamoto, K.R. 2002. Disassembly of transcriptional regulatory complexes by molecular chaperones. *Science* 296, 2232-2235.

Fronius, M., Rehn, M., Eckstein-Ludwig, U. and Clauss, W. 2001. Inhibitory non-genomic effects of progesterone on Na+ absorption in epithelial cells from *Xenopus* kidney (A6). *Journal of Comparative Physiology B* 171, 377-386.

Ganea, E. 2001. Chaperone-like activity of α-crystallin and other small heat shock proteins. *Current Protein and Peptide Science* 2, 205-225.

García-Mata, R., Bebök, Z., Sorscher, E.J. and Sztul, E.S. 1999. Characterization and dynamics of aggresome formation by a cytosolic GFP-chimera. *The Journal of Cell Biology* 146, 1239-1254.

Garrido, C., Brunet, M., Didelot, C., Zermati, Y., Schmitt, E. and Kroemer, G. 2006. Heat shock proteins 27 and 70: anti-apoptotic proteins with tumorigenic properties. *Cell Cycle* 5, 2592-2601.

Gauley, J. and Heikkila, J.J. 2006. Examination of the expression of the heat shock protein gene, *hsp110*, in *Xenopus laevis* cultured cells and embryos. *Comparative Biochemistry and Physiology A* 145, 225-234.

Gebel, T.W. 2001. Unanswered questions in arsenic toxicology. *Journal of Environmental Pathology, Toxicology and Oncology* 20, 299-309.

Gellalchew, M. and Heikkila, J.J. 2005. Intracellular localization of *Xenopus* small heat shock protein, hsp30, in A6 kidney epithelial cells. *Cell Biology International* 29, 221-227.

Glickman, M. H. and Ciechanover, A. 2002. The ubiquitin-proteasome proteolytic pathway: destruction for the sake of construction. *Physiology Reviews* 82, 373–428.

Goldbaum, O. and Richter-Landsberg, C. 2004. Proteolytic stress causes heat shock protein induction, tau ubiquitination, and the recruitment of ubiquitin to tau-positive aggregates in oligodendrocytes in culture. *The Journal of Neuroscience* 24, 5748-5757.

Gordon, S., Bharadwaj, S., Hnatov, A., Ali, A. and Ovsenek, N. 1997. Distinct stress-inducible and developmentally regulated heat shock transcription factors in *Xenopus* oocytes. *Developmental Biology* 181, 47-63.

Gothard, L.Q., Ruffner, M.E., Woodward, J.G., Park-Sarge, O-K. and Sarge, K.D. 2003. Lowered temperature set point for ativation of the cellular stress response in T-lymphocytes. *The Journal of Biological Chemistry* 278, 9322-9326.

Graf, J. and Kobel, H. R. 1991. Genetics of *Xenopus laevis*. In "Methods in cell biology" 36: pp. 19-34, Academic Press, Inc.: England.

Guerra, L., Favia, M., Fanelli, T., Calamita, G., Svetlo, M., Bagorda, A., Jacobson, K.A., Reshkin, S.J. and Casavola, V. 2004. Stimulation of *Xenopus* P2Y1 receptor activates CFTR in A6 cells. *European Journal of Physiology* 449, 66-75.

Gupta, M., Vavasis, C. and Frishman, W.H. 2004. Heat shock proteins in cardiovascular disease a new therapeutic target. *Cardiology in Review* 12, 26-30.

Hamilton, A.M. and Heikkila, J.J. 2006. Examination of the stress-induced expression of the collagen binding heat shock protein, hsp47, in *Xenopus laevis* cultured cells and embryos. *Comparative Biochemistry and Physiology A* 143, 133-141.

Harris, G.K. and Shi, X. 2003. Signaling by carcinogenic metals and metal-induced reactive oxygen species. *Mutation Research* 533, 183-200.

Haslbeck, M. 2002. sHsps and their role in the chaperone network. *Cellular and Molecular Life Sciences* 59, 1649-1657.

Haas, A. and Rose, I. 1982. The mechanism of ubiquitin activating enzyme: A kinetic and equilibrium analysis. *The Journal of Biological Chemistry* 257, 10329–10337.

Heikkila, J.J., Ohan, N., Tam, Y., and Ali, A. 1997. Heat shock protein gene expression during *Xenopus* development. *Cellular and Molecular Life Sciences* 53, 114-121.

Heikkila, J.J., Darasch, S.P., Mosser, D.D. and Bols, N.C. 1987. Heat and sodium arsenite act synergistically on the induction of heat shock gene expression in *Xenopus laevis* A6 cells. *Biochemistry and Cell Biology* 65, 310-16.

Heikkila, J.J. 2003. Expression and function of small heat shock protein genes during *Xenopus* development. *Seminars in Cell and Developmental Biology* 14, 259-266.

Helbing, C., Gallimore, C. and Atkinson, B.G. 1996. Characterization of a *Rana catesbeiana* HSP30 gene and its expression in the liver of this amphibian during both spontaneous and thyroid hormone-induced metamorphosis. *Developmental Genetics*18, 223-233.

Herkovits, J., Cardellini, P., Pavanati, C. and Pérez-Coll, C.S. 1998. Cadmium uptake and bioaccumulation in *Xenopus laevis* embryos at different developmental stages. *Ecotoxicology and Environmental Safety* 39, 21-26.

Hershko, A., Ciechanover, A., Heller, H., Haas, A.L. and Rose, I.A. 1980. Proposed role of ATP in protein breakdown: conjugation of proteins with multiple chains of the polypeptide of ATP-dependent proteolysis. *Proceedings of the National Academy of Science USA* 77, 1783–1786.

Hohfeld, J. and Jentsch, S. 1997. GrpE-like regulation of the hsc70 chaperone by the anti-apoptotic protein BAG-1. *EMBO Journal* 16, 6209– 6216.

Holm, K., Hernroth, B. and Thorndyke, M. 2008. Coelomocyte numbers and expression of HSP70 in wounded sea stars during hypoxia. *Cell Tissue Research* 334, 319-325.

Hough, R., Pratt, G. and Rechsteiner, M. 1987. Purification of two high molecular weight proteases from rabbit reticulocyte lysate. *The Journal of Biological Chemistry* 262, 8303–8313.

Hughes, M.F. 2002. Arsenic toxicity and potential mechanisms of action. Toxicol Lett 133, 1-16.

Ichigi, J. and Asashima, M. 2000. The gene expressions and morphogenesis of *Xenopus* kidney A6 cells cultured in simulated microgravity and hypergravity. *Biological Science in Space* 14, 198-199.

Iijima, R., Homma, K.J. and Natori, S. 2003. Participation of proteasomes in *Xenopus* embryogenesis. *Journal of Biochemistry* 134, 467-471.

Imai, J., Yashiroda, H., Maruya, M., Yahara, I. and Tanaka, K. 2003. Proteasomes and molecular chaperones: cellular machinery responsible for folding and destruction of unfolded proteins. *Cell Cycle* 2, 585-590.

Ito, H., Kamei, K., Iwamoto, I., Inaguma, Y., García-Mata, R., Sztul, E. and Kato, K. 2002. Inhibition of proteasomes induces accumulation, phosphorylation, and recruitment of HSP27 and alphaB-crystallin to aggresomes. *Journal of Biochemistry* 131, 593-603.

Ito, H., Okamoto, K. and Kato, K. 1998. Enhancement of expression of stress proteins by agents that lower the levels of glutathione in cells. *Biochimica et Biophysica Acta* 1397, 223-230.

Jentsch, S. and Pyrowolakis, G. 2000. Ubiquitin and its kin: how close are the family ties? *Trends Cell Biology* 10, 335–342.

Johnston, J.A., Ward, C.L. and Kopito R.R. 1998. Aggresomes: a cellular response to misfolded proteins. *The Journal of Cell Biology* 143, 1883-1898.

Jong, W.W., Caspers, G.J. and Leunissen, J.A.M. 1998. Genealogy of the α-crystallin-small heat-shock protein superfamily. *Internation Journal of Biological Macromolecules* 22, 151-162.

Katoh, Y., Fujimoto, M., Nakamura, K., Inouye, S., Sugahara, K., Izu, H. and Nakai, A. 2004. Hsp25, a member of the Hsp30 family, promotes inclusion formation in response to stress. *FEBS Letters* 565, 28-32.

Katschinski, D.M. 2004. On heat and cells and proteins. *News in Physiological Science* 19, 11-15.

Kawazoe, Y., Nakai, A., Tanabe, M. and Nagata, K. 1998. Proteasome inhibition leads to the activation of all members of the heat-shock-factor family. *European Journal of Biochemistry* 255, 356-362.

Kim, D., Kim, S.H. and Li, G.C. 1999. Proteasome inhibitors MG132 and lactacystin hyperphosphorylate HSF1 and induce *hsp70* and *hsp27* expression. *Biochemical and Biophysical Research Communications* 254, 264-268.

Klemenz, R., Andrews, A-C, Fröhli, E., Schäfer, R. and Aoyama, A. 1993. Expression of the murine small heat shock proteins hsp25 and αB crystalline in the absence of stress. *The Journal of Cell Biology* 120, 639-645.

Kloetzel, P.M. 2001. Antigen processing by the proteasome. *Nature Reviews Molecular Cell Biology* 2, 179-187.

Kovacs, I., Lentini, K.M., Ingano, L.M. and Kovacs, D.M. 2006. Presenilin 1 forms aggresomal deposits in response to heat shock. *Journal of Molecular Neuroscience* 29, 9-19.

Krebs, R.A. and Feder, M.E. 1997. Tissue-specific variation in Hsp70 expression and thermal damage in *Drosophila melanogaster* larvae. *The Journal of Experimental Biology* 200, 2007-2015.

Krone, P. and Heikkila, J.J. 1988. Analysis of *hsp30, hsp70,* and *ubiquitin* gene expression in *Xenopus laevis* tadpoles. Development 103, 59-67.

Lambert, H., Charette, S.J., Bernier, A.F., Guimond, A. and Landry, J. 1999. HSP27 multimerization mediated by phosphorylation-sensitive intermolecular interactions at the amino terminus. *The Journal of Biological Chemistry* 274, 9378-9385.

Lang, L., Miskovic, D., Fernando, P. and Heikkila, J.J. 1999. Spatial pattern of constitutive and heat shock-induced expression of the small heat shock protein gene family, *hsp30*, in *Xenopus laevis* tailbud embryos. *Developmental Genetics* 25, 365-374.

Lang, L., Miskovic, D., Lo, M. and Heikkila J.J. 2000. Stress-induced, tissue-specific enrichment of *hsp70* mRNA accumulation in *Xenopus laevis* embryos. *Cell stress and Chaperones* 5, 36-44.

Laroia, G., Cuesta, R., Brewer, G. and Schneider, R.J. 1999. Control of mRNA decay by heat shock-ubiquitin-proteasome pathway. *Science* 284, 499-502.

Le Goff, P., Le Dréan, Y., Le Péron, C., Le Jossic-Corcos, C., Ainouche, A. and Michel, D. 2004. Intracellular trafficking of heat shock factor 2. *Experimental Cell Research* 294, 480-493.

Lee, B.S., Chen, J., Angelidis, C., Jurivich, D.A. and Morimoto, R.I. 1995. Pharmacological modulation of heat shock factor 1 by anti-inflammatory drugs results in protection agaist stress-induced cellular damage. *Proceedings for the National Academy of Sciences USA* 92, 7207-7211.

Lee, D.H. and Goldberg, A.L. 1998a. Proteasome inhibitors: valuable new tools for cell biologists. *Trends in Cell Biology* 8, 397-403.

Lee, D.H. and Goldberg, A.L. 1998b. Proteasome inhibitors cause induction of heat shock proteins and trehalose, which together confer thermotolerance in *Saccharomyces cerevisiae*. *Molecular and Cellular Biology* 18, 30-38.

Li, W. and Chou, I.N. 1992. Effects of sodium arsenite on the cytoskeleton and cellular glutathione levels in cultured cells. *Toxicology and Applied Pharmacology* 114, 132-139.

Liang, P., Amons, R., Clegg, J.S. and MacRae, T.H. 1997. Molecular characterization of a small heat shock/α-crystallin protein in encysted *Artemia* embryos. *The Journal of Biological Chemistry* 272, 19051-19058.

Linder, B., Jin, Z., Freeman, J.H. and Rubin, C.S. 1996. Molecular characterization of a novel, developmentally regulated small embryonic chaperone from *Caenorhabditis elegans*. *The Journal of Biological Chemistry* 271, 30158-30166.

Lindquist, S. and Craig, E.A. (1988) The heat shock proteins. *Annual Reviews in Genetics* 22, 631-677.

Liu, J., Kadiiska, M.B., Liu, Y., Lu, T., Qu, W. and Waalkes, M.P. 2001. Stress-related gene expression in mice treated with inorganic arsenicals. *Toxicological Sciences* 61, 314-320.

Luders, J., Demand, J. and Hohfeld, J. 2000. The ubiquitin-related BAG-1 provides a link between the molecular chaperones Hsc70/Hsp70 and the proteasome. *The Journal of Biological Chemistry* 275, 4613– 4617.

Lundgren, J., Masson, P., Mirzaei, Z. and Young, P. 2005. Identification and characterization of a *Drosophila* proteasome regulatory network. *Molecular and Cellular Biology* 25, 4662-4675.

Lüss, H., Schmitz, W. and Neumann, J. 2002. A proteasome inhibitor confers cardioprotection. *Cardiovascular Research* 54, 140-151.

MacRae, T.H. 2000. Structure and function of small heat shock/α-crystallin proteins: established concepts and emerging ideas. *Cellular and Molecular Life Sciences* 57, 899-913.

Madden, E.F., Akkerman, M. and Fowler, B.A. 2002. A comparison of 60, 70, and 90 kDa stress protein expression in normal rat NRK-52 and human HK-2 kidney cell lines following in vitro exposure to arsenite and cadmium alone or in combination. *Journal of Biochemical and Molecular Toxicology* 16, 24-32.

Manwell, L. A. and Heikkila, J. J. 2007. Examination of KNK437- and quercetin-mediated inhibition of heat shock-induced heat shock protein gene expression in *Xenopus laevis* cultured cells. *Comparative Biochemistry and Physiology A* 148, 521-530.

Marin, R. and Tanguay, R.M. 1996. Stage-specific localization of the small heat shock protein Hsp27 during oogenesis in *Drosophila melanogaster*. *Chromosoma* 105, 142-149.

Masliah, E., Rockenstein, E., Veinbergs, I., Mallory, M., Hashimoto, M., Takeda, A., Sagara, Y., Sisk, A. and Mucke, L. 2000. Dopaminergic loss and inclusion body formation in alpha-synuclein mice: implications for neurodegenerative disorders. *Science* 287, 1265-1269.

Mazroui, R., Di Marco, S., Kaufman, R.J. and Gallouzi, I.E. 2007. Inhibition of the ubiquitin-proteasome system induces stress granule formation. *Molecular Biology of the Cell* 18, 2603-2618.

McMillan, D.R., Christians, E., Forster, M., Xiao, X., Connell, P., Plumier, J.C., Zuo, X., Richardson, J., Morgan, S. and Benjamin, I.J. 2002. Heat shock transcription factor 2 is not essential for embryonic development, fertility, or adult cognitive and psychomotor function in mice. *Molecular and Cellular Biology* 22, 8005-8014.

Melikova, M.S., Kondratov, K.A. and Kornilova, E.S. 2006. Two different stages of epidermal growth factor (EGF) receptor endocytosis are sensitive to free ubiquitin depletion produced by proteasome inhibitor MG132. *Cell Biology International* 30, 31-43.

Michaud, S., Marin, R. and Tanguay, R.M. 1997. Regulation of heat shock gene induction and expression during *Drosophila* development. *Cellular and Molecular Life Sciences* 53, 104-113.

Michaud, S., Morrow, G., Marchand, J. and Tanguay, R.M. 2002. *Drosophila* small heat shock proteins: cell and organelle-specific chaperones? *Progress in Molecular and Subcellular Biology* 28, 79-101.

Mimnaugh, E.G., Chen, H.Y., Davie, J.R., Celis, J.E. and Neckers, L. 1997. Rapid deubiquitination of nucleosomal histones in human tumor cells caused by proteasome inhibitors and stress response inducers: effects on replication, transcription, translation, and the cellular stress response. *Biochemistry* 36, 14418-14426.

Miskovic, D., Salter-Cid, L., Ohan, N., Flajnik, M.F. and Heikkila, J.J. 1997. Isolation and characterization of a cDNA encoding *Xenopus* immunoglobulin binding protein, BiP (GRP78). *Comparative Biochemistry and Physiology B* 116, 227-234.

Morimoto, R.I. 2008. Proteotoxic stress and inducible chaperone networks in neurodegenerative disease and aging. *Genes and Development* 22, 1427-1438.

Morimoto, R. I. 1998. Regulation of heat shock transcriptional response: cross talk between a family of heat shock factors, molecular chaperones, and negative regulators. *Genes and Development* 12, 3788-3796.

Morimoto, R.I., Tissieres, A., and Georgopoulos, C. 1994. Regulation of heat shock gene transcription by a family of heat shock factors. In: "The Biology of Heat Shock Proteins and Molecular Chaperones". R.I. Morimoto, A. Tissieres, and C. Georgopoulos (Eds.). Cold Spring Harbor Laboratory Press.: Cold Spring Harbor, NY.

Morimoto, R. I. and Milarski, K. L. 1990. Expression and function of vertebrate *hsp70* genes. In: Stress proteins in biology and medicine. R. Morimoto, A Tissieres and C. Georgopoulos (Eds). Cold Spring Harbor Press.: Cold Spring Harbor, NY.

Morrow, G., Inaguma, Y., Kato, K. and Tanguay, R.M. 2000. The small heat shock protein Hsp22 of *Drosophila melanogaster* is a mitochondrial protein displaying oligomeric organization. *The Journal of Biological Chemistry* 275, 31204-31210.

Mosser, D. D., Caron, A. W., Bourget, L., Meriin, A. B., Sherman, M. Y., Morimoto, R. I. and Massie, B. 2000. The chaperone function of hsp70 is required for protection against stress-induced apoptosis. *Molecular and Cellular Biology* 20, 7146-7159.

Mosser, D. D., Kotzbauer, P. T., Sarge, K. D. and Morimoto, R. I. 1990. *In vitro* activation of heat shock transcription factor DNA-binding by calcium and biochemical conditions that affect protein conformation. *Proceedings of the National Academy of Sciences USA* 87, 3748-3752.

Muller, M., Gauley, J. and Heikkila, J.J. 2004. Hydrogen peroxide induces heat shock protein and proto-oncogene mRNA accumulation in *Xenopus laevis* A6 kidney epithelial cells. *Canadian Journal of Physiology and Pharmacology* 82, 523-529.

Muller, W.E.G., Koziol, C., Jurelec, B., Dapper, J., Batel, R. and Rinkevich, B. 1995. Combinatory effects of temperature stress and non-ionic organic pollutants on stress protein (hsp70) gene expression in the freshwater sponge *Ephydatia fluviatilis*. *Environmental Toxicology and Chemistry* 14, 1203-1208.

Murata, S., Minami, Y., Minami, M., Chiba, T. and Tanaka, K. 2001. CHIP is a chaperone-dependent E3 ligase that ubiquitylates unfolded protein. *EMBO Journal* 2, 1133-1138.

Neutzner, A., Benard, G., Youle, R.J. and Karbowski, M. 2008. Role of the ubiquitin conjugation system in the maintenance of mitochondrial homeostasis. *Annals of the New York Academy of Sciences* 1147, 242-253.

Nickson, R., McArthur, J., Burgess, W., Ahmed, K.M., Ravenscroft, P. and Rahman, M. 1998. Arsenic poisoning of Bangladesh groundwater. *Nature* 395, 338-346.

Norris, C.E., Brown, M.A., Hickey, E., Weber, L.A. and Hightower, L.E. 1997. Low-molecular-weight heat shock proteins in a desert fish (*Poeciliopis lucida*): homologs of human Hsp27 and *Xenopus* Hsp30. *Molecular Biology and Evolution* 14, 1050-1061.

Norris, C.E., diIorio, P.J., Schultz, R.J., and Hightower, L.E. 1995. Variation in heat shock proteins within tropical and desert species of *Poeciliid* fishes. *Molecular Biology and Evolution* 12, 1048-1062.

Ohan, N.W. and Heikkila, J.J. 1995. Involvement of differential gene expression and mRNA stability in the developmental regulation of the *Hsp30* gene family in heat-shocked *Xenopus laevis* embryos. *Developmental Genetics* 17, 176-184.

Ohan, N.W., Tam, Y., Fernando, P. and Heikkila, J.J. 1998a. Characterization of a novel group of basic small heat shock proteins in *Xenopus laevis* A6 kidney epithelial cells. *Biochemistry and Cell Biology* 76, 665-671.

Ohan, N.W., Tam, Y. and Heikkila, J.J. 1998b. Heat-shock-induced assembly of Hsp30 into high molecular weight aggregates in *Xenopus laevis* cultured cells. *Comparative Biochemistry and Physiology* B 119, 381-389.

Ohtsuka, K., Liu, Y.C. and Kaneda, T. 1993. Cytoskeletal thermotolerance in NRK cells. *International Journal of Hyperthermia* 9, 115-124.

Omura, S., Matsuzaki, K., Fujimoto, T., Kosuge, K., Furuya, T., Fujita, S. and Nakagawa A. 1991. Structure of lactacystin, a new microbial metabolite which induces differentiation of neuroblastoma cells. J. Antibiot. 44, 117-118.

Ovsenek, N. and Heikkila, J.J. 1990. DNA sequence-specific binding activity of the heat shock transcription factor is heat-inducible before midblastula transition of early *Xenopus* development. *Development* 110, 427-433.

Panasenko, O.O., Kim, M.V., Marston, S.B. and Gusev, N.B. 2003. Interaction of the small heat shock protein with molecular mass 25 kDa (hsp25) with actin. *European Journal of Biochemistry* 270, 892-901.

Parcellier, A., Gurbuxani, S., Schmitt, E., Solary, E. and Garrido, C. 2003. Heat shock proteins, cellular chaperones that modulate mitochondrial cell death pathways. *Biochemical and Biophysical Research Communications* 304, 505-512.

Parsell, D.A. and Lindquist, S. 1993. The function of heat shock proteins in stress tolerance: degradation and reactivation of damaged proteins. *Annual Reviews in Genetics* 27, 437-439.

Phang, D., Joyce, E.M. and Heikkila, J.J. 1999. Heat shock-induced acquisition of thermotolerance at the levels of cell survival and translation in *Xenopus* A6 kidney epithelial cells. *Biochemistry and Cell Biology* 77, 141-151.

Pritts, T.A., Hungness, E.S., Hershko, D.D., Robb, B.W., Sun, X., Luo, G.J., Fischer, J.E., Wong, H.R. and Hasselgren, P.O. 2002. Proteasome inhibitors induce heat shock response and increase IL-6 expression in human intestinal epithelial cells. *American Journal of Physiology: Regulatory, Integrative and Comparative Physiology* 282, 1016-1026.

Quinlan, R. and van den Ijssel, P. 1999. Fatal attraction: when chaperone turns harlot. *Nature Medicine* 5, 25-26.

Rafferty, K. A. 1965. Mass culture of amphibian cells: Methods and observations concerning stability of cell type. In "Biology of amphibian tumors" pp. 52-81, Springer-Verlag: Berlin.

Reinstein, E., Scheffner, M., Oren, M., Ciechanover, A. and Schwartz, A. 2000. Degradation of the E7 human papillomavirus oncoprotein by the ubiquitin-proteasome system: targeting via ubiquitination of the N-terminal residue. *Oncogene* 19, 5944-5950.

Ritossa, F. 1962. A new puffing pattern induced by heat shock and DNP in *Drosophila*. *Experimentia* 571-573.

Rivett, A.J, Palmer, A. and Knecht, E. 1992. Electron microscopic localization of the multicatalytic proteinase complex in rat liver and in cultured cells. *Journal of Histochemistry and Cytochemistry* 40, 1165-72.

Robert, J. 2003. Evolution of heat shock protein and immunity. *Developmental and Comparative Immunology* 27, 449-464.

Rock, K.L., Gramm, C., Rothstein, L., Clark, K., Stein, R., Dick, L., Hwang, D. and Goldberg, A.L. 1994. Inhibitors of the proteasome block the degradation of most cell proteins and the generation of peptides presented on MHC class I molecules. *Cell* 78, 761-771.

Rodenheiser, D.I., Jung, J.H. and Atkinson, B.G. 1986. The synergistic effect of hyperthermia and ethanol on changing gene expression of mouse lymphocytes. *Canadian Journal of Genetics and Cytology* 28, 1115-1124.

Sarge, K.D. 1995. Male germ cell-specific alteration in temperature set point of the cellular stress response. *The Journal of Biological Chemistry* 270, 18745-18748.

Scherrer, K. and Bey, F. 1994. The prosomes (multicatalytic proteinases; proteasomes) and their relationship to the untranslated messenger ribonucleoproteins, the cytoskeleton, and cell differentiation. *Progress in Nucleic Acid Research and Molecular Biology* 49, 1-63.

Scheufler, C., Brinker, A., Bourenkov, G., Pegoraro, S., Moroder, L., Bartunik, H., Hartl, F.U. and Moarefi, I. 2000. Structure of TPR domain–peptide complexes: critical elements in the assembly of the Hsp70–Hsp90 multichaperone machine. *Cell* 101, 199–210.

Shamovsky, I. and Nudler E. 2008. New insights into the mechanism of heat shock response activation. *Cellular and Molecular Life Sciences* 65, 855-861.

Sheng, X., Hu, Z., Lü, H., Wang, X., Baluska, F., Samaj, J. and Lin, J. 2006. Roles of the ubiquitin/proteasome pathway in pollen tube growth with emphasis on MG132-induced alterations in ultrastructure, cytoskeleton, and cell wall components. *Plant Physiology* 141, 1578-1590.

Silverthorn, D.U. 2004. Human Physiology: an integrated approach (3rd Ed.) Pearson Education Inc: New York.

Singh, D., Raman, B., Ramakrishna, T. and Rao, C.M. 2006. The cataract-causing mutation G98R in human alphaA-crystallin leads to folding defects and loss of chaperone activity. *Molecular Vision* 12, 1372-1379.

Sive, H. L., Grainger, R. M. and Harland, R. M. 2000. Early development of *Xenopus laevis*. Cold Spring Harbor Laboratory Press: New York.

Smith, J. C. and Tata, J. R. 1991. *Xenopus* cell lines. In "Methods in cell biology" 36, pp. 635-654, Academic Press, Inc.: England.

Sondermann, H., Scheufler, C., Schneider, C., Hohfeld, J., Hartl, F.U. and Moarefi, I. 2001. Structure of a Bag/Hsc70 complex: convergent functional evolution of Hsp70 nucleotide exchange factors. *Science* 291, 1553-1557.

Sreedhar, A. S. and Csermely, P. 2004. Heat shock proteins in the regulation of apoptosis: new strategies in tumor therapy: a comprehensive review. *Pharmacology and Therapeutics* 101, 227-257.

Stangl, K., Günther, C., Frank, T., Lorenz, M., Meiners, S., Röpke, T., Stelter, L., Moobed, M., Baumann, G., Kloetzel, P.M. and Stangl, V. 2002. Inhibition of the ubiquitin-proteasome pathway induces differential heat-shock protein response in cardiomyocytes and renders early cardiac protection. *Biochemical and Biophysical Research Communications* 291, 542-549.

Stromer, T., Ehrnsperger, M., Gaestel, M., and Buchner, J. 2003. Analysis of the interaction of small heat shock proteins with unfolding proteins. *The Journal of Biological Chemistry* 278, 18015-18021.

Stokoe, D., Engel, K., Campbell, D.G., Cohen, P. and Gaestel, M. 1992. Identification of MAPKAP kinase 2 as a major enzyme responsible for the phosphorylation of the small mammalian heat shock proteins. *FEBS Letters* 313, 307-313.

Tabb, A.L., Utsugi, T., Wooten-Kee, C.R., Sasaki, T., Edling, S.A., Gump, W., Kikuchi, Y. and Ellis, S.R. 2001. Genes encoding ribosomal proteins Rps0A/B of *Saccharomyces cerevisiae* interact with TOM1 mutants defective in ribosome synthesis. *Genetics* 157, 1107-1116.

Takemoto, L., Emmons, T. and Horwitz, J. 1993. The C-terminal region of α-crystallin:involvement in protection against heat-induced denaturation. *The Biochemical Journal* 294, 435-438.

Tam, Y. and Heikkila, J.J. 1995. Identification of members of the HSP30 small heat shock protein family and characterization of their developmental regulation in heat-shocked *Xenopus laevis* embryos. *Developmental Genetics* 17, 331-339.

Tanaka, K., Ii, K., Ichihara, A., Waxman, L. and Goldberg A.L. 1986. A high molecular weight protease in the cytosol of rat liver. I. Purification, enzymological properties, and tissue distribution. *The Journal of Biological Chemistry* 261, 15197-15203.

Tanaka, M. and Atomi, Y. 2000. Gravitational response of A6 cells. *Biological Science in Space* 14, 200-201.

Taylor, J.P., Hardy, J. and Fischbeck, K.H. 2002. Toxic proteins in neurodegenerative disease. *Science* 296, 1991-1995.

Tseng, C.H., Tseng, C.P., Chiou, H.Y., Hsueh, Y.M., Chong, C.K. and Chen, C.J. 2002. Epidemiologic evidence of diabetogenic effect of arsenic. *Toxicology Letters* 133, 69-76.

Vabulas, R.M. and Hartl, F.U. 2005. Protein synthesis upon acute nutrient restriction relies on proteasome function. *Science* 310, 1960-1963.

Van den Ijssel, P., Norman, D.G. and Quinlan, R. 1999. Molecular chaperones: Small heat shock proteins in the limelight. *Current Biology* 9, 103-105.

Van Montfort, R., Slingsby, C. and Vierling, E. 2002. Structure and function of the small heat shock protein α-crystallin family of molecular chaperones. *Advances in Protein Chemistry* 59, 105-156.

Verschuure, P., Croes, Y., van den IJssel, P.R., Quinlan, R.A., de Jong, W.W. and Boelens, W.C. 2002. Translocation of small heat shock proteins to the actin cytoskeleton upon proteasomal inhibition. *Journal of Molecular and Cellular Cardiology* 34, 117-128.

Voellmy, R. 2004. On mechanisms that control heat shock transcription factor activity in metazoan cells. *Cell Stress and Chaperones* 9, 122-133.

Voyer, J. and Heikkila, J.J. 2008. Comparison of the effect of heat shock factor inhibitor, KNK437, on heat shock- and chemical stress-induced *hsp30* gene expression in *Xenopus laevis* A6 cells. *Comparative Biochemistry and Physiology A* 151, 253-261.

Waters, E.R., Lee, G.J. and Vierling, E. 1996. Evolution, structure and function of the small heat shock proteins in plants. *Journal of Experimental Botany* 47, 325-338

Westerheide, S.D. and Morimoto, R.I. 2005. Heat shock response modulators as therapeutic tools for diseases of protein conformation. *The Journal of Biological Chemistry* 280, 33097-33100.

Wiegant, F.A., van Bergen en Henegouwen, P.M., van Dongen, G. and Linnemans, W.A. 1987. Stress-induced thermotolerance of the cytoskeleton of mouse neuroblastoma N2A cells and rat Reuber H35 hepatoma cells. *Cancer Research* 47, 1674-1680.

Wilkinson, K. D., Urban, M. K. and Haas, A. L. 1980. Ubiquitin is the ATP-dependent proteolysis factor I of rabbit reticulocytes. *The Journal of Biological Chemistry* 255, 7529–7532.

Woolfson, J.P. and Heikkila, J.J. 2009. Examination of cadmium-induced expression of the small heat shock protein gene, *hsp30*, in *Xenopus laevis* A6 kidney epithelial cells. *Comparative Biochemistry and Physiology A* 152, 91-99.

Wotton, D., Freeman, K. and Shore, D. 1996. Multimerization of Hsp42p, a novel heat shock protein of *Saccharomyces cerevisiae*, is dependent on a conserved carboxyl-terminal sequence. *The Journal of Biological Chemistry* 271, 2717-2723.

Wu, B.J., Kingston, R.E. and Morimoto, R.I. 1996. Human HSP70 promoter contains at least two distinct regulatory domains. *Proceedings of the National Academy of Sciences USA* 83, 629-633.

Xu, W., Marcu, M., Yuan, X., Mimnaugh, E., Patterson, C. and Neckers, L. 2002. Chaperone-dependent E3 ubiquitin ligase CHIP mediates a degradative pathway for c-ErbB2/Neu. *Proceedings of the National Academy of Sciences USA* 99, 12847– 12852.

Zou, J., Salminen, W.F., Roberts, S.M. and Voellmy, R. 1998. Correlation between glutathione oxidation and trimerization of heat shock factor 1, an early step in stress induction of the Hsp response. *Cell Stress and Chaperones* 3, 130-141.